INFLUENCE OF MOLECULAR PARAMETERS ON THE MISCIBILITY OF METALLOCENE LLDPE AND HDPE BLENDS: RHEOLOGICAL AND MOLECULAR DYNAMICS SIMULATION INVESTIGATION

BY

ADAM MUSA GIRI ARBAB

A Thesis Presented to the

DEANSHIP OF GRADUATE STUDIES

KING FAHD UNIVERSITY OF PETROLEUM & MINERALS

DHAHRAN, SAUDI ARABIA

In Partial Fulfillment of the
Requirements for the Degree of

MASTER OF SCIENCE

In

CHEMICAL ENGINEERING
January 2003

UMI Number: 1412289

ProQuest Information and Learning Company
300 North Zeeb Road
P.O. Box 1346
Ann Arbor, MI 48106-1346

بسم الله الرحمن الرحيم

In the name of Allah the Most beneficent, the Most Merciful

" و قل ربی زدنی علمًا "

" But say: O my Lord advance me in knowledge "

KING FAHD UNIVERSITY OF PETROLEUM & MINERALS
DHAHRAN 31261, SAUDI ARABIA

DEANSHIP OF GRADUATE STUDIES

This thesis, written by ADAM MUSA GIRI under the direction of his thesis advisor and approved by his thesis committee, has been presented to and accepted by the Dean of Graduate Studies, in partial fulfillment of the requirements for the degree of MASTER OF SCIENCE IN CHEMICAL ENGINEERING.

Thesis Committee

18/1/03

Dr. I.A. Hussein
(Thesis Advisor)

Dr. B.F. Abu-Sharkh
(Member)

Prof. A.M. AL-Amer
(Member)

Prof. Mohammed B. Amin
(Department Chairman)

Prof. Osama Ahmed Jannadi
(Dean of Graduate Studies)

3-3-2003

Date

ACKNOWLEDGMENT

All the praises are due to Allâh, the Lord of the worlds, and may Allâh send prayers of blessings upon Prophet Muhammad, the chosen, the trustworthy, and upon his family and all of his companions.

Thanks are due to King Fahd University of Petroleum & minerals for providing the support for this research. This research project was supported by the Faculty of Graduate Studies and Research through project # CHE/Rheology/223. The efforts of Dr. Al-Ohali and research committee are appreciated

I wish to express my special gratitude and appreciation to my supervisor, Dr. Ibenlwaleed A. Hussein for his constructive and patient guidance and persistent encouragement both in the whole thesis work and in daily life.

My heartfelt gratitude and appreciation also due to my co-supervisor, Dr. Basel F. Sharkh, for helpful suggestions and enlightening discussions concerning Molecular dynamics simulation part of the thesis. I would also like to thank my thesis committee member Professor Adnan M. AL-Amer for his constructive suggestions and advice for the thesis work.

Thanks are also due to the former and current Chairmen of the Chemical Engineering department Professors Abdullah A. Shaikh and Mohamad B. Amin.

TABLE OF CONTENTS

	List of Tables	VIII
	List of Figures	IX
	Abstract (English)	XI
	Abstract (Arabic)	XII
	CHAPTER 1	
	Introduction	1
	CHAPTER 2	
	Literature Review	6
2.1	Phase Separation in PE/PE Blends	7
2.2	Rheology and Miscibility of Multiphase Blends	12
2.3	Miscibility of HDPE/LLDPE Blends	18
	CHAPTER 3	
	Methodology	33
3.1	Molecular Dynamics Simulation	33
3.2	Experimental	51
	CHAPTER 4	
	Results and Discussion: Molecular Dynamics Simulation	57
	CHAPTER 5	
	Results and Discussion: Rheology	70
5.1	Influence of Branch Content	72
5.2	Influence of Molecular Weight on Blend Miscibility	96
5.3	Influence of the Composition Distribution	113

CHAPTER 6

	Conclusions and Recommendations	**127**
6.1	Conclusions.	**127**
6.2	Recommendations	**131**
	APPENDICES	**132**
A	Supplement to Chapter 4	**132**
B	Supplement to Chapter 5.1	**137**
C	Supplement to Chapter 5.2	**146**
D	Supplement to Chapter 5.3	**153**
	REFERENCES	**162**

List of Tables

Table 3.1 Characteristics of the Models Used in the Simulation 50

Table 3.2 Characteristic of the Materials Used in this Work 53

List of Figures

Figure 4.1a	Configuration of the blend of HDPE with m-LLDPE Containing 10 branches/1000C	58
Figure 4.1b	Configuration of the blend of HDPE with m-LLDPE Containing 20 branches/1000C	59
Figure 4.1c	Configuration of the blend of HDPE with m-LLDPE Containing 30 branches/1000C	60
Figure 4.1d	Configuration of the blend of HDPE with m-LLDPE Containing 40 branches/1000C	61
Figure 4.1e	Configuration of the blend of HDPE with m-LLDPE Containing 60 branches/1000C	62
Figure 4.2	Like Nonbonded RDF of LLDPE CH_2 with LLDPE CH_2	64
Figure 4.3	Like Nonbonded RDF of HDPE CH_2 with HDPE CH_2	65
Figure 4.4	Bond order correlation function for the two components of the blend (LLDPE with 30 branches/1000C	66
Figure 4.5	Bond order correlation function for the two components of the blend (LLDPE with 60 branches/1000C	67
Figure 5.1a	Comparison of the rheology of as-received and conditioned m-EO2	73
Figure 5.1b	$\eta'(\omega)$ and $G'(\omega)$ for 50% blend of m-EO2 with HDPE: Reproducibility test	74
Figure 5.2a	$\eta'(\omega)$ for blends of m-EO2 with HDPE	76
Figure 5.2b	$\eta'(\omega)$ for blends of m-EO3 with HDPE	77
Figure 5.3a	Cole-Cole plot for blends of m-EO2 with HDPE	79
Figure 5.3b	Cole-Cole plot for blends of m-EO3 with HDPE	80
Figure 5.4a	$\eta'(\phi)$ for blends of m-EO2 with HDPE	82
Figure 5.4b	$\eta'(\phi)$ for blends of m-EO3 with HDPE	83
Figure 5.5a	$\eta_o(\phi)$ for blends of m-EO2 with HDPE computed from BPU equation for NDB	84
Figure 5.5b	$\eta_o(\phi)$ for blends of m-EO3 with HDPE computed from Cross model	85
Figure 5.6a	$N_1(\dot{\gamma})$ for blends of m-EO2 with HDPE	87
Figure 5.6b	$N_1(\dot{\gamma})$ for blends of m-EO3 with HDPE	88
Figure 5.7a	Comparison of $\eta^*(\omega)$ and $\eta(\dot{\gamma})$ for blends of m-EO3 with HDPE	91
Figure 5.7b	Comparison of $\eta^*(\omega)$ and $\eta(\dot{\gamma})$ for blends of m-EO2 with HDPE	92
Figure 5.8a	$N_1(t)$ for blends of m-EO2 with HDPE	93
Figure 5.8b	$N_1(t)$ for blends of m-EO3 with HDPE	94

Figure 5.9a	$\eta'(\omega)$ for m-EO1 blend with HDPE	**97**
Figure 5.9b	$\eta'(\omega)$ for blends of m-EO3 with HDPE	**98**
Figure 5.10	Cole-Cole plot m-EO1 blends with HDPE	**100**
Figure 5.11a	$\eta'(\phi)$ for blends of m-EO3 with HDPE	**102**
Figure 5.11b	$\eta'(\phi)$ for blends of m-EO1 with HDPE	**103**
Figure 5.12a	$\eta_o(\phi)$ for blends of m-EO3 with HDPE computed from Cross model	**105**
Figure 5.12b	$\eta_o(\phi)$ for blends of m-EO1 with HDPE computed from Cross model	**106**
Figure 5.13a	$N_1(\dot{\gamma})$ for blends of m-EO1 with HDPE	**108**
Figure 5.13b	$N_1(\dot{\gamma})$ for blends of m-EO3 with HDPE	**109**
Figure 5.14	Comparison of $\eta^*(\omega)$ and $\eta(\dot{\gamma})$ for blends m-EO1 with HDPE	**110**
Figure 5.15	$N_1(t)$ for blends of m-EO3 with HDPE	**112**
Figure 5.16	$\eta'(\omega)$ for ZN-EO blends with HDPE	**114**
Figure 5.17	Cole-Cole plot for blends of ZN-EO with HDPE	**116**
Figure 5.18	$\eta'(\phi)$ for blends of ZN-EO with HDPE	**117**
Figure 5.19	$\eta_o(\phi)$ for blends of ZN-EO with HDPE computed from Cross model	**119**
Figure 5.20	Comparison of $\eta^*(\omega)$ and $\eta(\dot{\gamma})$ for the blends of ZN-EO with HDPE	**121**
Figure 5.21	$N_1(\dot{\gamma})$ for blends of ZN-EO with HDPE	**123**
Figure 5.22	$N_1(t)$ for blends of ZN-EO with HDPE	**124**

THESIS ABSTRACT

***NAME**: Adam Musa Giri Arbab*

***TITLE OF STUDY**: INFLUENCE OF MOLECULAR PARAMETERS ON THE MISCIBILITY OF METALLOCENE LLDPE AND HDPE BLENDS: RHEOLOGICAL AND MOLECULAR DYNAMICS SIMULATION INVESTIGATION*

***MAJOR FIELD:** CHEMICAL ENGINEERING*

***DATE OF DEGREE:** January, 2003*

The melt miscibility of linear high-density polyethylene (HDPE) and octene-based metallocene linear low-density polyethylene (m-LLDPE) was investigated by rheological and molecular dynamics (MD) simulation techniques. The effects of molecular parameters, like branch content (BC), composition distribution (CD), and molecular weight (M_w) were studied. In the MD simulation study, branch content of m-LLDPE was varied in the range 10 to 80 branches/1000 C. Both Rheology and MD simulation suggest a strong influence for BC on blend miscibility, and blends start to phase separate when the branch content of LLDPE is 40 branches/1000C. The separation becomes sharper at higher branch content of 60 branches/1000C. At high-BC, mismatch of the molecular conformation of highly branched m-LLDPE and HDPE was observed. Interlayer morphology was suggested by rheology and observed in MD simulations. Also, Ziegler-Natta LLDPE was found to be more miscible than m-LLDPE of the same M_w and BC. However, increasing the M_w of m-LLDPE from 70 to 100 kg/mol is of insignificant effect on its miscibility with HDPE. This research suggests the strong influence of molecular parameter of BC, and CD on miscibility of LLDPE/HDPE blends.

خلاصة الرسالة

الاسم : آدم موسى جرى

عنوان الرسالة : بحث تأثير العوامل الجزينية على ذوبان البولى إيثلين الخطى منخفض الكثافة المتالوسينى فى البولى إيثلين الخطى عالى الكثافة بواسطة الريولوجيا و المحاكاة الجزينية

التخصص : الهندسة الكيميانية

تاريخ الرسالة : يناير ٢٠٠٣

فى هذا البحث تمت دراسة ذوبان البولى إيثلين الخطى عالى الكثافة فى البولى إيثلين الخطى منخفض الكثافة المبلمر من الإيثلين والأوكتين بواسطة الريولوجيا و المحاكاة الجزينية. كما تمت دراسة تأثير كمية التفرع، الوزن الجزيىء وتوزيع التفرع. فى دراسة المحاكاة تم توزيع كمية التفرع فى المدى من ١٠ الى ٨٠ فرع / ١٠٠٠ ذرة كربون. أشارت نتائج إختبارات الريولوجيا والمحاكاة الجزينية الى تأثير قوى لكمية التفرع على درجة إمتزاج خليط البولى إيثلين. وجد أن المزيج ينفصل عندما تصل كمية التفرع للبولى إيثلين منخفض الكثافة الى ٤٠فرع/١٠٠٠ ذرة كربون وينفصل عنه تماما فى التفرعات الأعلى أى فى مدى ٦٠فرع/١٠٠٠ ذرة كربون. لوحظ تباين واضح فى شكل البولى إيثلين الخطى عالى الكثافة والبولى إيثلين الخطى منخفض الكثافة عندما تكون درجة تفرع الأخير عالية. كما لوحظ تكون الطبقة البينية المنزلقة بين خليطى البولى إيثلين بواسطة الريولوجيا و المحاكاة الجزينية. أيضا وجد أن البولى إيثلين الخطى منخفض الكثافة المحضر بواسطة حفاز زقلر- ناتا يمتزج فى البولى إيثلين عالى الكثافة أكثر مما يمتزجه البولى إيثلين الخطى منخفض الكثافة الميتالوسينى فى نفس كمية التفرع والوزن الجزيىء. كما وجد أن زيادة الوزن الجزيىء للبولى إيثلين الخطى منخفض الكثافة الميتالوسينى من ٧٠ الى ١٠٠ كلجم/مول ليس له أى تأثير يذكر على ذوبانه فى البولى إيثلين عالى الكثافة. تبين نتائج هذه الدراسة على تأثير قوى للتركيب الجزيئ ككمية التفرع وتوزيعها على درجة إمتزاج البولى إيثلين منخفض الكثافة فى البولى إيثلين عالى الكثافة.

CHAPTER 1

INTRODUCTION

Polyethylene (PE) is the most widely used polymer nowadays. Nevertheless, it is distinguished by some peculiarities making it unique polymer. It has an extremely high crystallization rate, arising from its high chain flexibility, mostly from its perfect chain structure, particularly, in the case of high-density polyethylene (HDPE). For this reason, PE is not commonly available in amorphous state, and therefore many characteristics of amorphous PE are derived via extrapolation of semicrystalline samples.

PE is produced in different forms, each of which has different properties resulting from variations in structure. HDPE molecule is mainly linear and it may contain very little branching with density in the range 0.940 to 0.965 g/cm^3. Also, low-density polyethylene (LDPE) contains short-chain branches (SCB) as well as long chain branches (LCB) with density in the range 0.910 to 0.925 g/cm^3 (Cho et al., 1998). The third type is linear low-density polyethylene (LLDPE), which is produced by copolymerizing ethylene with α-olefins such as 1-butene, 1-hexene, or 1-octene, and has a wide range of branch contents depending on catalyst and concentration of added comonomer. The density of conventional LLDPE is in the range 0.900 to 0.935 g/cm^3. It has long been recognized that one of the major differences between LLDPE prepared by

metallocene catalysts is the distribution of the comonomers along the backbone of the molecule (Karbashewski et. al. 1992). In particular, LLDPE prepared by Ziegler-Natta catalysts (ZN-LLDPE) has more uneven co-monomer distribution. However, LLDPE synthesized by metallocene catalyst (m-LLDPE) is claimed to possess relatively uniform distribution (Karbashewski et. al. 1992; Wignall et al. 2000, Zhang et al., 2001). It is generally believed that such differences in comonomer distribution is mainly attributed to the difference in the number of active-sites available in the two catalysts and manifests itself in the rheology and mechanical properties of the polymers as well as their melt miscibility with HDPE (Karbashewski et al. 1992, Kazatchrov et al. 1999; Tanem and Stori 2001).

ZN or m-LLDPEs are available in different grades and find use in different applications either as pure resins or blended with other polymers. The main distinguishing feature of all of these commercial grades is the comonomer type, branch content, and composition distribution (i.e. whether ZN or m-LLDPE). The details of branching strongly influence the processing and the properties of final product (Kazatchkov et al., 1999). Also, the details of branching affect molecular conformations and dimensions, which again affect solution and melt properties of LLDPE. In addition, molecular structure influences the miscibility of PEs as acknowledged in both theoretical (Fredrickson et al., 1994; Fredrickson and Lui, 1995) and experimental research (Hussein and Williams, 2001; Tanem and Stori, 2001; Lee and Denn, 2000; Hill and Barham, 1997).

Blends of HDPE, LDPE and LLDPE are widely used in industry. However, as aforementioned, various PEs exhibit different characteristics and properties. Therefore, different types of polyethylenes are often blended together to meet various kinds of requirements of processing and final product properties for example LLDPE has advantage characteristics such as flexibility, resistance to the environment, shear strength, and thermal properties compared to HDPE (Cho et al., 1998). However, LLDPE has disadvantages in yield stress, melt strength, and hardness. In order to modify these properties, the LLDPE is usually blended in small amounts with HDPE to improve flexibility and reduce extruder backpressure (Karbashewski et al. 1993; Utracki and Schlund, 1987; Hu et al. 1987; Barham et al. 1988; Tashiro et al. 1992). Thus, miscibility studies of PE blends in the liquid state have both industrial and scientific significance. The polyethylene melt processing industry is concerned about the miscibility of the components because miscibility affects the melt rheology. This in turn is expected to affect the solid-state morphology and final product properties. However, understanding of the mechanical and melt flow properties of such blends is handicapped by the consensus concerning the melt miscibility of HDPE/LLDPE mixtures. For example, different views were expressed in the literature about PE/PE blends ranging from liquid –liquid phase segregation (Hill et al. 1993; Barham et al. 1988; Hill et al., 1991, 1992 and 1994; Hill and Puig, 1997) to complete homogeneity in the melt (Alamo et al., 1990,1994 and 1997, Agamalian et al., 1999; Fan et al., 2002). However, in the case of HDPE/LLDPE blends, researchers have demonstrated unanimously that the average number of brunches per thousand backbone carbons of LLDPE is the major

factor that controls miscibility (Hill et al., 1993; Alamo et al., 1997; Choi., 2000). It was also predicted by the Small Angle Neutron Scattering (SANS) and Molecular Dynamics Simulations (MD) that the cut-off value for this blend is around 40 branches/1000C carbons (Alamo et al., 1997; Choi P. 2000). However, when the branch content is higher than 80, the blends phase separate (Alamo et al., 1997). But the authors (Alamo et al., 1997) made no comments on the miscibility of such blends with branch contents of LLDPE intermediate between 40 and 80. On the other hand, using transmission electron microscopy (TEM) different researchers (Hill et al., 1993; Barham et al., 1993; Hill and Barham, 1994; Morgan et al., 1999) have shown that the threshold value for the same blends is about 60. Furthermore, the critical value of branch content for systems of HDPE and a new type of LLDPE to form two separate crystal populations was reported by Zhao et al., (1997) to be about 25 branches/1000C. Thus the question is not simply whether linear and branched molecules are miscible, because it is evident that there will be miscibility when the branch level is very low and immiscibility when it is high (Hill et al., 1993; Barham et al., 1993; Hill and Barham, 1994, and Alamo et al., 1997). Rather, the question is about the level of branches that is required to phase separate the system. Recently, Fan et al., (2000) and Choi (2000) used MD simulation to calculate Flory-Huggins interaction parameter, χ and infer miscibility of LLDPE/HDPE blends.

In this study, a different approach was used. Initially, LLDPE and HDPE molecules were totally mixed at 500 K. The branch content of LLDPE was varied from 10 to 60

CHAPTER 2

LITERATURE REVIEW

Polymer blends have attracted considerable interest both in research community and in industry. One crucial issue is the miscibility of the polymer in a blend. For most applications, it is desirable that phase behavior of the polymer blend be accurately known, since it will affect the physical properties and, consequently, the use of the blend for specific application. As mentioned before, different polyethylene, i.e. linear and branched, were often blended together to increase the stiffness of LDPE and toughness and flexibility of linear polyethylene, mainly, HDPE, in the early stage of polyethylene industry.

ZN-LLDPE, and metallocene m-LLDPE are produced by copolymerization of a small percentage (0.1-8%) of 1-butene, 1-hexene, or 1-octene with ethylene resulting in SCB containing two to six methylene units. The branching commercial ZN-LLDPE chains is random and actual composition contains linear as well as highly branched molecules (Usami et al., 1986); however branching is more uniformly distributed along the m-LLDPE chains.

It was believed that the blends of different types of polyethylene would form homogeneous crystal due to their similar chemical composition, i.e., CH_2 group.

Kazatchkov et al, (1999); have studied two series of LLDPE resins, one having nearly constant M_w and different MWD, and the other series having nearly constant MWD and different M_w. Both series had the same degree of short chain branching. It was concluded that an increase in the weight average molecular weight of a resin increases its apparent melt viscosity and extrudate swell but decreases its shear rate and shear stress for the on set melt fracture. Wardhaugh and Williams (1995) reported that melts of pure LLDPE are likely to phase separate. LDPE on the other hand has a very chaotic molecular structure, with both short and long branches that may affect its rheology and blend miscibility in different ways.

2.1.1 Blends of Homopolymers

Blends of HDPE/HDPE and LDPE/LDPE (different M_w fractions) were reported to be miscible (Munoz-Escalona, 1997; Hill and Barham, 1995) and the viscosity vs. composition relationship followed the log-addtivity rule. For LLDPE/LLDPE systems studied by Utracki (1989b), one pair was found miscible; however, another blend was reported to be immiscible. It should be noted that ZN-LLDPEs were likely used in that study. This could explain these results, since each ZN-LLDPE is a "unique" soup of molecular structures.

2.1.2 HDPE/LDPE Blends

Barham et al. (1988), reported experimental data that support the view of a phase-segregated melt in blends of HDPE/LDPE with concentration higher than 50% of the latter. The branch content of the LDPE is close to one branch per hundred CH_2. Garcia-Rejon and Alvarez (1987) reported the incompatibility (immiscibility) of HDPE/LDPE blends. It was observed that low concentrations of HDPE (10%) had increased the LDPE G' by 50% (strong positive deviation behavior, PDB). Martinez-Salazar et al. (1991); Plans et al. (1991) correlated PDB of HDPE/LDPE systems to the branch content of LDPE, and reported a critical branch content below which miscibility was assured for their components. Furthermore, Curto et al. (1983) indicated good superposition of reduced η ($\dot{\gamma}$) capillary flow data for a series of HDPE/LDPE blends at T=160° to 200° C, interpreted as support for likely miscibility (or stable morphology). Similarly, the results of Lee et al. (1997) supported the miscibility of HDPE/LDPE blends.

2.1.3 HDPE/LLDPE Blends

Hu et al. 1987; Lee et al. 1997; Lee and Denn 2000, reported the miscibility of certain HDPE/ ZN-LLDPE pairs. However, Hill and co-workers (Thomas et al., 1993; Hill and Barham, 1995) detected liquid-liquid phase separation with HDPE/O-LLDPE systems with heavily branched LLDPE (branched content > 40 branches/1000C), produced by polymerization with a (promoted) catalyst system, consisting of $VOCl_3$ and $Et_3Al_2Cl_3$.

2.1.4 LDPE/LLDPE systems

Blends of LLDPE and LDPE combine the favorable mechanical properties of the LLDPE with the ease of processing of LDPE. Muller and Balsamo, (1994); Lee and Denn, (2000); reported that blends of LLDPE/LDPE partially miscible. However blends of LLDPE with other LLDPE or LDPE may show a widely diverse behavior, dependent on small changes in molecular structure caused by; for example using different catalyst, polymerization method or composition (Utracki, 1989 b). Hussein and Williams (2001) have reported dynamics and steady shear measurements of the miscibility of ZN-LLDPE/LDPE blends. It was concluded that blends of ZN-LLDPE (butene-based) and LDPE mixed at 190° and 220° C is partially miscible. Immiscibility is likely to occur around the 50/50 composition and in the LDPE-rich blends. Blends are likely miscible in the LLDPE-rich range. It was suggested that the complexity of the molecular mixture constituting ZN-LLDPE and the "mismatch" in the molecular conformation of LLDPE and LDPE are likely responsible for the immiscibility. Also, authors concluded that the mixing temperature did not influence the miscibility/immiscibility of blends. However, degradation of LLDPE was accelerated by the high mixing temperature (220°C) and extra antioxidant was needed to prevent degradation.

For immiscible blend systems, the state of dispersion and specifically the shape of dispersed phase (i.e. droplets) generally influence the rheological responses of

immiscible polymer blends. As a basic rule phase separation causes G' and G'' to increase as result of "emulsion morphology" present in phase separated systems. The emulsion morphology with consequent surface tension (α) gives rise to a non-zero storage modulus (G') even in a mixture of two Newtonian liquids.

Scholz et al. (1989) presented a constitutive equation for dilute emulsions of spherical, monodisperse droplets of Newtonian liquids. The two liquids are assumed to be incompressible, and totally immiscible. In the linear viscoelastic range of deformation the dynamic viscosity (and loss modulus) are given by:

$$\frac{G''(\omega)}{\omega} = \eta' = \eta_m\left[1+\phi\left(\frac{2.5k+1}{k+1}\right)\right] \quad \text{.....(2.1)}$$

Where, η_m is the viscosity of the matrix liquid.

$k=\eta_d/\eta_m$; η_d = the viscosity of the matrix liquid and ϕ = volume fraction of the disperse phase.

Chuang and Han (1984) reported that $\eta'(\omega)$ obtained at low ω for immiscible polymer blends, other than PE/PE systems, is found to be higher than those of the components as predicted by equation (2.1). This principle was applied to differentiate between miscible phase-separated polymeric blends. The high ω data ($\omega > 10$ rad/s) is not generally useful for similar interpretation of the miscibility of a blend (Scholz et al. 1989).

2.2 Rheology and Miscibility of Multiphase Systems

Chuang and Han (1984) illustrated that rheological behavior of immiscible blends is strongly affected by the type of applied shear. While shear-induced mixing that alters blend morphology is observed in some steady shear experiments (Larson, 1992; Minale et al., 1997), no such effects are reported for small amplitude dynamic shear (Utracki, 1988; Chuang and Han, 1984).

Generally, phase separation causes the storage and loss moduli G' and G'' to exceed values for the matrix phase, due to the presence of droplets of the dispersed phase. The storage modulus $G'(\omega)$ obtained experimentally at low-ω for immiscible polymer blends was reported by (Fujiyama and Kawasaki, 1991; Gramespacher and Meissner, 1992) to be higher than those of the components. Ajji and Choplin (1991) found the effects of phase separation on G' to be more pronounced than on G''.

The similarity of dynamic and steady shear properties e.g., between $\eta(\dot{\gamma})$ and $\eta^*(\omega)$, and between $N_1(\dot{\gamma})$ and $2G''(\omega)$ must not be expected for immiscible blends (Utracki and Schlund, 1987; Chuang and Han, 1984). While the lack of superposition of dynamic and steady shear viscosities does indicate immiscibility, success of superposition cannot be taken as proof of miscibility (Utracki and Schlund, 1987).

2.2.1 Rheological Models

Two types of two-phase flow may be distinguished, by their degree of phase separation. One type is dispersed two-phase flow, in which one component exists as the discrete phase dispersed in the other component, which form continuous phase. The other type stratified two-phase flow, in which both components form continuous phases separated from each other by a continuous boundary.

Einstein (1906) was the first to make a theoretical study of predicting the viscosity of a dilute suspension of rigid spheres and obtained, for suspension viscosity η:

$$\eta/\eta_o = 1 + 2.5\phi \quad \text{.....(2.2)}$$

η_o is the viscosity of the suspending medium, ϕ is the volume fraction of the spheres

2.2.1.1 Emulsion Models

The emulsion model of Palierne (1990) has been very successful in characterizing the linear viscoelastic behavior of immiscible blends of flexible polymer melts. One characteristic of such systems is an elevated value of the storage modulus at low frequencies relative to the matrix because of an elastic response associated with interfacial tension. For an emulsion of two viscoelastic phases with a uniform particle size and constant interfacial tension, the complex modulus of a blend, $G_b^*(\omega)$, is given by:

$$G_b^* = G'(\omega) + iG_b''(\omega) = G_m^* \frac{1+3\phi H(\omega)}{1-2\phi H(\omega)} \quad \text{.....(2.3)}$$

where:

$$H^* = \frac{4(\alpha/R)\left[2G_m^*(\omega)+5G_d^*(\omega)\right]-\left[G_m^*(\omega)-G_d^*(\omega)\right]*\left[16G_m^*(\omega)+19G_d^*(\omega)\right]}{40(\alpha/R)\left[G_m^*(\omega)+G_d^*(\omega)\right]+\left[3G_m^*(\omega)+2G_d^*(\omega)\right]*\left[16G_m^*(\omega)+19G_d^*(\omega)\right]} \quad \text{.....(2.4)}$$

G^*_m and G^*_d are the complex moduli of matrix and dispersed phases respectively; α is the interfacial tension, ϕ the volume fraction of disperse phase, and R the radius of disperse phase.

Recently, Bousmina (1999) extended Kerner's model for modulus of composite solid elastic media (1956) to an emulsion of viscoelastic liquid interfacial tension undergoing deformation of small amplitude. Bousmina obtained the following simple expression for $G^*_b(\omega)$:

$$G_b^* = G_m^* \frac{2\left(G_d^*+\alpha/R\right)+3G_m^*+3\phi\left(G_d^*+\alpha/R-G_m^*\right)}{2\left(G_d^*+\alpha/R\right)+3G_m^*-2\phi\left(G_d^*+\alpha/R-G_m^*\right)} \quad \text{----------(2.5)}$$

Scholz et al. (1989) derived a constitutive equation for dilute emulsions of noninteracting, spherical and monodisperse droplets of Newtonian liquids. The two liquids were assumed to be incompressible, and totally immiscible. For the linear viscoelastic range of deformation, the emulsion was shown to have dynamic moduli given by:

$$\frac{G''(\omega)}{\omega} = \eta' = \eta_m\left[1+\phi\left(\frac{2.5k+1}{k+1}\right)\right] \quad \text{----------(2.6)}$$

However, the difference between the fluidity-additivity equation and Lin's dependence equation is the presence of the interlayer interaction parameter. However, Bousmina, Palierne and Utracki (BPU) proposed a new model describing NDB.

$$1/\eta_{eff} = k\,(\phi_1\phi_2)^{1/2} + [\phi_1/\eta_1) + (\phi_2/\eta_2] \quad \text{.....(2.10)}$$

η_{eff}: effective viscosity; k: parameter for NDB

2.3 Miscibility of HDPE/LLDPE blends

Several research groups have studied the phase behavior of HDPE with LLDPE blends. Liquid-liquid phase separation in blends containing copolymers (two ethylene-butene and one ethylene-hexene) produced using metallocene catalyst has been investigated by Hill and Barham (1997). It was examined the blends by using indirect experimental methods to analyze the blend phase behavior in the melt. It was reported that all of the three systems show phase separation in the melt at low linear PE content at temperatures between ~ 125°C and 170°C. The behavior of the HDPE/hexene-LLDPE system was very similar to the behavior of the two HDPE/b-LLDPE systems.

Wignall et al., (2000) investigated the solid-state morphology of blends of linear HDPE and model short-chain branched b-LLDPE by four different techniques, differential scanning calorimetry (DSC), transmission electron microscopy (TEM), SANS and small angle X-ray (SAXS) scattering. The SANS results indicated that the mixtures were homogeneous in the melt for all compositions when the ethyl branch content was low (i.e., < 40 branches/1000 C ($M_w \sim 10^5$). However, due to structural and melting point differences between HDPE and LLDPE, the components may phase segregate in the solid state. The degree of separation is therefore controlled by the crystallization kinetics. On the other hand their results from DSC, TEM, SANS, and SAXS showed that the combination of scattering, microscopy, and calorimetric techniques can provide detailed insight into the compositions of the various populations of the lamellar and the

amorphous regions that surround them. Alamo, et al. (1997), examined the level of branching that is required to phase separate the systems of linear HDPE and branched b-LLDPE using SANS. It was observed that mixtures are homogeneous in the melt when the branch content is low (i.e., < 40 branches /1000 C). However, when the branch content is high (>80 braches/1000 C), the blends phase separate. Moreover, phase segregation could be driven by isotope effects if the molecular weight of deuterated PE was sufficiently high so that the product of degree of polymerization and χ between deuterated and hydrogenated species exceeds 2. The isotope effect driven phase separation could also be observed in the isotopic mixtures of the same species, say a deuterated and hydrogenated HDPE blend. It was further indicated that for a LLDPE system itself with a wider range of distribution of branch contents, a fraction of the highly branched molecules could phase separate from the lightly branched majority, even when the average branch content was low, say, 10-20 branches/1000 backbone carbon atoms (Alamo et al., 1997). It was commented that the key factor would be the level of branch content that would determine the miscibility of the components in the blend systems.

Kyu et al. (1987), extensively investigated blend system of b-LLDPE with HDPE by wide angle x-ray diffraction (WAXD), SAXS, Raman longitudinal acoustic mode spectroscopy (LAM), light scattering (LS) and DSC. The molecular information is as follows: LLDPE: M_w=114000; M_w/Mn =4.5, 18 SCB/1000C; HDPE: M_w=126000;

M_w/Mn =5.3; 1.0 SCB/1000C. Blend compositions were chosen with 20, 50 and 80% HDPE for HDPE/LLDPE blends. A single melting peak in DSC measurements was observed for all HDPE/LLDPE blend for both slowly cooled and quenched samples. Results from different techniques were believed to be quite consistent, whenever a single endotherm was found in DSC (for HDPE/LLDPE blends). It was concluded that cocrystallization (which implies that the components are miscible in crystalline phase), between the LLDPE and HDPE components occurred; no segregation was observed at high order structural levels of crystalline lamellae or spherulite. These arguments were based on the assumption that HDPE and LLDPE polyethylenes are miscible in the liquid state, which is still controversial topic.

Hill and Barham (1995) have investigated blends of LLDPE of differing M_w four linear PE (LPE) fractions, of M_{ws} between $2*10^6$ and $2.5*10^3$ were used. It was observed that all LPE fractions mix in the melt in all proportions between 160° and 120°C. Phase separation does not take place on quenching, but some small-scale spatial separation can be observed on isothermal crystallization when M_w differences between the two fractions were very large. Thus, the phase separation observed in blends of linear with branched PE does not take place as a result of some small-scale spatial separation can be observed on isothermal crystallization when M_w differences alone.

Further, Rego and Gedde (1989), Iragorri et al. (1991), Conde Brana and Gedde (1992) studied the crystallization kinetics and melting behavior of PE blends using DSC,

polarized light microscopy (PLM), TEM and small-angle light scattering (SALS) techniques. (HDPE: M_w of 2500; M_w/M_n=1.15; LLDPE: M_w=166000; M_w/M_n=6.1; 7.5 ethyl branches /1000C). It was pointed out that the presence of a single melting peak would be a necessary but not sufficient condition for the existence of cocrystals. It was found that a sample displaying unimodal melting might have two separate crystallite populations of the same melting temperature. It was suggested that reported that the HDPE and LLDPE blends show two distinct crystalline types. Also, the crystallization behavior (cocrystals or distinct crystallite populations) of PE blends would be strongly influenced by crystallization temperature and blend composition. Therefore, care should be exercised to analyze unimodal type of experimental results when cocrystallization issue is raised.

Tashiro et al. (1992), observed different cocrystallization degrees in the blends of HDPE with two b-LLDPE samples having a close composition. No explanation was given for this phenomenon. However, it could be seen from this paper that these two LLDPE samples were prepared by two different methods: one from hydrogenation of polybutadiene and the other with heterogeneous ZN catalyst. The DSC melting curve of the former were much narrower than the latter, indicating a more homogeneous composition distribution (Tashiro et al., 1992).

Lee et al. (1997) investigated the miscibility behavior of the blends of ZN-LLDPE/HDPE and m-LLDPE/HDPE in liquid state by WAXD technique. (HDPE:

M_w=142000; PD=3.5; ZN-LLDPE: M_w=178000; PD =3.9; m-LLDPE: M_w=164000; PD=2.4). It was observed that the ZN-LLDPE is more miscible in HDPE than the m-LLDPE. Zhao et al. (1997) have investigated crystallization behavior of blends of HDPE and a m-LLDPE produced by copolymerization of ethylene and 1-octene. In that study, m-LLDPE with different branch contents were used and blended with the same HDPE at 20, 50, 70, and 90% weight fraction. (HDPE: M_w=53000; PD=3.3; o- LLDPE: M_w =113000; 3.6 branches/1000 and M_v=68000; 7.15 branches/1000C and M_w=46000; 24.1 branches/1000C). DSC, SAXS and WAXD techniques were used. It was found that the crystallization behavior of the blends of HDPE with m-LLDPE differed significantly from that of blends of HDPE with conventional octene ZN-LLDPE. Further, authors reported that when branch content of m-LLDPE was low (3.6 branches/1000 carbons, or 0.72% in mole percentage), the components mixed well and formed uniform cocrystals. However, when branch content was increased, separate crystallization occurred between the two components. There was a continuous transformation from cocrystallization to separate crystallization depending on the branch content. When branch content was above about 8 branches per 1000 carbons, separate crystallization began to take place. When branch content was above about 25 branches per 1000 carbons, it was observed completely separate crystallization. In addition, it was reported that the critical value of branch content for separate crystallization to occur in the blends of HDPE and m-LLDPE was much lower than that in the blends of HDPE and conventional octene LLDPE reported in the literature (Zhao et al., 1997). Also, it was suggested that the

miscibility (in solid state) of the linear and branched polyethylenes would be affected by both the branch content and how the branches were distributed on the backbone.

Nicholson et al. (1990) investigated blends of HDPE and hydrogenated polybutadienes having different levels of ethyl branching along the backbone, which are model polymers of b-LLDPE with very narrow MWD and branching distributions. Authors examined melt HDPE/ b-LLDPE blend by SANS technique. Polybutadiene polymers were produced by anionic polymerization so as to give from 18 to 106 ethyl groups per 1000 backbone carbon atoms. However, in SANS experiments, the contrast is due to the deuteration of one of the species, either HDPE or hydrogenated polybutadiene in this case. Therefore, isotope effect will become an issue when phase behavior is being discussed using SANS technique. This effect was analyzed and the χ value that the isotope effect contributes in SANS experiments was evaluated. It was reported that an expression was obtained for χ of 50/50 HDPE/LLDPE blends at temperatures 150±15°C, as following:

$$\chi = 0.4 * 10^{-4} + 0.014 \Delta X_b^2 \quad \text{.....(2.11)}$$

Where χ is the Flory-Huggins interaction parameter based on SANS; ΔX is the fraction of the repeat units with ethyl branches. The first was attributed to the isotope effect and the second term to the chemical composition differences between the components. Authors implied that the information drawn from this study of the model systems could

be used to understand the phase behavior in complex copolymer systems such as those involving LLDPE.

Further, Rhee and Crist (1991) continued this work by examining the critical value of the branch content of hydrogenated polybutadiene for the blend to phase separate using SANS and morphological study with scanning electron microscopy (SEM) associated with etching and quenching techniques. It was concluded with their study that branch content over 60/1000C of the modeled branched polyethylene would be the critical value to phase segregate with HDPE in the blends with molecular weight M_w =118000 at 150° C. The domain sizes they observed ranged from 0.1 to 16 μm.

Hill and co-workers (1988-1998) performed a series of studies on polyethylene blends by using DSC, TEM and some other techniques. Author's main interest was focused on the liquid-liquid phase separation (LLPS) behavior in polyethylene blends. It was assumed that liquid state morphology existing at high temperatures ($T>T_m$) would be preserved if rapid quenching were applied to the melt. It was suggested that define rapid cooling impedes the movements of the molecules in the melt such that further segregation, which will need molecular diffusion, is not feasible (Kyu et al., 1987; and Barham, 1992). Hence the morphology observed in the quenched samples should be closely related to the morphology in the liquid state

Blends of HDPE with octene-based LLDPE obtained by polymerization with a (promoted) catalyst system consisting of $VOCl_3$ and $Et_3Al_2Cl_3$, of different branched content have been investigated by Barham et al., (1993). TEM and DSC techniques were used to examine phase behavior of the blends. It was observed that for lower branch contents (less than 8% in mole or 40 branches/1000C) of the LLDPE the phase diagram of the HDPE/LLDPE system was similar to those obtained previously from the studies of HDPE/LDPE blends. However, an unexpected behavior regarding the size of the LLPS region was observed. With the increase of branch content of the octene-based LLDPE (beyond 8%), the size of the LLPS region (closed-loop) was decreased. Later, it was investigated blends of HDPE and b-LLDPE with differing branch contents (Hill et al., 1993). What authors found was that the phase of this blend system was basically the same as that contained o-LLDPE. In addition, authors showed that the length of the LLDPE branches had to be of secondary importance in determining the phase behavior of the PE blends, as molecular of HDPE was based on the above studies and the investigation of the effect of molecular weights, further, it was reported that branch content of branched polyethylenes would be the major factor that determines the phase behavior of LLDPE blends with HDPE.

Hill and Puig (1997) have investigated melt miscibility of blends of o-LLDPE and LDPE. TEM and DSC, techniques were used to see if authors previous studies on HDPE/LDPE and HDPE/LLDPE blends could be applied to understand the phase behavior of complex LDPE/LLDPE blend system. In fact, many researchers suggested

that LLDPE was not single component system itself (Wardhaugh and Williams, 1995; Mirabella et al, 1988; Channel et al., 1994). If it is true that LLDPE itself phase separated, then it is not surprising that blends containing LLDPE components can have multiphase behavior. Based on experiment, Hill and Puig deduced that the previous work could be applied to explain phase behavior of the LDPE/LLDPE system with similar conclusions: there was a closed-loop phase diagram at low LLDPE composition and the phase domain size was around some microns in diameter. Two different types of LLDPE were used in the study; one was an ethylene-octene copolymer and the other had more than one branch type. However, different blends of LDPE with either one of above LLDPE showed similar phase behavior, i.e., similar LLPS region and domain size. Accordingly, authors further contended that it would be the number of branches that was of primary importance and that branch type was not of importance in determining the extent of phase separation. It was suggested that the phase separation in melts would very likely affect the rheological properties of these blends.

Alamo et al., (1997) addressed the hypothesis that HDPE/ZN-LLDPE blends would be homogeneous in the melt for all compositions by further studies of the blends of linear and branched PE and focused on the effect of branching on the miscibility of the components in the blends. Hydrogenated polybutadiene (HPB) was used, as model PE with different levels of branching that are essentially monodisperse model LLDPEs. It was reported that mixtures of linear and branched polyethylene would be homogeneous for all compositions when the branch content of the branched polyethylene was low,

typically less than 40 branches/1000C when Mw ~ 10^5. However, linear and branched PE molecules would phase separate if the branch content of branched PE was higher, typically larger than 80 branches/1000 C. Moreover, isotope effects could drive phase segregation if molecular weight of deuterated polyethylene was sufficiently high so that the product of degree of polymerization and χ between deuterated and hydrogenated species exceeds 2. The isotope effect driven phase separation could also be observed in the isotopic mixtures of the same species, say a deuterated and hydrogenated HDPE blend.

Extensive review on the miscibility studies of the polyolefin melts blends, namely polyethylene was reported by Crist and Hill (1997). It was indicated that more complicated systems such as blends of commercial polyethylenes could be understood by studying blends with model polymers that have uniform chemical structures and narrow molecular weight and branch content distributions. HPB model polymers were good examples. Most of the studies regarding miscibility issue for polyolefin blends are based on the Flory-Huggins interaction parameter theory. This approach shows its simplicity and power for expressing thermodynamic interactions in terms of a single parameter, χ. It has been pointed out that morphological investigations on this issue must be taken very carefully in order to draw a conclusion on the melt miscibility between the components in the blends based on the morphologies observed in the solid state. As mentioned before, Hill et al. developed an indirect method by using TEM and DSC to characterize the PE melt morphology based on observation of quenched samples. Hill

emphasized that the Ostwald ripening behavior was exhibited in the previous work regarding the LLPS of PE blends, thus assuring that the conclusions based on the solid state morphological studies were applicable to the liquid state. As for SANS technique, it is very powerful in determining the melt miscibility through evaluating thermodynamic interaction (χ) between chemically different polyolefins but this technique requires one of the components to be deuterated, which may cause additional ambiguity. Therefore, isotope effect must be taken into account. In general, measurements of interaction parameter, χ, should be done twice for each set of components, once with one of the two components deuterated and once with the other component deuterated. The geometric mean of the value of χ should be taken as reliable value without isotope effect (Mark, 1996).

Choi (2000) used MD simulation technique to compute Hildebrand solubility parameter (δ) for models of HDPE and a series of b-LLDPE with different branch contents. The branches were distributed randomly on the skeletal chains. The model molecules resemble LLDPE produced by ZN type of catalysts. The respective branch content was set at 10, 20, 40, 50, and 80/1000C for each LLDPE model. Author's reasons using of long chains rather than short chains (e.g. 100 backbone carbon chains) is to capture the branch content effect with statistically representative models. The molecular mass information was as follows: model HDPE had molecular mass, 17,029 g/mol, and the molecular volume is approximately 17,874 cm^3/mol; and model LLDPE had molecular mass range from 14,310-16,273 g/mol. δ values were used to calculate the

corresponding χ between HDPE and various B-LLDPE models. It was concluded that the level of branch content of B-LLDPE required to phase separate the blends in the liquid state is about 40 branches/1000 carbon atoms, regardless of temperature. Comparing these results with those recently investigated by Fan et al., (2002); using HDPE/LDPE blends, suggest the influence of long chain branching on the miscibility of polyethylene blends at elevated temperature. It was found that the level of branch content for LDPE above which the blends are immiscible and segregate in the melt was 30 branches/1000C. This value was significantly lower than that of b-LLDPE/HDPE blends (40 branches/1000C) computed by Choi (2000). It can be noted that the major differences between LDPE and LLDPE models is that each modeled LDPE molecule has three long chains while each modeled LLDPE molecule had only one long chain.

Tanem and Stori (2001) have investigated blends of a low-M_w weight LPE and several different ethylene-hexene copolymers using DSC, TEM. All blend components were made by single-site metallocene catalysts. It was observed that (a) In the blend containing 10 wt% of the LPE, even 1.8 mol% comonomer in the branched blend component is sufficient to create two separate crystal populations. This limit is lower than observed in blends containing ZN-based materials, indicating a more homogeneous distribution of short chain branching (SCB) in the single-site materials. However, a limited degree of cocrystallization seems to be present even for relatively high amount of comonomer in these blends. This is most probably the result of some structural heterogeneity in the branched blends components. In the blend containing 50 and 70wt%

many interesting results regarding rheology and morphology of polyolefin blends in the literature (Schlund and Utracki 1987, Utracki and Schlund 1987, Vega et al., 1996, Munoz-Escalona et al., 1997, Hill and Barham 1997, Cho et al., 1997). Utracki and Schlund (1987) have extensively studied various rheological properties of LLDPEs, including the LLDPE blend with LLDPE and LDPE. It was reported that the LLDPE/LLDPE blend showed miscibility, whereas the LLDPE/LDPE blend was thermodynamically immiscible but a possibility of a compatible mixture of emulsion type was suggested. The blend of high and low molecular weights of HDPE (Vega et al., 1996) made by the metallocene catalyst, was reported miscible themselves by rheological study. It was observed that the LLDPE/HDPE blend was miscible, but the LLDPE/LDPE and HDPE/LDPE blends were not miscible in the crystalline state, but they are all miscible in the melt state (Cho et al., 1998).

However, most of the above studies have used either SANS, differential scanning calorimetry (DSC), wide-angle X-ray diffraction (WAXD), or TEM techniques except the recent work of Choi (2000) and Fan et al. (2001) that used MD simulations (Fredrickson and Liu, 1995, Bates and Fredrickson, 1994). In that study, LLDPE molecule was constructed with a total of 500 C atoms and random distribution of branches. Also, both LLDPE and HDPE molecules were evaporated separately and cohesive energy density, E_{CED}, and Florry-Huggins interaction parameter, χ, were then calculated (Florry, 1941). Miscibility was predicted from χ values.

CHAPTER 3

METHODOLOGY

The techniques used for the investigation of the miscibility of HDPE/LLDPE, are essentially, MD simulations and rheological methods. MD simulations were used to study the effect of branch content on blend miscibility. On the other, rheological methods were employed to study the effect of M_w, BC, and CD on the miscibility of ZN and m-LLDPE blends with HDPE.

3.1 Molecular Dynamics Simulation

3.1.1 A Brief Description of the Molecular Dynamic Method

MD simulations calculate the 'real' dynamics of the system, from which time averages of properties can be calculated. Sets of atomic positions are derived in sequence by applying Newton's equations of motion. Basically, one needs to solve Hamilton's equations or any other formulation of the classical equations of motion, starting with some initial positions and momenta of all atoms in the molecules involved, and propagate the solution in a series of usually equally spaced time steps. The MD simulation runs until the equilibrium is reached, i.e. all thermodynamic properties start

to fluctuate randomly around certain steady mean values as in Monte Carlo (MC) simulations (Colbourn 1994).

Simulations are usually performed with relatively large numbers of atoms over many iterations or time steps. The intra- and intermolecular interactions are therefore almost always described by an empirical (i.e. molecular mechanics) energy model. Having chosen an energy model, the simulation itself can be broken into four distinct stages. First, an initial configuration for the system must be established. An equilibrium phase is then performed, during which the system evolves from initial configuration. Thermodynamic and structural properties are monitored during the equilibration until stability is achieved. At the end of the equilibration, the production phase commences. It is during the production phase that simple properties of the system are calculated. Finally, the simulation is analyzed; properties not calculated during the simulation are determined and the configurations are examined. This leads not only to discover how the structure of the system had changed, but also provides means for checking any unusual behavior that might determine the success or failure of a simulation (Colbourn 1994).

3.1.2 Thermodynamics of Mixtures

It is generally accepted that local molecular structure plays a crucial role in determining the thermodynamic properties of pure simple liquid and their mixtures. Accordingly, the

theory of simple liquid has received a great deal of attention. The concept of miscibility for polymer mixtures means that the components of the mixtures mingle well at segmental level. Flory (1942) and Huggins (1942) were among the first individuals to present a statistical mechanical theory that deals with the random-walk nature of polymer solutions and melts. However, the resulting expressions for the free energy of mixing bear a striking resemblance to classical regular solution theory, where the ideal combinatorial entropy of mixing for simple fluids is normalized by degree of polymerization. All excess free energy contributions are included in the well-known χ parameter,

$$\chi = \chi_H + \chi_S \quad \text{.....(3.1)}$$

$$\chi_H = -T\frac{\partial \chi}{\partial T} \quad \text{.....(3.2)}$$

$$\chi_S = -\partial(\chi T/\partial T) \quad \text{.....(3.3)}$$

So that on this basis χ should vary, as a+b/T. χ_H is enthalpic component, excess entropies, arising from specific interactions such as hydrogen bonding and segment packing constraints, are accounted for by χ_S. In general, contributions to excess entropy of mixing have been associated with local (i.e. monomer length scale) effects, with little attention paid to the nonlocal (i.e. length scales greater than the persistence, or Kuhn length). The expression of entropy of mixing based upon an incompressible lattice model, Flory (1941; 1942) and Huggins (1941; 1942),

$$\Delta S_{mix} = -k(N_1 \ln\phi_1 + N_2 \ln\phi_2) \quad \text{.....(3.4)}$$

where ϕ_1, ϕ_2 are volume fractions of component 1 and 2, respectively, $N_t$represents the number of molecules of solvent for polymer-solvent system but it represents the number of segments of polymer one for polymer-polymer systems, N_2 represents the number of segments of polymer 2, not the number of polymer molecules. It is worth noting that volume fraction must be used in the polymer field because the ratio of segments occupying adjacent lattice sites, not the ratios of whole molecules, determines the interaction energies. Flory-Huggins lattice theory of free energy of mixing per monomer, ΔG_m, is:

$$\Delta G_{mix} = kT[N_1 \ln\phi 1 + N_2 \ln\phi_2 + \chi_{12}(N_1 + N_2)\phi_1\phi_2] \quad \text{.....(3.5)}$$

Where ϕ, N_i, are volume fractions and degree of polymerization respectively. Thermal energy is given by kT, and χ is Flory-Huggins interaction parameter, which represents energetic repulsion ($\chi > 0$) or, more rarely, attraction ($\chi < 0$) between monomer of two polymers.

If using number of moles (n_i) instead of the number of molecules (N_i) in the above equation ($n_i = N_i/A$, A is the Avogadro's constant), the above equation can be rewritten as follows:

$$\Delta H_{mix} = RT\, \chi_{12}(n_1+n_2)\, \phi_1\, \phi_2 \quad \text{..... (3.6)}$$

$$\Delta S_{mix} = -R[n_1 \ln \phi_1 + n_2 \ln \phi_2] \quad \text{.....(3.7)}$$

Note, that in Equation 4.5, the first two terms (the entropy contribution to mixing) in the bracket are always negative because volume fractions are less than unity and the sign of

the third term (enthalpy contribution to mixing) depends on the sign of the Flory-Huggins interaction parameter. χ_{12} can be positive or negative in nature depending on the characteristics of the interactions between solvents and segments of polymers or between polymer-polymer segments. In favor of miscibility, the value of χ_{12} must be negative or, positive, small enough in order to have negative ΔG_{mix}. Altering the temperature of a binary blend changes the size of the Flory-Huggins interaction parameter χ. The most common situation is when χ is positive and decreases with increasing temperature:

$$\chi(T) = A+B/T \quad \text{.....(3.8)}$$

Here, the constant B is greater than zero. Lowering the absolute temperature T enhances χ. Based on Equation 4.5, increasing molecular weight of polymer components of a mixture at fixed ϕ_2 will decrease the total number of molecules, N_2, while keeping other variables constant. Therefore, it will reduce the negative entropic term and result in a less negative Gibbs free energy change, indicating that higher-molecular-weight polymers are more difficult to dissolve in solvents or other polymers than are lower-molecular-weight polymers.

The interaction parameter χ can be interpreted in terms of the difference in solubility parameters (square root of cohesive energy density) of repeat units constituting polymer 1 and 2 (Hildebrand and Scott, 1964).

$$\chi_{12} = \frac{V_s}{kT}(\delta_1 - \delta_2)^2 \quad (3.9)$$

where $V_s = V/(n_1-n_2)$ is the molar volume of the solvent for polymer-solvent mixtures or the molar volume of the smallest polymer segment for polymer-polymer mixtures. In this expression for V_s, n_1 is the number of moles of the solvent while n_2 is the number of moles of polymer segments for polymer-solvent systems, not the number of moles of polymer molecules and usually not the number of moles of polymer repeat unit. For polymer-polymer systems, n_1 and n_2 represent the number of moles of segments of polymer one and polymer two, respectively. By using this simple expression, χ_{12} can be calculated from individual solubility parameters of the pure components without appealing to the simulations of the blends, which saves much computation work. Because χ_{12} is always positive, the smaller χ_{12}, the more miscible or compatible the components. For polymer blends, the critical value of $\chi_{12,\,critical}$ for the components to phase-separate is rather small and close to zero in many cases. In polyethylene blends, the χ_{12} values of linear and branched polyethylene blends are usually larger when the branch content is high.

3.1.3 Common Statistical Ensembles

An ensemble is a collection of a large number of systems (microstates) having the same observed microstate. There are four ensembles in common use: the microcanonical, or constant-NVT ensemble, corresponding to close system. If the system is defined in terms of N, V, E (E is the total energy of the system), it is called microcanonical ensemble, indicating an isolated system. If the system has fixed values of V, T, and chemical potential, denoted as μ, it is called grand canonical ensemble, representing an open system.

In practice, we often make averages over a series of microstates as the result of the evolution of the system with time as MD does instead of ensemble averages. Therefore, ergodicity must be assumed. In statistical thermodynamics, we always study systems in equilibrium. Therefore, an ensemble being studied is usually a stationary one. Thus, the ensemble average of any thermodynamic property should be independent of time. Accordingly, the ensemble average must be the same as the time average. This is the so-called ergodicity hypothesis (Lucas, 1991) in statistical mechanics. Strictly speaking, it is not proper to define a given macro system in terms of microstates specified by the position and momentum coordinates of all particles in the system simultaneously according to Heisenberg's uncertainty principle. Quantum effects have to be taken into account in describing molecular world. However, in classical statistical mechanics,

quantum effects are not considered explicitly. Firstly, because statistical mechanics calculations use force field and require a molecular model that collects all the necessary information about the molecular system and lumps it together and simplifies the actual problem. A force field is the collection of expressions and parameters that are used to describe molecular systems. Therefore, quantum effects have been taken into account when the expressions of the force field are set up or the parameters are experimentally determined. Secondly, if the systems dealt with are at high temperatures, far above zero K, the quantum effect is usually negligible. Thus, the system can be treated as a continuous phase space at high temperatures. In this study, temperatures of 450 and 500K are used; hence, quantum effects are negligible.

3.1.4 Force Field

The fundamental computation at the core of a force field-based simulation is the calculation of the potential energy for a given configuration of atoms (and cells, if requested and possible). The calculation of this energy, along with its first and second derivatives with respect to atomic coordinates (and cell coordinates), yields the information necessary for minimization, harmonic vibrational analysis, and dynamic simulations. The calculation is actually done by the simulation engine, or force field based program.

Simulation engines are the computational packages that handle the application of force fields in minimization, dynamics, and other molecular mechanics simulations.

The goal of the force field is to describe entire classes of molecules with reasonable accuracy. In a sense, the force field interpolates and extrapolates from the empirical data of the small set of models used to parameterize the force field to a larger set of related models. Some force fields aim for high accuracy for limited set of element types, thus enabling good prediction of many molecular properties. Other force fields aim for the broadest possible coverage of the periodic table, with necessary lower accuracy (Colbourn, 1994).

The physical significance of most of the types of interactions in a forcefield is easily understood, since describing a model's internal degree of freedom in terms of bonds, bond angles, and torsions seems natural. The analogy of vibrating balls connected by springs to describe molecular motion is equally familiar. However, it must be remembered that such models have limitations. Consider for example the difference between such a mechanical model and a quantum mechanical "bond".

The total potential energy, E_{tot}, in the MD simulations consists of four parts: the bond-stretching energy, $E_{stretch}$, for adjacent united atoms, the bond-bending energy E_{bend}, among three adjacent united atoms, and the torsion energy, $E_{torsion}$ among four adjacent

united atoms, and the 12-6 Lennard-Jones potential, E_{vdW}. Between two Nonbonded atoms,

$$E_{tot} = E_{stretch} + E_{bend} + E_{torsion} + E_{vdw} \quad \text{.....(3.10)}$$

$$E_{tot} = \sum_{i=2}^{n} \frac{1}{2} k_d (d_i - d_0)^2 + \sum_{i=3}^{n} \frac{1}{2} k_\theta (\theta_i - \theta_0)^2 + \sum_{i=4}^{n} \frac{1}{2} k_\phi [1 - \cos(3\phi_i)]$$

$$+ \sum_{i=1}^{n-4} \sum_{j=i+3}^{n} 4\varepsilon \left[\left(\frac{\sigma}{r_{ij}} \right)^{12} - \left(\frac{\sigma}{r_{ij}} \right)^{6} \right] \quad \text{.....(3.11)}$$

Where d_0 is the equilibrium bond length and d_i is the bond length between atoms I-1 and I, θ_o is the bond angle, θ_i is the bond angle between bonds (i-2, i-1) and (i –1,i), ϕ_i is the dihedral angle between the (i –3, i-2, i-1) and (i-2, i-1, i) planes, and r_{ij} is the distance between atoms I and j. Nonbonding interactions are not calculated between atoms bonded to each other (I, 2 interactions) or atoms involved in angle interactions (1,3 interactions), since it is assumed that these interactions are included in the bond angle energy terms (Mayo et al., 1990; Fujiwara and Sato, 1997; Liao and Jin, 1999). Basically, there are three categories of force fields. First category of force fields was developed on the purpose of being very generic so that these force fields can cover as many as possible atom types and their combinations. UFF (universal force field) [Rappe et al., 1992] is an excellent general-purpose force field. All the universal force field parameters are generated from a set of rules based on element, hybridization, and connectivity. Also, DREIDING force field [Mayo et al., 1990] is a good, robust, and all-purpose forcefield. While a specialized forcefield is more accurate for predicting a

limited number of structures, the Deriding force field allows reasonable predictions for a very much larger number of structures, including those with novel combinations of elements and those for which there is little or no experimental data. It can be used for structure prediction and dynamic calculations on organic, biological, main group inorganic molecules. This category of force fields is usually expected to produce only approximately correct predictions of molecular structures due to the generic parameterization. The category of force fields was developed on the purpose of improving the quality of prediction in a relatively focused area of applications, especially in biochemistry field. Examples of these force fields are new version of CHARM (Mackerell et al., 1995), AMBER (Cornell et al. 1, 1995; Cornell et al. 2,1996) and OPLS/AMBER (Jorgensen et al., 1996). Similar to the first category, these force fields still use simple functions in potential energy expressions but parameterization is more precise. Another category belongs to high-precision prediction of various molecular properties with relatively large coverage of atom types. Unlike the above two categories, complicated potential expressions and high-order force constants are utilized in these force fields in order to achieve the high accuracy of prediction of molecular properties. It can be noted that atomic force field used here is the DREIDING potential.

works well with quantum mechanics may not be the most suitable for use with molecular mechanics. This is partly because quantum mechanics is usually used to model systems with smaller numbers of atoms than molecular mechanics. Some operations that are integral to certain minimization procedures (such as matrix inversion) are trivial for small systems but formidable for systems containing thousands of atoms. Quantum mechanics and molecular mechanics also require different amounts of computational effort to calculate the energies and the derivatives of various configurations. Thus an algorithm that takes many steps may be appropriate for molecular mechanics but inappropriate for quantum mechanics (Leach, 1996).

3.1.6 Nose' Formulation for NVT Canonical Ensemble Dynamics

Molecular dynamics studies the evolution of a molecular system with time. In order to achieve this, a trajectory file needs to be created when an MD run is completed. A trajectory is a set of records of position and velocity coordinates of a molecular system for the whole MD simulation run. In MD simulations, trajectory files are obtained by solving Newton's equation of motion step by step. At the beginning of an MD run, the initial position coordinates are determined by a Monte Carlo method subjected to density and conformational constraints. An energy minimization step is performed and the initial velocity coordinates are assigned based on the Boltzmann principle at the simulation temperature before an MD run. Thus, MD simulations cannot be repeated exactly

because of the random selection of the initial position coordinates and velocity coordinates. However, MD run results should not depend on the initial condition although no identical trajectories can be generated. This is assured by appropriate selection of the initial configurations of the molecules (or atoms) and their momenta. This includes proper construction of molecular models and suitable energy minimization. If this is done correctly, the energy (energies) of the modeled system at equilibrium for each MD run should be kept at the same level regardless of the difference of the trajectories.

Once the initial condition is selected, the position and velocity coordinates of the next time step can be calculated using a numerical method (called an integrator in MD simulation engines) according to the present position and velocity coordinates. In cerius2 MD simulation engine, the Verlet leapfrog integrator is used (Verlet, 1967). This method requires only one energy evaluation at each step and requires only modest memory and also permits large time step applications. However, if the time step is too large, instability and inaccuracy will occur in the integration process.

There are many statistical ensembles that can be used in MD simulations [MSI, 1997; Lucas, 1991; Pathria, 1972; McQuarrie, 1976]. In particular, the constant-number of particles, constant-temperature and constant-volume (NVT) ensemble (also called canonical ensemble) is used in this study. By using the NVT ensemble, the densities

(N/V) of the simulated systems can be easily controlled at experimental values. It was reported that an NPT ensemble approach would be slightly worse than an NVT approach in predicting solubility parameter (Sun and Rigby, 1997). Nose', 1984 developed a controlled-temperature dynamics method. The central theme of Nose' formalism is that an additional term is put into the original equation of motion to balance the heat bath with the system. In Nose' dynamics, the smaller the time step, the closer it reaches the controlled temperature.

3.1.7 Model and Simulation Method

Four chains of PE composed of 125 backbone CH_2 units each with various levels of octene incorporation and four chains of linear HDPE composed of 125 backbone segments were initially constructed. A limited number of simulations were conducted with two chains of PE composed of 250 backbone CH_2 segments each and 2 chains of HDPE composed of 250 CH_2 segments each to investigate the influence of molecular weight on miscibility. The branch content of the m-LLDPE was 10, 20, 30, 40 and 60 branches/1000 backbone carbons. The branches were randomly distributed along the chain to simulate the structure of LLDPE produced by metallocene catalysis Zhang et al. 2001). The branches were composed of five methylene units and an end methyl unit simulating the copolymerization of ethylene with 1-octene. Initially, chains with random torsion angle distribution were constructed. Energy of the chains was initially minimized in vacuum to eliminate high-energy overlaps. The chains were subsequently placed in a periodic MD cell of size that corresponds to the experimental density of the melt (Rudin 1970). The chains of the two polymers were completely entangled and mixed at the beginning of the simulation. Each methylene and methyl unit is treated as a spherical united atom. The united atom representation may introduce some errors especially in modeling the torsional potential. However, at the elevated temperature (450K and 500K) used in this investigation, the chain will sample more of its phase space. The simulations were carried out using Cerius2 (version 4.2, Accelerys Inc.) molecular modeling code. Simulations were carried out in the canonical (NVT) ensemble using the Nose-Hoover

method at densities averaged over the experimental bulk densities of both polymers (Rudin et al. 1970). Periodic boundary conditions were applied. The simulation temperatures were limited to 450K and 500K to represent PE melt conditions. An integration time step of 0.005 ps was used. Reducing the time step to 0.003 ps had no effect on the equilibrated structure and properties of the melt. A relaxation constant of 0.1 for the relaxation heat variable bath was applied throughout the simulations. The Dreiding II force field potential was employed. The geometric and energetic parameters were as described by Mayo et. al (1990). Nonbonded interactions were modeled using a Lennard-Jones potential with a cutoff distance of $10\,\mathring{A}$. Standard tail corrections were applied.

The time evolution of conformation of the chain was simulated for 20 ns. Equilibration was monitored by observing the change in total, torsion and van der Waal's energies and total pressure of the system with simulation time. Figure 1.a shows the change in energy of the 20 branches/1000C systems with simulation time at 450K. The energy of the system initially decreased because the simulations were started from a high energy configuration resulting from arranging the chains in the periodic boundary box. The energy fluctuated about a constant value after 2 ns. The pressure followed a similar trend. The equilibrium pressure was close to zero for all simulations conducted at experimental densities.

3.2 Experiment

3.2.1 Materials and Sample Preparation

Three commercial available m-LLDPE resins and one ZN-LLDPE resins were blended with linear HDPE. All resins were supplied from Exxon Mobil except the ZN-LLDPE, which was obtained from professor Michael C. Williams laboratory in Edmonton, Alberta. Characterization of polymers used is given in Table 3.2. The densities, M_w, polydispersity indices (PDI) and melt flow indices (MI) of polymers are those quoted by Exxon Mobil. The branch contents of LLDPEs were measured by ^{13}C NMR spectroscopy. Here, resins were labeled the polymers by M_w and comonomer type, for instance m-LLDPE copolymer of (M_w =73*10^3, BC=18.76) octene comonomer would be labeled m-EO1, similarly m-EO2 denote (m-LLDPE, M_w=95*10^3, BC= 32.67) and m-EO3 denote (m-LLDPE, M_w=90*10^3, BC=16.32). Blends of m-EO1and m-EO3, were chosen to study the effect of molecular weight; blends of m-EO2 and m-EO3 for the effect of the branch content. As seen from the Table3.2, these resins were paired to study one molecular variable at a time. For example, m-EO1 and m-EO2 had similar branch content and MWD; however, M_w, is the primary factor. Also, m-EO2 and m-EO3 had similar M_w and MWD, with the branch content as the major difference between the two resins.

All samples were melt blended with HDPE in proportion to the weight ratio (m-EOs/HDPE): 0/100, 10/90, 30/70, 50/50, 70/30, 90/10, and 100/0. For instance a 0/100 is one containing pure HDPE and a 10/90 blend is one containing 10% m-EOs with 90% HDPE and so forth.

Melt blending was carried out in a Haake PolyDrive melt blender. The polymers were blended at 190°C for 10 min at 50 rpm. The mixtures of the polymers were stabilized by addition of 1000 ppm of a 50/50 mixture of Irganox 1010 [phenol B, tetrakis (methylene 3-(3,5-di-t-butylphenol) propionate) methane, M_w =1178, the primary antioxidant] and the phosphorous-containing compounds Irgafos 168 [P-1, tris (2,4-di-t-butylphenol) phosphite, M_w =646, the secondary antioxidant], to prevent the thermo-oxidative degradation process (Bair, 1997). Both antioxidants are made by Ciba specialty Chemicals.

The conditioned (blended) samples were then removed from the mixing bowl, and air-cooled and then small samples were prepared. The specimens were compression molded using a Carver press as follows: The polymers were sandwiched between Mylar sheets, heated at 170°C (338°F) for 4 min under minimal pressure, then 4 min at 3 metric tons, and for 4 min at 7 metric tons.

The disc was then water-cooled for 10 min. The 25mm and 2mm thickness discs were then removed and inserted between the rheometer platens for rheological characterization.

Table 3.2

Characteristic of the materials used in this work

Sample	M_w, kg/mol	M_w/M_n	MI, g/10min	Density, g/cm^3	BC, CH_3/1000C
ZN-EO	105	6.1	1.02	0.9021	35
m-EO1	74	2.1	3.0	0.902	18.67
m-EO2	95	1.99	1.10	0.8820	32.67
m-EO3	90	2.04	1.10	0.9020	16.32
HDPE	101	6.71	0.7	0.9610	0

3.2.2 Rheological Measurements

Advance Rheometeric Expansion system (ARES) with cone-and-plate geometry (25mm diameter, 0.1radians cone angle and 0.048 mm gap) was used to measure the rheological properties. ARES equipped with sensitive force rebalance transducer (normal force range 2-2000 g, and torque range 2-2000 g-cm) was used in the low-and high frequency ranges. For all samples, the measurements were performed at 15% strain, which was within the linear viscoelastic region, at temperature 190°C, with continuous liquid nitrogen purging of environmental chamber to avoid thermal degradation. It should be noted that during the measurements the maximum temperature difference as read by thermocouple, did not exceed (±0.01). The circular discs samples were placed between the cone-and-plate geometry in an oven at 190°C and allowed a 3 min temperature equilibration period. The gap between the plates was subsequently reduced to 0.048 mm, and melt extruded beyond the platen rim was removed by a razor blade, then the oven allowed to reaches test temperature of 190°C.

The following rheological measurements were carried out: 1) Oscillatory shearing flow properties where dynamic viscosity (η'), storage modulus (G'), and loss modulus (G''), were measured for all pure component and blends as function of frequency (range $\omega=10^{-2}$ to 10^{2} rad/sec). 2) Steady shear flow properties, where, viscosity (η), shear stress (τ_{12}), and the first normal stress difference (N_1), were measured at 190°C as function of shear rate ($\dot{\gamma}$) between 10^{-2} to 5 s^{-1}. Delay before measurement of 200s and measurement time

of 30s were used. 3) Transient flow properties where, N_1 (t) was measured at 190°C, shear rate 1.0 s^{-1}, zone time 200s, points per zone 100s, and relaxation time 100s.

3.2.3 Polyethylene Characterization

Nuclear magnetic resonance spectroscopy (^{13}C NMR) spectroscopy was used Hansen (1997) to evaluate the amount of branches for the three of the m-LLDPE samples. Polymer sample (0.255g) was taken in 10 mm NMR-tube, and 1mL of 1,2,4-trichlorobenzene was added. The NMR-tube was thereafter placed in an oil bath at 150°C for 2h, allowing the polymer to dissolve in the solvent. Then 0.005g of Fe (acac)$_3$ was added as nuclear spin relaxation agent. Then a few drops of deuterated benzene was added before being run at 130°C on ^{13}C NMR spectrometer operating at 500 MHZ carbon resonance frequency. The summary of ^{13}C NMR results is given in Table 3.2. The short chain branch frequency was calculated from relative areas of the CH_2 peaks at (β carbon resonance, ω=27.38), (backbone carbon resonance =30.1), (γ carbon resonance, ω=30.61) and (α carbon resonance, ω=35.25) ppm, the CH peak at branch point (ω=38.4), and that of the 3B6 carbon at 32.30 ppm, yielding a measure of short chain branches per 1000 backbone carbons (Hansen et al., 1997 and Karbashewski et al., 1992). The NMR spectrum of PE samples at 130°C are displayed in Appendix (A.1, A.2, and A.3)

The number-average (M_n) and M_w as well as PD were obtained by a gel permeation chromatography (GPC). GPC data was collected using 1,2,4 trichlorobenzene as solvent at 150°C in a WATERS GPC2000 instrument. Polystyrene standards were used for calibration.

CHAPTER 4

Results and Discussion

4.1 MD Simulation Results and Discussion

Figures 1a-d shows the final conformation of the blends after 8-10 ns of simulation. It can be seen in Figure 1a, b and c that the HDPE and LLDPE containing 10, 20 and 30 branches/1000C are compatible and are well mixed in the simulation box. The HDPE chains are shown in purple which the LLDPE are shown in gray and the branches are red in color. Increasing the branch content to 40 causes the two polymers to phase separate as shown in Figure 1-d. The phase separation becomes more evident at a branch content of 60/1000C when chains occupy distinct domains in the simulation box. The snapshots shown are representative of the structure of the melt and the systems with 40 and 60 branches/1000C remain phase segregated after the initial equilibration period. The level of segregation increased as the branch content increases from 40 to 60/1000C. For example, some overlap is observed between the two polymers in the case of 40/1000C while the polymers occupy totally distinct domains in the 60/1000C case. This is a direct demonstration of the influence of branch content on miscibility of linear and branch PE'S.

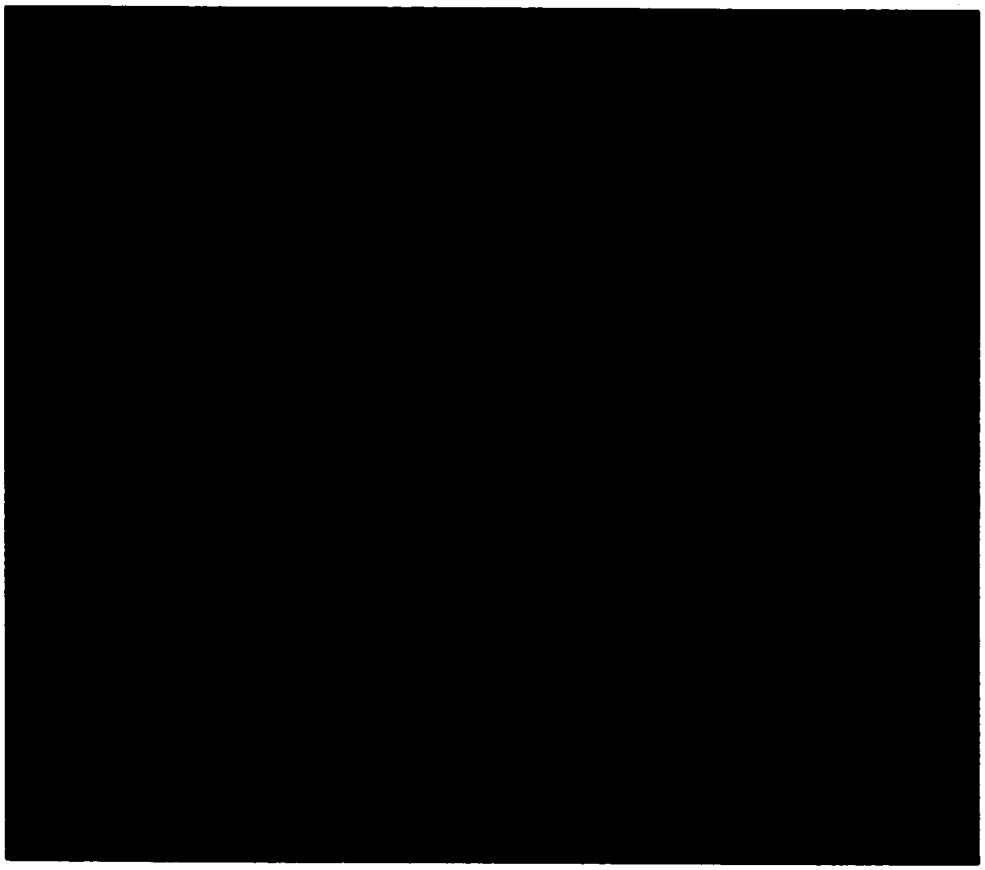

Figure 4.1 a: Configuration of the blend of HDPE with m-LLDPE containing 10 branches/1000 C.

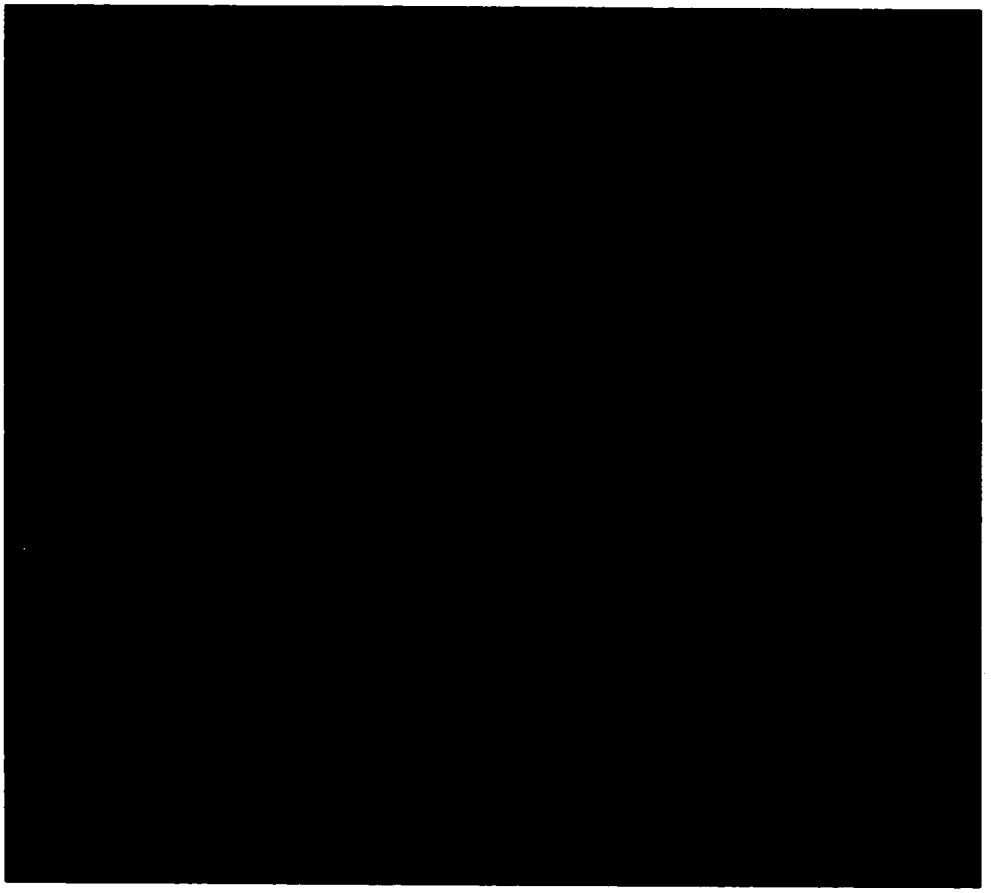

Figure 4.1 b: Configuration of the blend of HDPE with m-LLDPE containing 20 branches/1000 C.

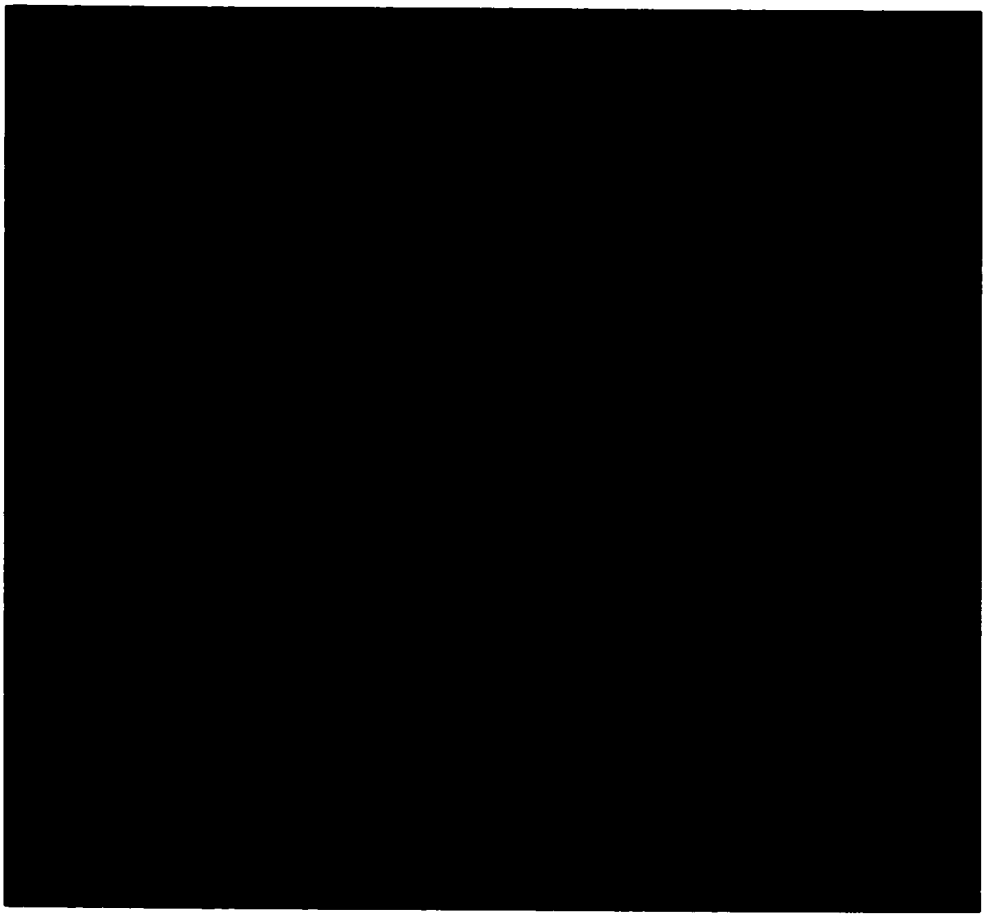

Figure 4.1 c: Configuration of the blend of HDPE with m-LLDPE containing 30 branches/1000 C.

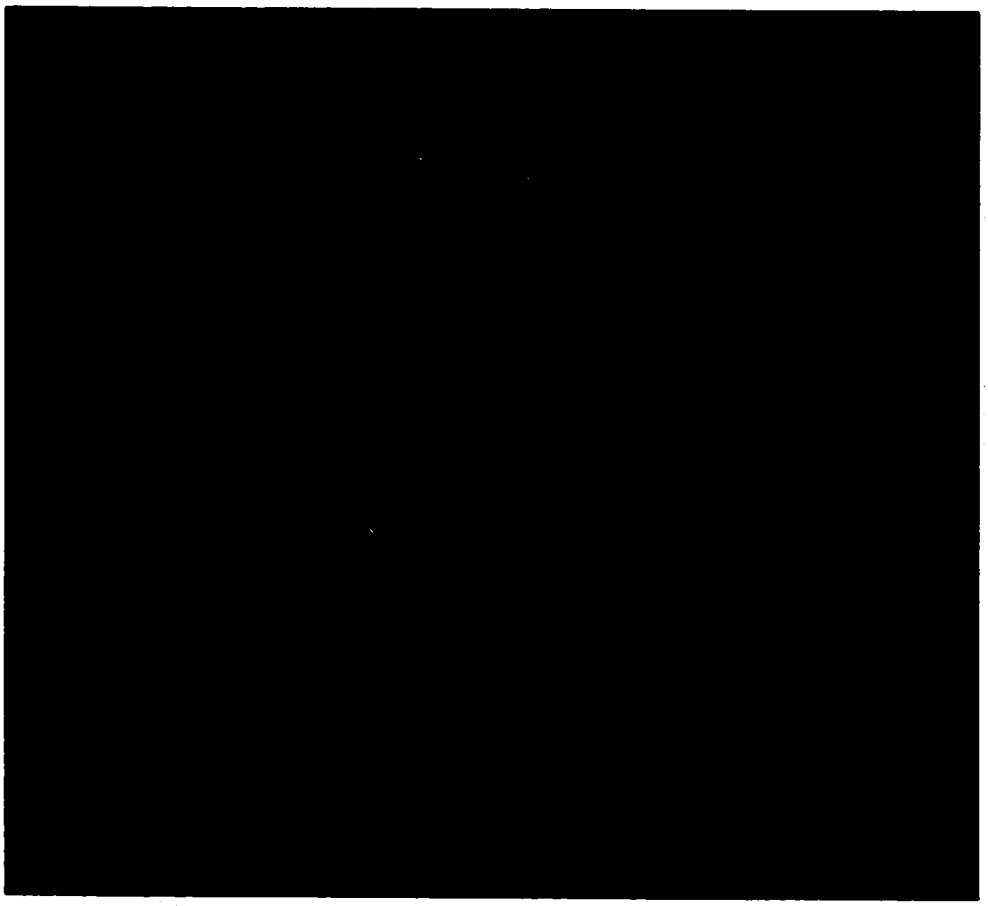

Figure 4.1 d: Configuration of the blend of HDPE with m-LLDPE containing 40 branches/1000 C.

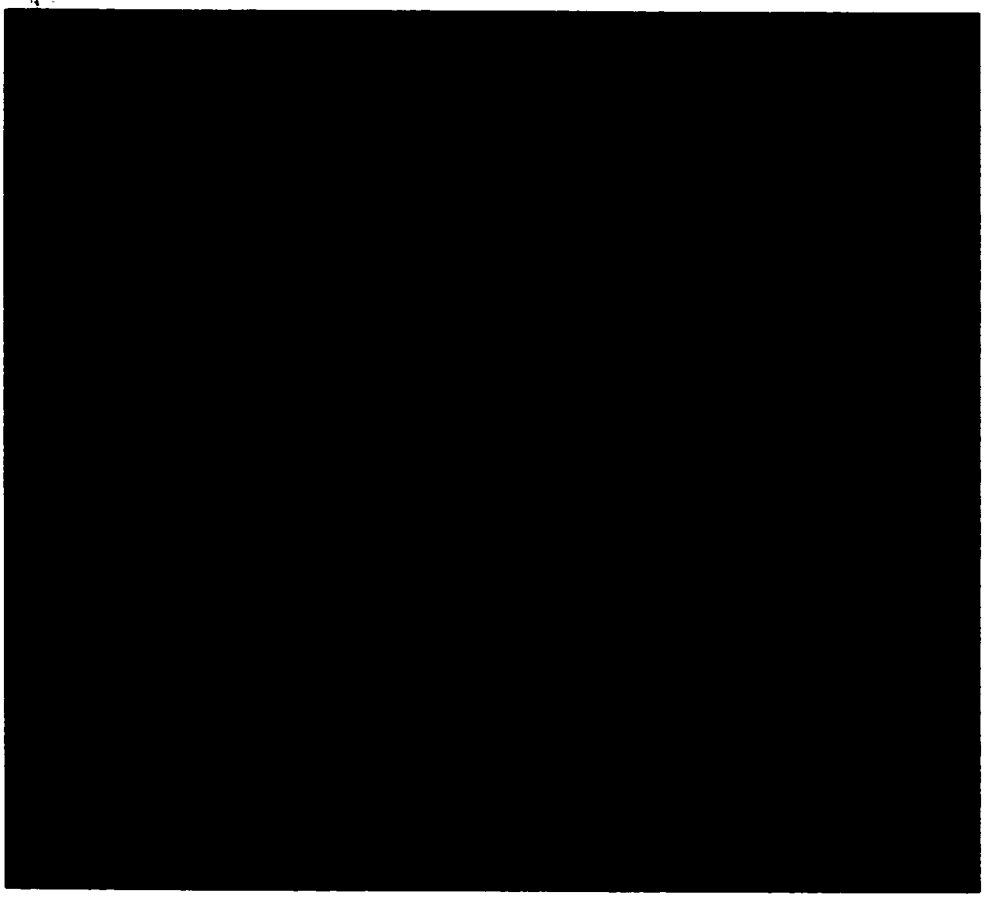

Figure 4.1 e: Configuration of the blend of HDPE with m-LLDPE containing 60 branches/1000 C.

In order to investigate the structure of the blend, we determined the like CH_2-CH_2 radial distribution function (RDF) for the different blends. A comparison of the Nonbonded RDF of the CH_2 segments in the LLDPE is shown in Figure 4.2. It can be observed that the self-correlation increases with increasing branch content from 20 to 60. The level of correlation at long distances (beyond 6 A°) is minimum for the 20, and 30. However, it is higher at 30 and is maximum at 40 branches/1000C. This increase in self-correlation indicates increased phase segregation with increased branch content. For the miscible systems, the RDF is almost exactly the same. However, differentiation is observed for the nonmiscible systems. A similar trend is observed in Figure 4.3 which shows the Nonbonded RDF for the HDPE CH_2 segments.

It is also observed that the two chain types assume different conformations in the melt in the immiscible systems. Figure 4.4 shows a comparison of the order parameters (Eq.4.1) for the HDPE and the 30 branches/1000C chains within the same system. The order parameter is a quantity that gives indication of the structural source of incompatibility of the two polymers. The order parameter, S(r), is defined by:

$$S(r) = \frac{3\langle \cos^2 \theta \rangle - 1}{2} \tag{4.1}$$

It can be observed that at low branch content the HDPE and m-LLDPE chains have a similar level of order. However, as the branch content increases, different levels of order are observed between the two polymers as shown in Figure 4.5 in which the level of

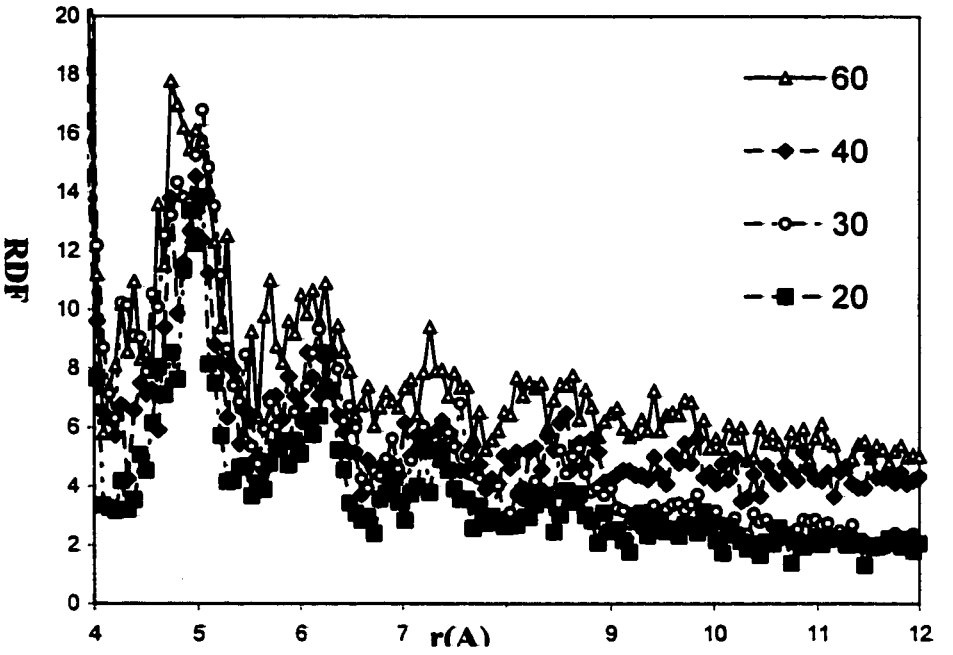

Figure 2. Like Nonbonded RDF of LLDPE CH_2 with LLDPE CH_2

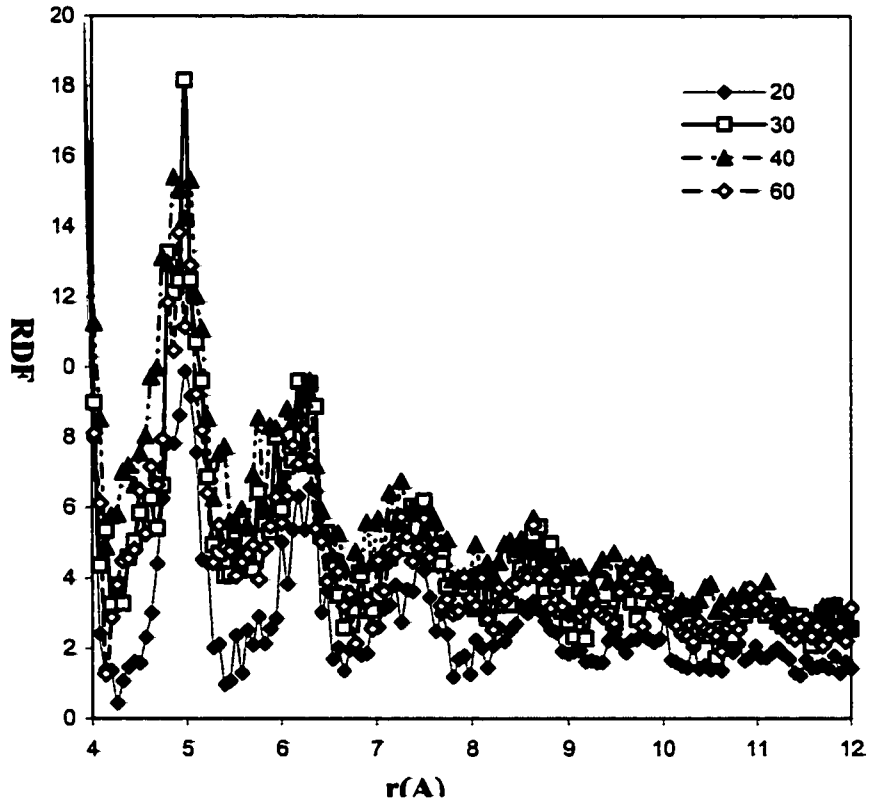

Figure 4.3 Like nonbonded RDF of HDPE CH_2-HDPE CH_2

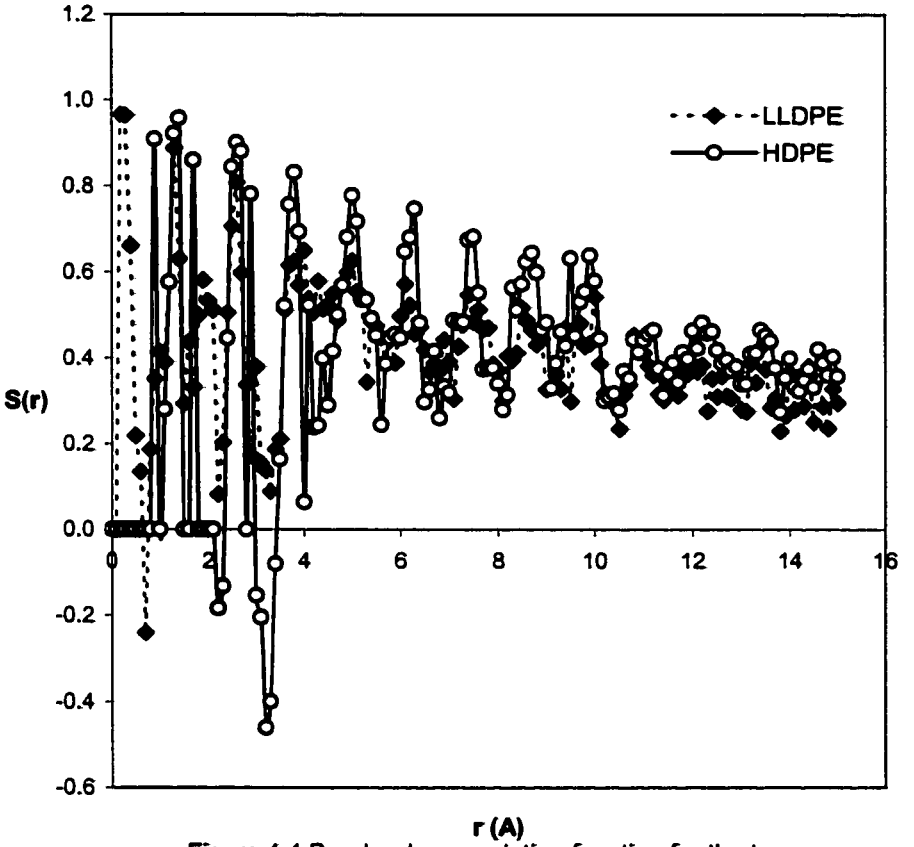

Figure 4.4 Bond order correlation function for the two components of the blend (LLDPE with 30 branches/1000C)

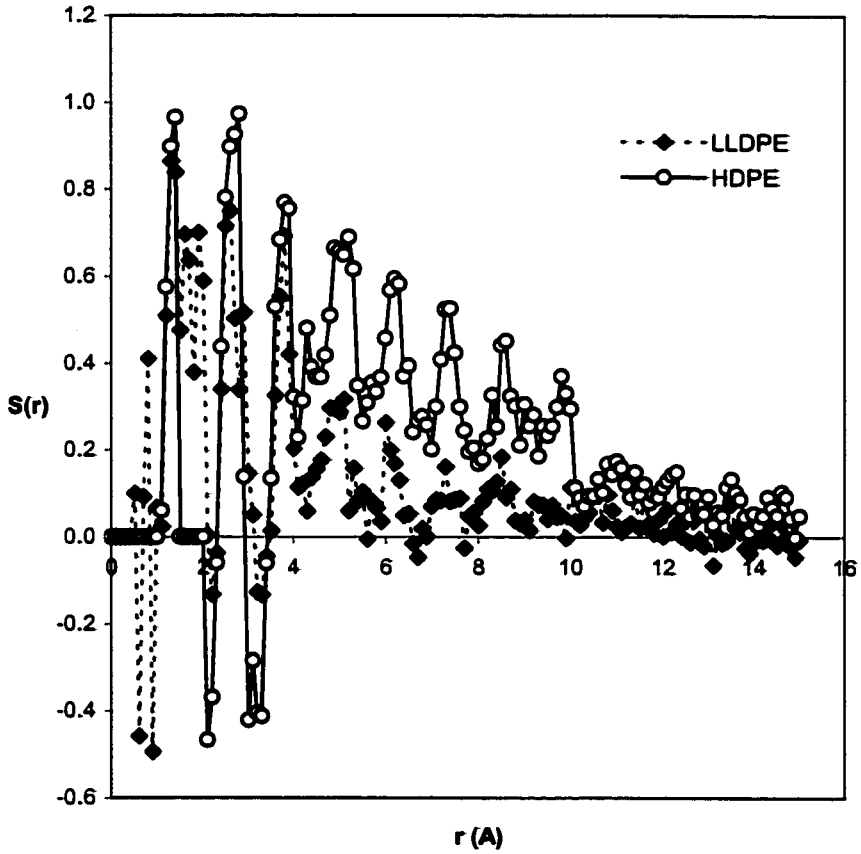

Figure 4.5 Bond order correlation function for the two components of the blend (LLDPE with 60 branches/1000C)

in the HDPE is higher than that of the LLDPE. These results suggest that the origin of the observed segregation in these simulations is the difference in the local structures of the two polymers in the blend at high branch content. In particular, the HDPE and the LLDPE with low branch content is capable of forming locally ordered structures in the fluid state in which a lower energy state is formed when CH_2 segments belonging to the same chain are neighbours to each other. The phase behavior of polymer mixtures has been traditionally described by extensions of the Flory-Huggins theory. In these extensions, the interaction parameter (χ) has been generally decomposed by many researchers into two components that correspond to the enthalpic contribution and entropic contribution to the excess Gibbs energy of mixing. This work shows that the local structures of the polymers should be considered when describing the excess Gibbs energy of the blend. It also shows that the local structure of the polymers in the blend may be one of the causes of the experimentally observed of demixing of different polyethylenes in the melt state. The observed lamellar morphology of the blend in the melt explains rheological observations which suggest that interlayer slip takes place during low shear investigation of HDPE/m-LLDPE blends.

Conclusion

This study shows that blends of HDPE and LLDPE are miscible up to a branch content of 30 branches/1000C. At a branch content of 40/1000C phase separation is observed and is found increase with increasing branch content to 60/1000C. The level of

separation was characterized by the radial distribution function and order parameter. The conformation of the different chains was found to be different as branch content increased. The MD simulation results were supported by experiments that shoed NDB rheology.

CHAPTER 5

Results and Discussion: Rheology

The effects of the molecular weight, branch content and composition distribution on the miscibility of LLDPE blends with HDPE were studied by rheological tools. Three m-LLDPEs and one ZN-LLDPE were blended with the same linear HDPE. The resins were chosen to have similar molecular characteristics with the exception of the parameter under investigation. Dynamic, steady-shear and transient flow measurements were performed using ARES rheometer. The different rheological data were analyzed in different ways:

The rheological functions, η' (or G'') and η''(or G') as functions of composition, ϕ, and frequency, ω; the first normal stress difference, N_1 ($\dot{\gamma}$), and N_1 (t) were obtained. The dynamic shear data of $\eta'(\omega)$ and $G'(\omega)$ were analyzed. Low-ω data were used in interpretations of blend miscibility as suggested by different researchers (Scholz et al., 1983; Hameed and Hussein, 2002). Plots of $\eta'(\phi)$ and $G'(\phi)$ were extracted from the $\eta'(\omega)$ and $G'(\omega)$ data. In the steady shear measurement, N_1 ($\dot{\gamma}$) and ϕ were analyzed.

For miscible blends addition of small amount of a more viscous component to a less viscous component leads to a proportional increase in viscosity. However, for a master immiscible blends positive deviation behavior (PDB); negative deviation behavior

(NDB) or positive-negative deviation behavior (PNDB) are obtained (Utracki, 1989). First, Cole-Cole (CC) plots were used in the analysis of polymer-polymer miscibility. These plots are widely used in the polymer blends literature (Scholz et al. 1989); Han and Kim, 1993; Nakajima and Harrell 1987; Chuang and Han 1984). The CC plot is a linear plot of η' vs. η'' or G' vs. G'' that corresponds to the linear addtivity rule of property-composition curve. However, the modified Cole-Cole (mCC) is a log-log plot similar to log-addtivity rule. The log-log plot of G' vs. G'' was reported by Chuang and Han (1984) and Munoz-Escalona et al. (1997) to be independent of composition for miscible blends, generating a master curve. The lack of superposition suggests immiscibility of blends as discuss by Chaung and Han (1984).

For polymers, it has been suggested that the Cole-Cole representation of the imaginary part (η'') of the complex viscosity versus its real part (η') shows certain important differences for homogeneous systems as compared to heterogeneous systems (Utracki and Kamal, 1982). According to this proposal for homogeneous systems, a unique circular arc is given which passes through the origin whereas for a heterogeneous system a series of interpenetrating arcs are given.

Also, the experimental data were fitted to rheological models like Carreau model or the Cross model. In this study, ARES software was used to fit the data to the Cross model,

Figure 5.1a Comparison of the rheology of as-received and conditioned m-EO2

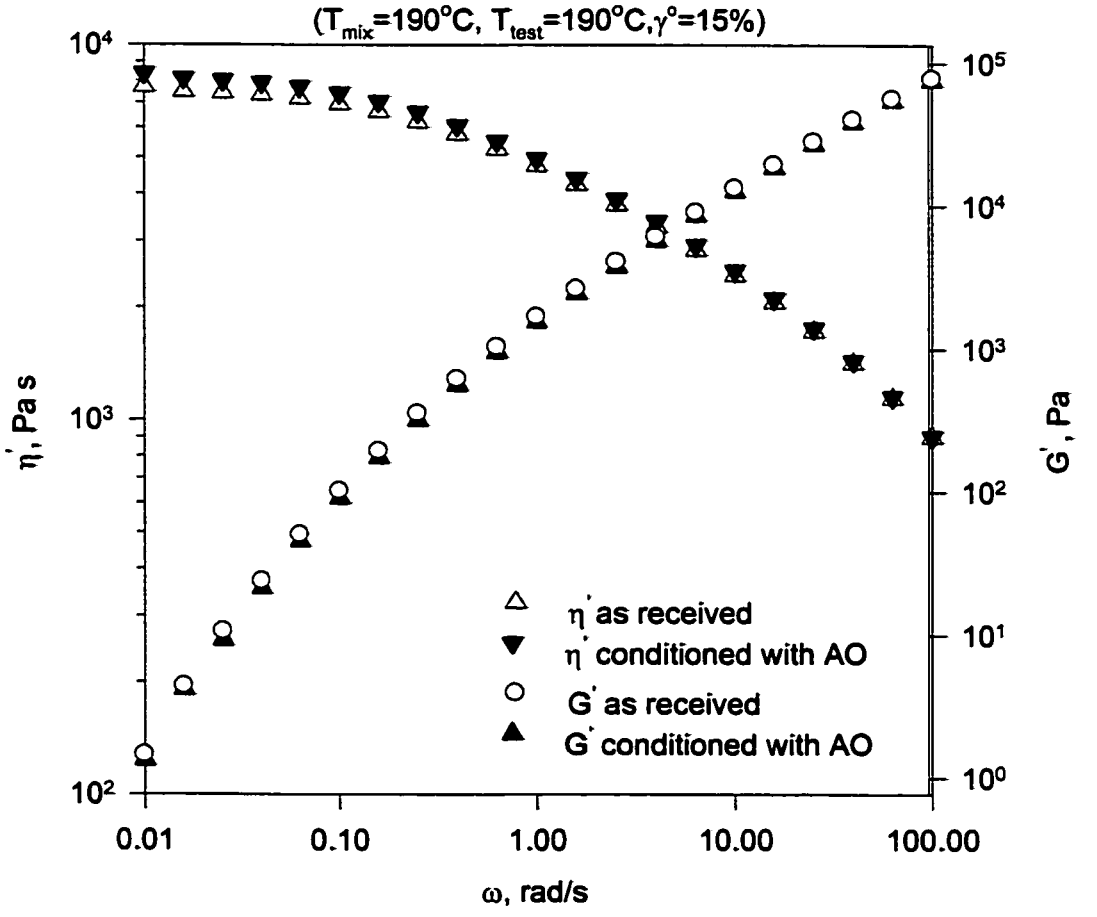

of reproducibility test are shown in Figure 5.1b. The excellent agreement between the $\eta'(\omega)$ and $G'(\omega)$ for samples prepared from different batches suggests the reproducibility of data. The dynamic, steady shear and transient measurements were conducted on the above-mentioned blends. The $\eta'(\omega)$ and $G'(\omega)$ data for blends of m-EO2 with HDPE and m-EO3 with HDPE and pure resins are displayed in Figures (5.2a &b) and in (Appendix, Figure B.1 & B.2), respectively. Figure 5.2a show that HDPE exhibits the highest viscosity and m-EO2 displays the lowest viscosity with a Newtonian limit that spans over a decade. The data given in Figure 5.2a for the high-BC pair show that the addition of up to 30% of HDPE (more viscous component) to m-EO2 did not influence the dynamic viscosity. Over the whole ω-range, $\eta'(\omega)$ for the 70% and 90% m-EO2 (LLDPE) blends with HDPE are almost the same as that of the pure m-EO2.

On the other hand, $\eta'(\omega)$ for blends of m-EO3 (low-BC) shows different behavior. The addition of the more viscous component (HDPE) to the less viscous component (m-EO2) resulted in a proportional increase in viscosity. The low-ω data is sensitive to morphological changes (Scholz et al. 1989) and will be used here for the assessment of miscibility. As shown in Figure 5.2b, high-ω data is not sensitive to the change in composition. The behavior of elastic component $G'(\omega)$ for m-EO2/HDPE and m-EO3/HDPE blends, are displayed in (Appendix, Figures B.1 & B.2). The overall behavior is similar to that of $\eta'(\omega)$ shown earlier in Figures 5.2a & b. At low-ω, $G'(\omega)$

Figure 5.2a $\eta'(\omega)$ for blends of m-EO2 with HDPE

(T_{mix}=190°C, T_{test}=190°C, γ^{o}=15%)

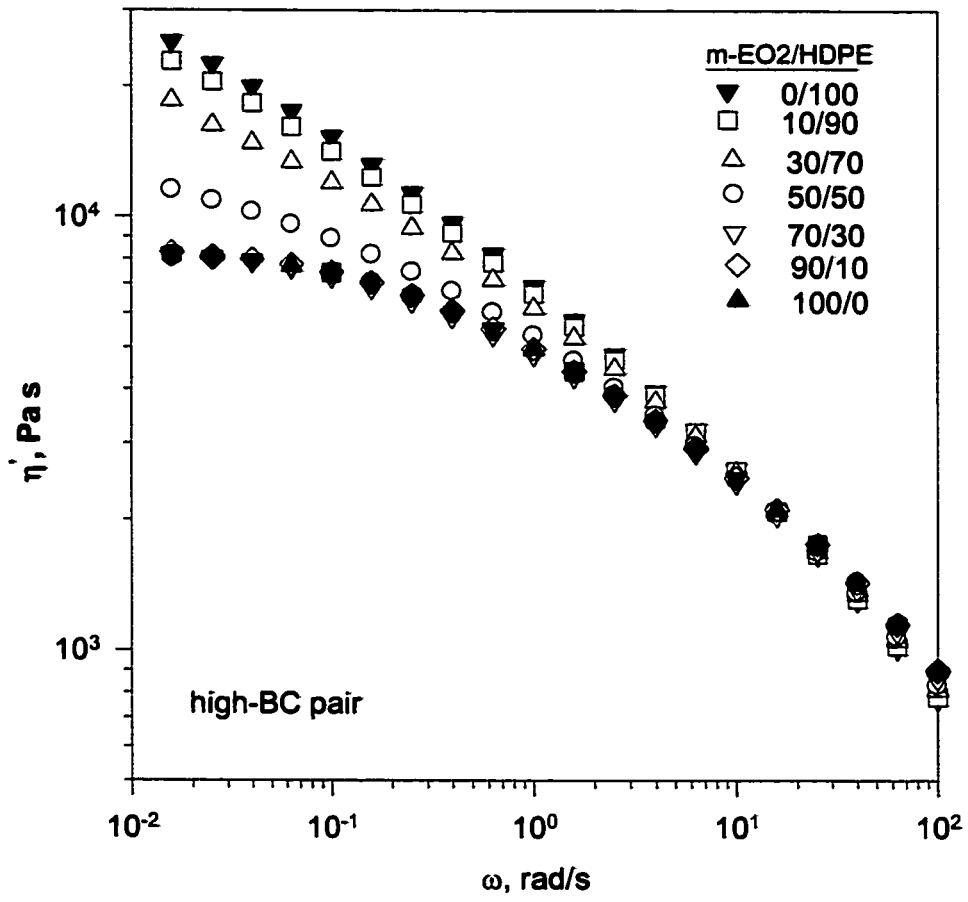

Figure 5.2b $\eta'(\omega)$ for blends of m-EO3 with HDPE
(T_{mix}=190°C, T_{test}=190°C, γ^{o}=15%)

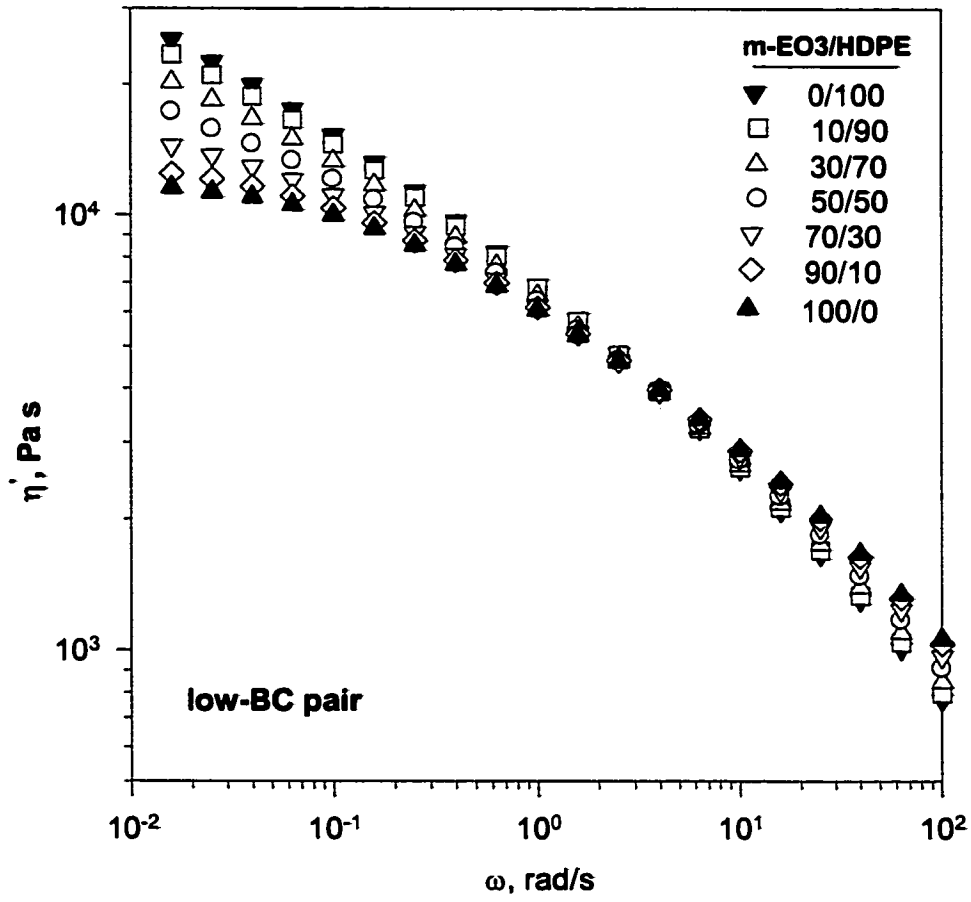

Figure 5.3a Cole-Cole plot for blends of m-EO2 with HDPE
(T_{mix}=190°C, T_{test}=190°C,γ°=15%)

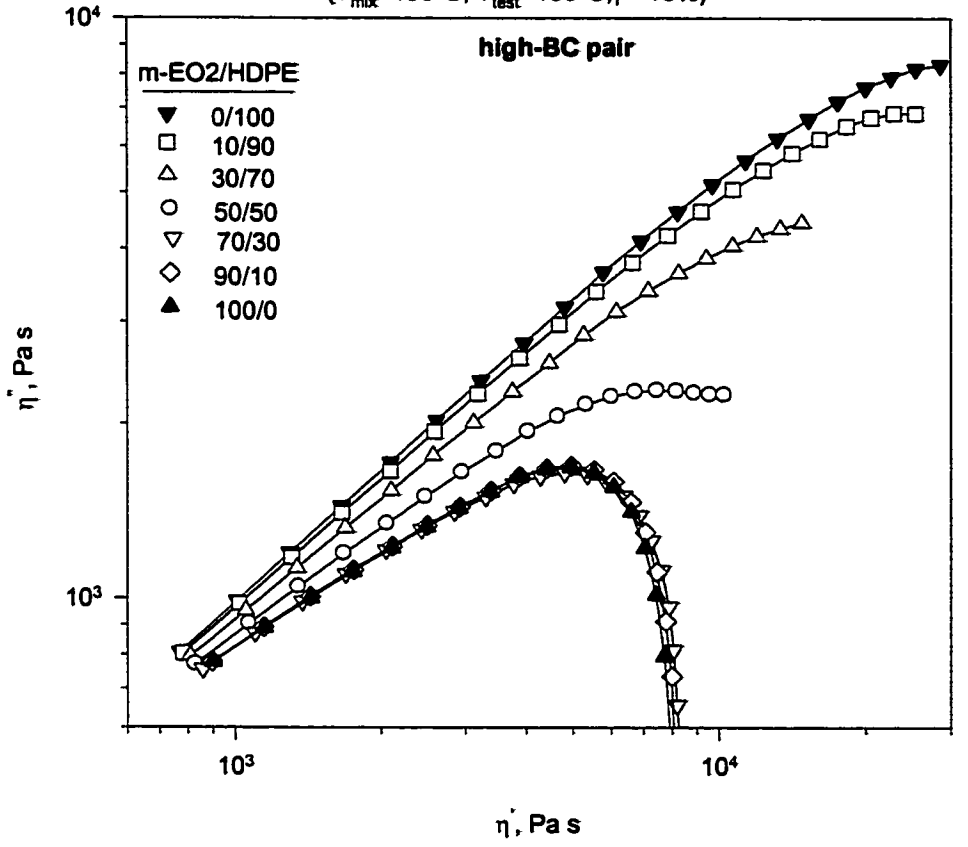

Figure 5.3b Cole-Cole plot for blends of m-EO3 with HDPE

(T_{mix}=190°C, T_{test}=190°C,γ^{o}=15%)

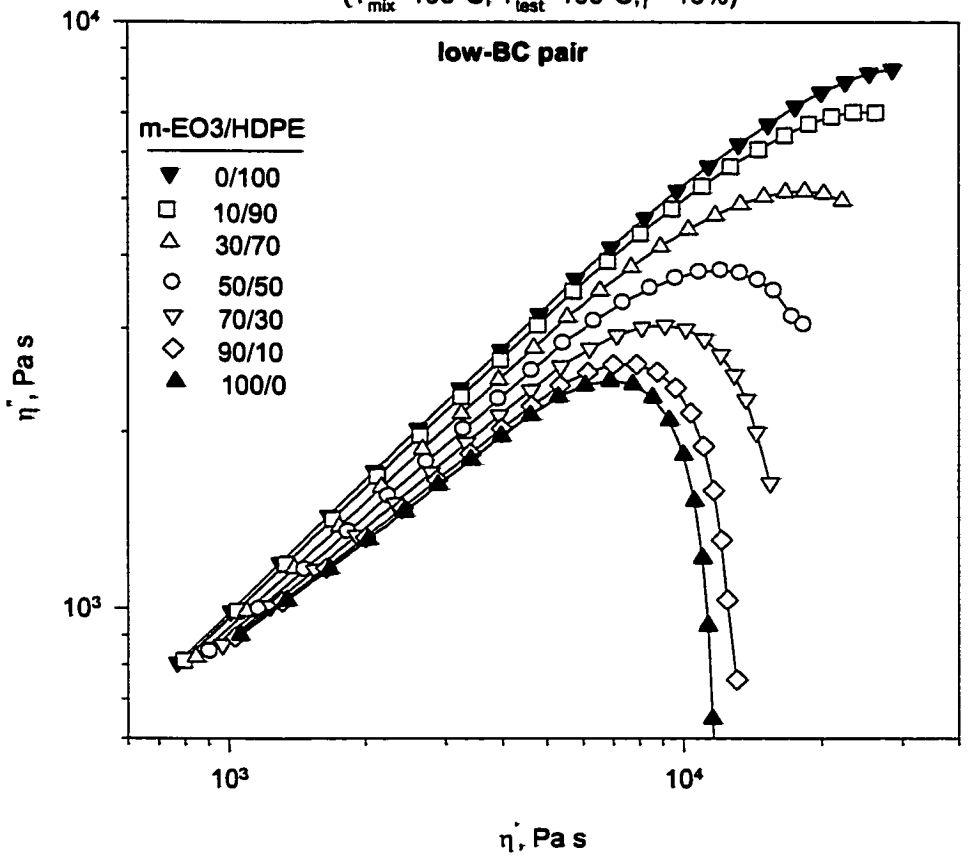

downward tailing was occurring. Thus, the large variances in slopes indicate poor miscibility, of m-EO2-rich blends (Rana et al. 2000). The third method of data analysis is a plot of the log η' vs. ϕ for all blends. Results are presented in Figures 5.4a and b. It can be seen that m-EO3/HDPE blends (low-BC) follows log-additivity rule, whereas m-EO2/HDPE (high-BC) indicated NDB from the log-additivity rule. Similarly, the plot of G' vs. ϕ shown in (Appendix, Figure B.3 & B.4), indicate the same trend as that of $\eta'(\phi)$ obtained in the low-ω range (sensitive to morphology). From the above three analysis, it can be reported that the m-EO3/HDPE (low-BC) is miscible in the whole composition range, while the m-EO2/HDPE (high-BC) is partially immiscible in the melt state. However, LLDPE-rich blends are suggested to be immiscible and HDPE-rich blends are miscible.

The fourth method of data treatment is the evaluation of η_o (ϕ) by fitting the η' (ω) data to Cross model using ARES Orchestrator software. Figure 5.5a (filled triangle) shows the plot $\eta_o(\phi)$ for m-EO2/HDPE blends. It is observed that η_o for m-EO2/HDPE blends exhibits a NDB from log-additivity rule; this unusual change will be discussed together with the result of the computed interlayer slip factor. On the other hand, blends of m-EO3 with HDPE (Figure 5.5b) followed log-additivity rule, suggesting miscibility of

Figure 5.4a $\eta'(\phi)$ for blends of m-EO2 with HDPE
(T_{mix}=190°C, T_{test}=190°C,γ^o =15%)

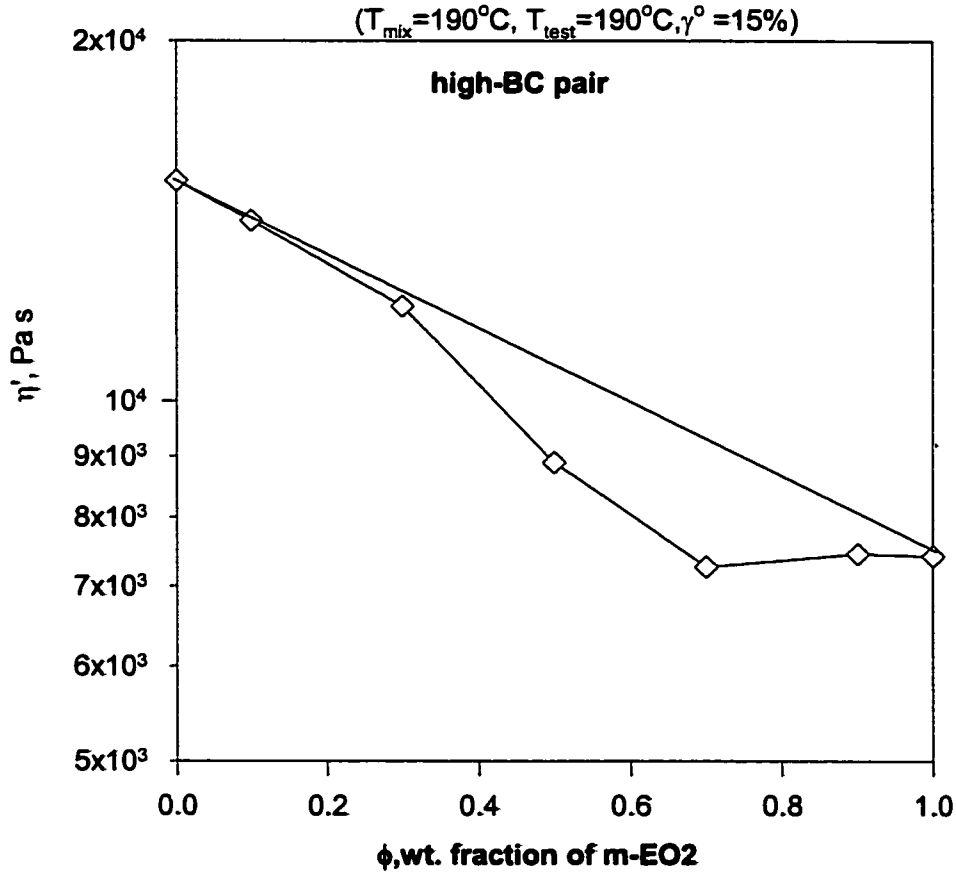

Figure 5.4b $\eta'(\phi)$ for blends of m-EO3 with HDPE
(T_{mix}=190°C, T_{test}=190°C, γ^{o}=15%)

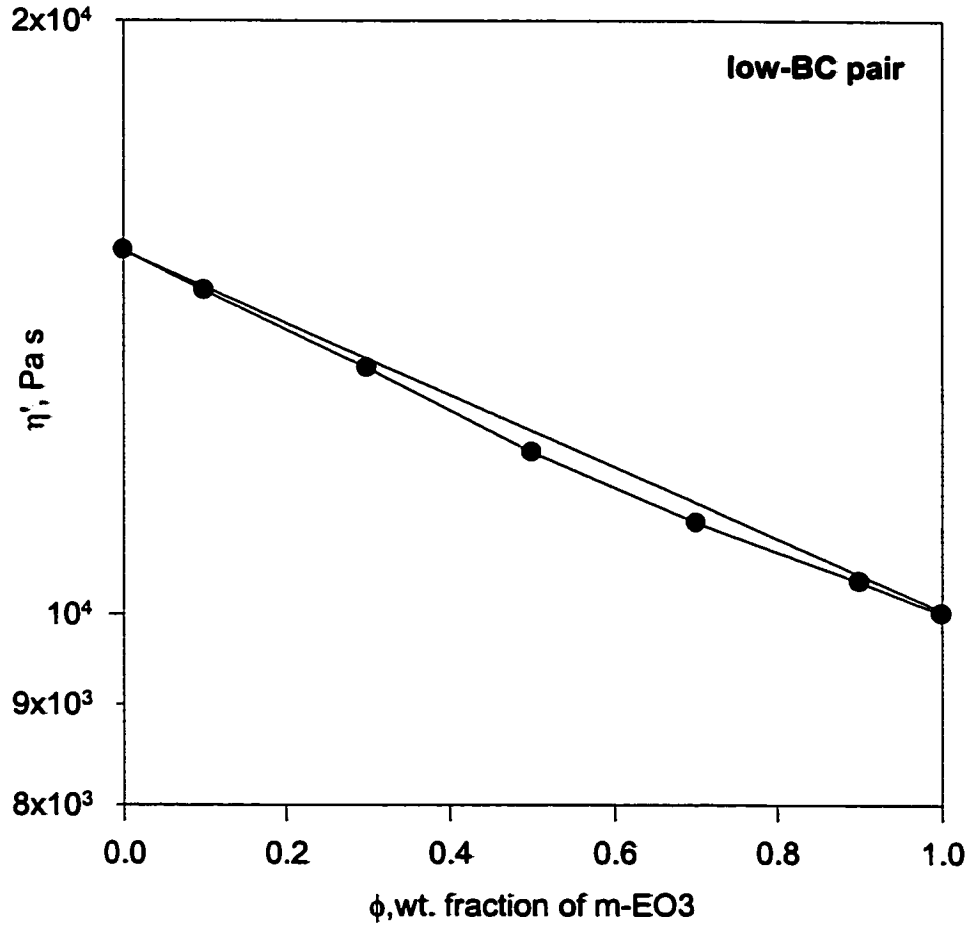

Figure 5.5a η_o (ϕ) for blends of m-EO2 with HDPE
Computed from BPU equation for NDB
(T_{mix}=190°C, T_{test}=190°C,γ^o =15%)

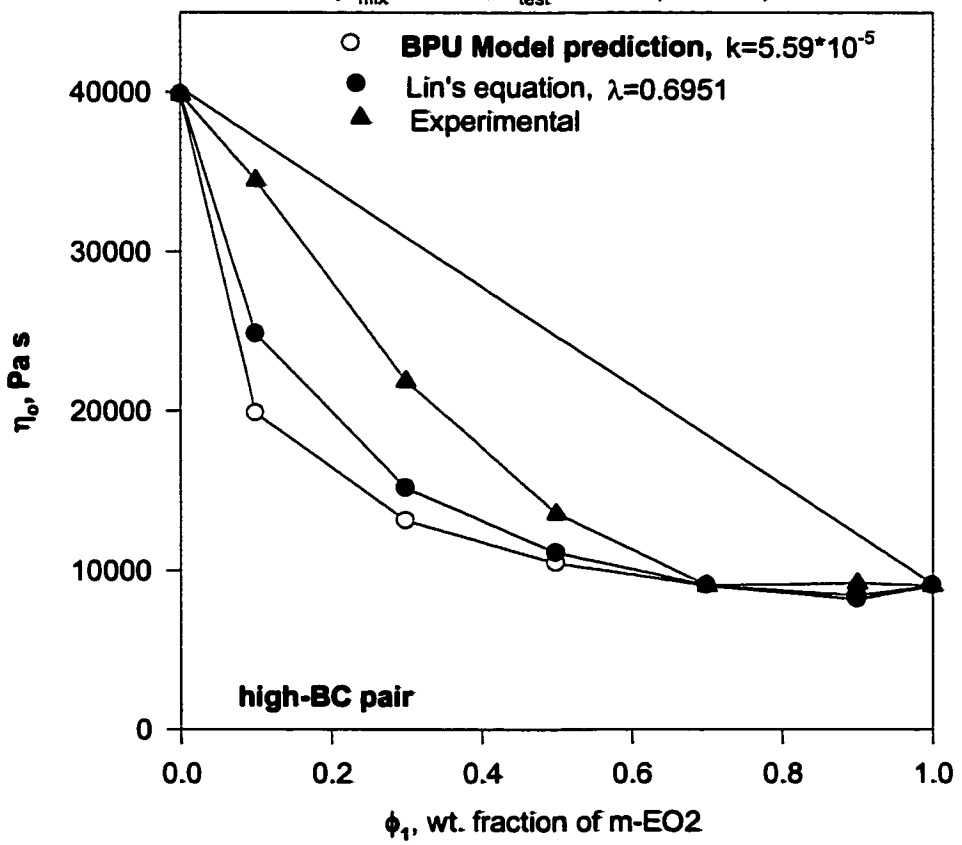

Figure 5.5b $\eta_o(\phi)$ for blends of m-EO3 with HDPE computed from Cross model

(T_{mix}=190°C, T_{test}=190°C, γ^o=15%)

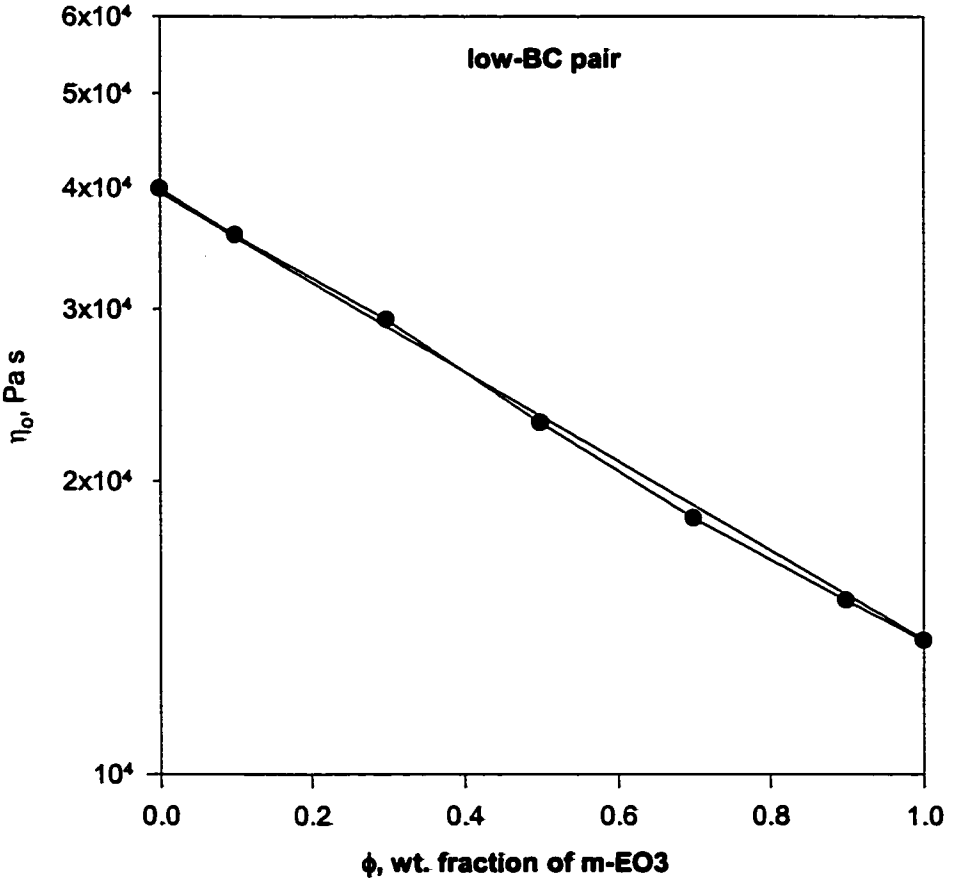

all ϕ. However, to determine the degree of immiscibility of EO2/HDPE blends, Bousmina-Palierne-Utracki (BPU, 1999), Lin's (1979) models that predict NDB rheology were used. Models predictions were shown as open and filled circles (Figure 5.5a). For LLDPE-rich blends experimental data are in agreement with model prediction, which suggest immiscibility of the LLDPE-rich blend. Also, interlayer slip is suggested to be reason for phase-separation. For HDPE-rich blends, model prediction and experimental data are in disagreement. This indicates improved miscibility in the HDPE-rich range. However, it can be observed that the plot of η_o (ϕ) was almost nonsymmetric for EO2/HDPE, while both models show symmetry. The values of interlayer slip factors were computed as $k=5.6*10^{-5}$ for BPU model and $\lambda=0.6951$ for Lin's model.

Furthermore, the steady shear measurements were carried out on all blends of m-EO2 and m-EO3 with HDPE following the earlier described procedure. Results of $N_1(\dot{\gamma})$ for the high-BC and low-BC blends obtained at 190°C are shown in Figures 5.6a and 5.6b, respectively. For the high-BC pair (Figure 5.6a), data show that HDPE exhibits the highest $N_1(\dot{\gamma})$ values. This is in agreement with previous G' data that suggested HDPE to be the more elastic blend component. In Figure 5.6a, experimental data show that the addition of 10% of the more viscous and elastic component (HDPE) has resulted in very little or no effect on $N_1(\dot{\gamma})$ of the less elastic component (m-EO2). Likewise, the

Figure 5.6b $N_1(\gamma)$ for blends of m-EO3 with HDPE
(T_{mix}=190°C, T_{test}=190°C)

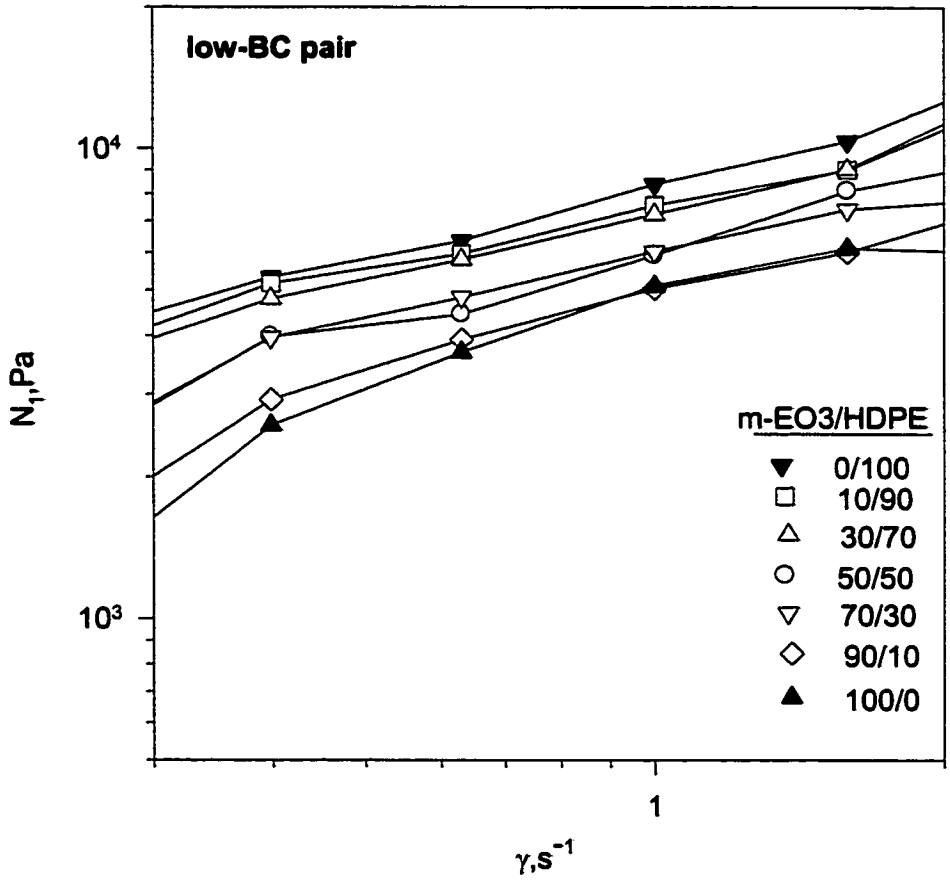

addition of 30% HDPE has even lead to $N_1(\dot{\gamma})$ that are lower than m-EO2 i.e. NDB. On the other side of HDPE-rich blends, the addition of 10% and 30% of m-EO2 to HDPE has resulted in a proportional decrease in the elasticity of HDPE. All of the above observations on $N_1(\dot{\gamma})$ for m-EO2 blends with HDPE suggest the immiscibility of this system with a possible interlayer slip as an explanation for the NDB. However, the low-BC blend of m-EO3 with the HDPE was more regular as shown in Figure 5.6b. $N_1(\dot{\gamma})$ data of pure resins and their blends increased in proportion to the increase in the more elastic component. This behavior is a clear indication of the miscibility of the low-BC blends of m-EO3 with HDPE in the whole composition range In addition to plots of $N_1(\dot{\gamma})$, plots of $N_1(\phi)$ at low $\dot{\gamma}$ ($\dot{\gamma}$=0.4) are extracted from Figures 5.6a and 5.6b. Results are displayed in (Appendix, Figures B.7 and B.8). The data for the high-BC pair showed NDB, while that for the low-BC have almost followed linear, additivity rule. The results support the previous findings from $N_1(\dot{\gamma})$ measurements.

Moreover, Cox-Merz (1958) rule was used. The rule proposes empirical relationship $\eta^*(\omega)$ and $\eta(\dot{\gamma})$ where $\eta(\dot{\gamma}) = \left|\eta^*(\omega)\right|_{\dot{\gamma}=\omega}$. This relationship holds for homogeneous polymer solutions and melts. However, Cox-Merz behavior has been used to identify the immiscibility of the binary blends. The similarity of dynamic and steady shear properties e.g., between $\eta(\dot{\gamma})$ and $\eta^*(\omega)$, must not be expected for immiscible blends (Utracki and

Schlund, 1987; Chuang and Han, 1984). However, while the lack of superposition of dynamic and steady shear viscosities does not indicate immiscibility, success of superposition cannot be taken as a proof of miscibility (Utracki and Schlund, 1987). Results of $\eta^*(\omega)$ and $\eta(\dot{\gamma})$ for blends of m-EO3 with HDPE (high-BC) and m-EO2 with HDPE (low-BC) are shown in Figures 5.7a & b, for the 10% and 90% blends. For the low-BC pair, the Cox-Merz rule is quite well verified over a wide range of shear rate suggesting the blend to be miscible (Figure 5.7a). On the other hand, the high-BC pair did not show the same agreement between $\eta^*(\omega)$ and $\eta(\dot{\gamma})$ as shown in Figure 5.7b. For the same shear range, the 10% m-EO2 blend with HDPE the disagreement is quite clear. However, for the 90% blend of m-EO2 with HDPE agreement of $\eta^*(\omega)$ and $\eta(\dot{\gamma})$ was obtained. This lack of supervision suggests the immiscibility of the high-BC pair and in the LLDPE-rich ranges supports the previous conclusions.

Furthermore, transient behavior of the blends was tested. All samples were sheared at 1.0 s^{-1} for 200 s and then relaxations were measured over a period of 10 s. Results of $N_1(t)$ obtained for the high-BC and the low-BC blends are given in Figures 5.8a & b, respectively. In Figure 5.8b the low-BC pair showed $N_1(t)$ data that are similar to the previous $N_1(\dot{\gamma})$ results (Figure 5.8b) and the $G'(\omega)$ data shown in (Appendix, Figure B.2). HDPE showed the highest $N_1(t)$, while m-EO3 was the least. For all other

Figure 5.7a Comparison of $\eta^*(\omega)$ and $\eta(\gamma)$ for beinds of m-EO3 with HDPE

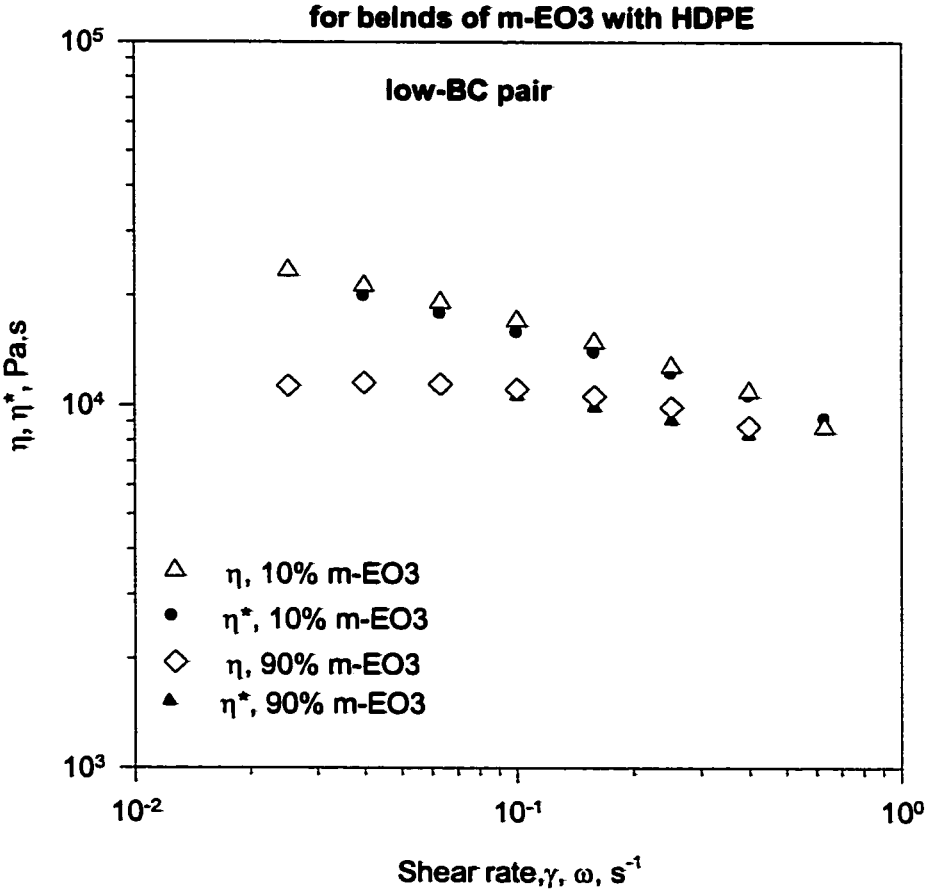

Figure 5.7b Comparison of $\eta^*(\omega)$ and $\eta(\gamma)$ for blends of m-EO2 with HDPE

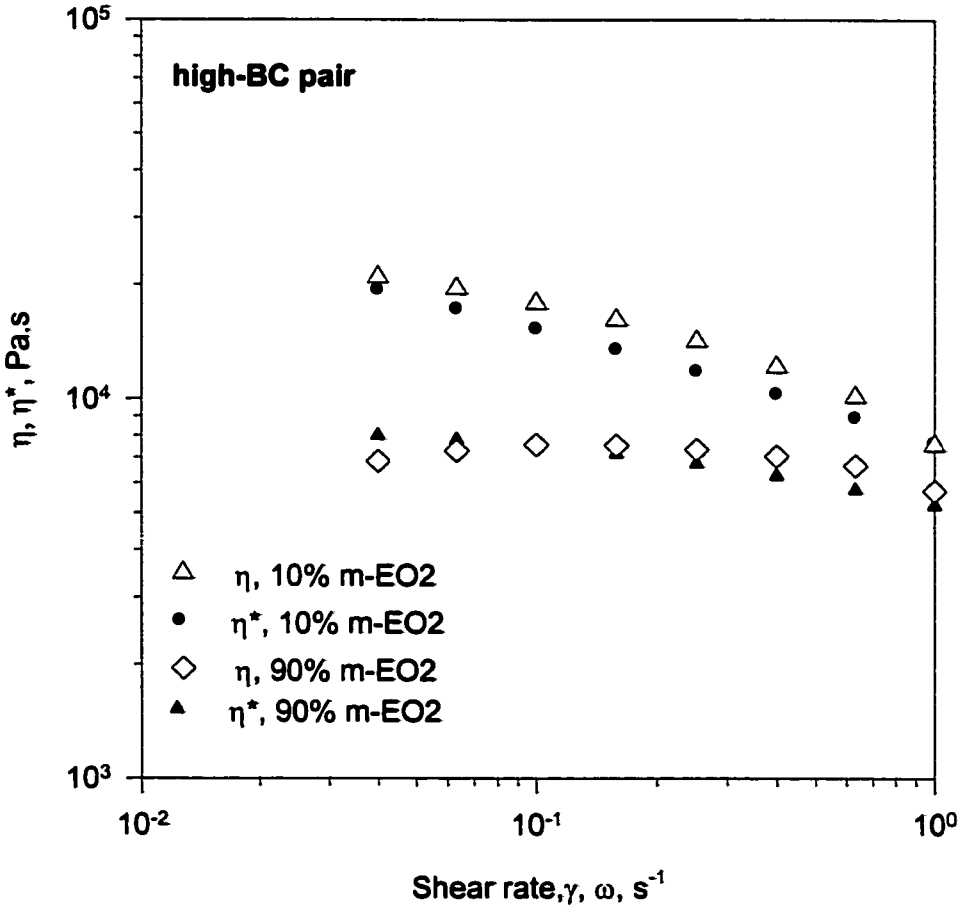

Figure 5.8b $N_1(t)$ for blends of m-EO3 with HDPE

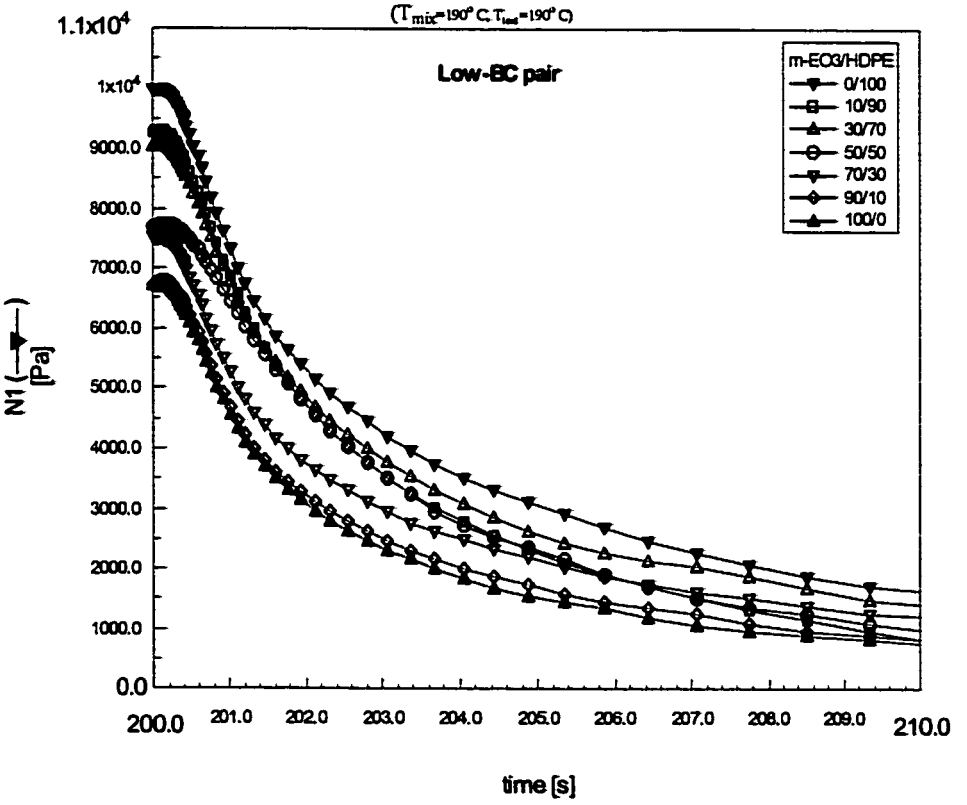

compositions, the values of N_1 (t) increased in proportion to the fraction of the more elastic component. This behavior suggests the miscibility of the low-BC pair. However, for the high-BC blends (Figure 5.8a) the behavior is different. The N_1 (t) data for the 70% and 90% blends of m-EO2 with HDPE were almost identical to N_1 (t) for pure m-EO2. This suggests that the addition of more elastic component (HDPE) did not influence the elasticity of the blend. This observation can only be explained by interlayer slip which was also observed and used to explain the $\eta'(\phi)$ and $G'(\phi)$ data for this pair. The different methods of presenting rheological data so far, suggest that blends rheology m-EO3 with HDPE results agrees well with log-additivity rule suggesting miscibility. On the other hand, different measurements and methods of data analysis on m-EO2 blends with HDPE showed NDB from the log-additivity rule suggesting the immiscibility of these blends especially in the range of m-EO2-rich blends. Since the two blends are similar in molecular structure except in the level of BC, hence we concluded that BC has a strong influence on miscibility of m-LLDPE blends with HDPE. High-BC is expected to lead to immiscibility of LLDPE-rich blends.

The previous MD simulations support this experimental observation. The blend studied in the MD simulation resembles the 50/50 blend of m-LLDPE/HDPE system investigated by rheological techniques. In both cases phases separation started to develop in m-LLDPE/HDPE blends when the level of BC exceeded 30 branches/1000 C.

Also, the MD simulation results shown in Figures (4.1a-e) predict that the morphology of m-LLDPE/HDPE blends is a layered morphology. This in fact supports the suggestion that the reason for the measured NDB behavior is likely the interlayer slip.

5.2 **Influence of M_w on Blend Miscibility**

The effect of M_w on the miscibility of octene-based m-LLDPE and HDPE blends was studied by comparing the rheology of m-EO1 and m-EO3 blends with HDPE. The $\eta'(\omega)$ and $G'(\omega)$ for the blends of m-EO1/HDPE and the pure resins are shown in Figures 5.16a & b and in (Appendix, Figures C.1 and C.2), respectively. Over the whole range of ω the viscosity of HDPE was higher than that of m-EO1 (low-M_w). Also, the viscosity and the elasticity of pure m-EO1 resin were the lowest (Figure 5.9a and Figure C.1). Both η' and G' of m-EO1 fractions lie between those of constituent components (pure m-EO1 and HDPE) and show high dependence on ω in the measured region. When ω was increased η' was found to decrease, while G' increased. Both material functions increased monotonically as the amount of HDPE in each blend was increased. HDPE was the more viscous and elastic blend component. Hence, for this blend the increase in η' and G' was proportional to the increase in the fraction of HDPE in the blend. At high-ω, the viscosity of all blends as well as pure components showed weak composition dependency. It should be mentioned that Liu et al. (2002) reported a

Figure 5.9a $\eta'(\omega)$ for m-EO1 blend with HDPE
(T_{mix}=190°C, T_{test}=190°C, γ^{o}=15%)

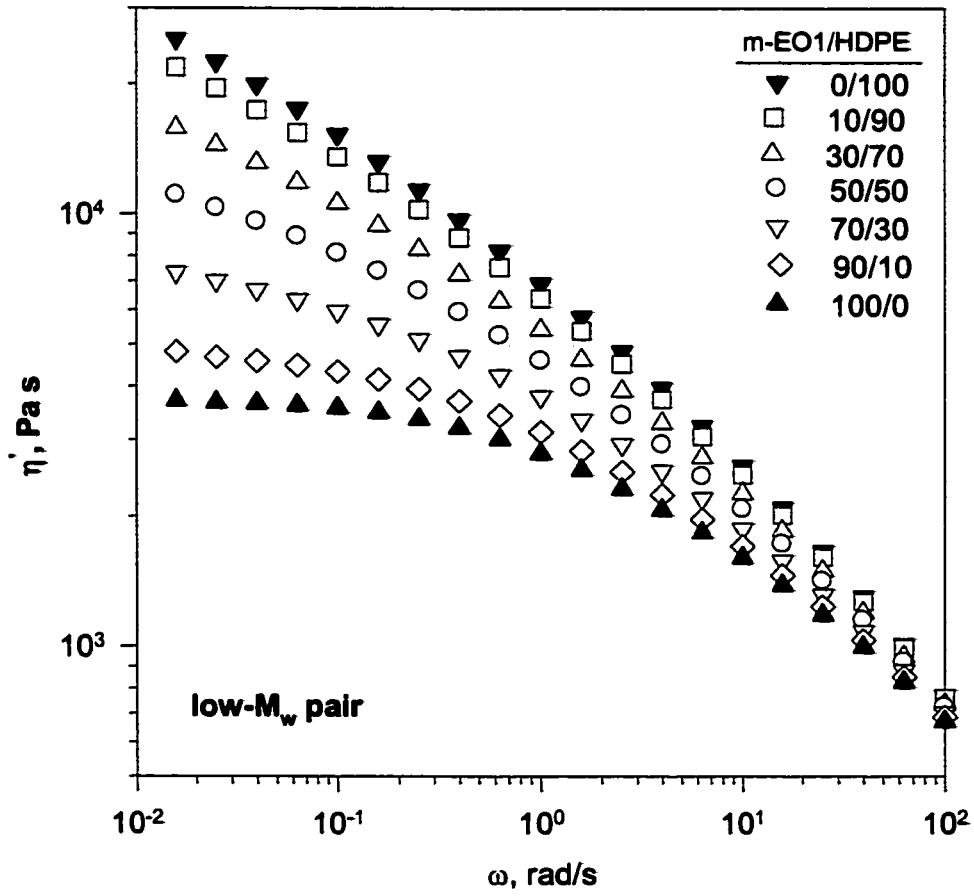

Figure 5.9b $\eta'(\omega)$ for blends of m-EO3 with HDPE
(T_{mix}=190°C, T_{test}=190°C, γ^{o}=15%)

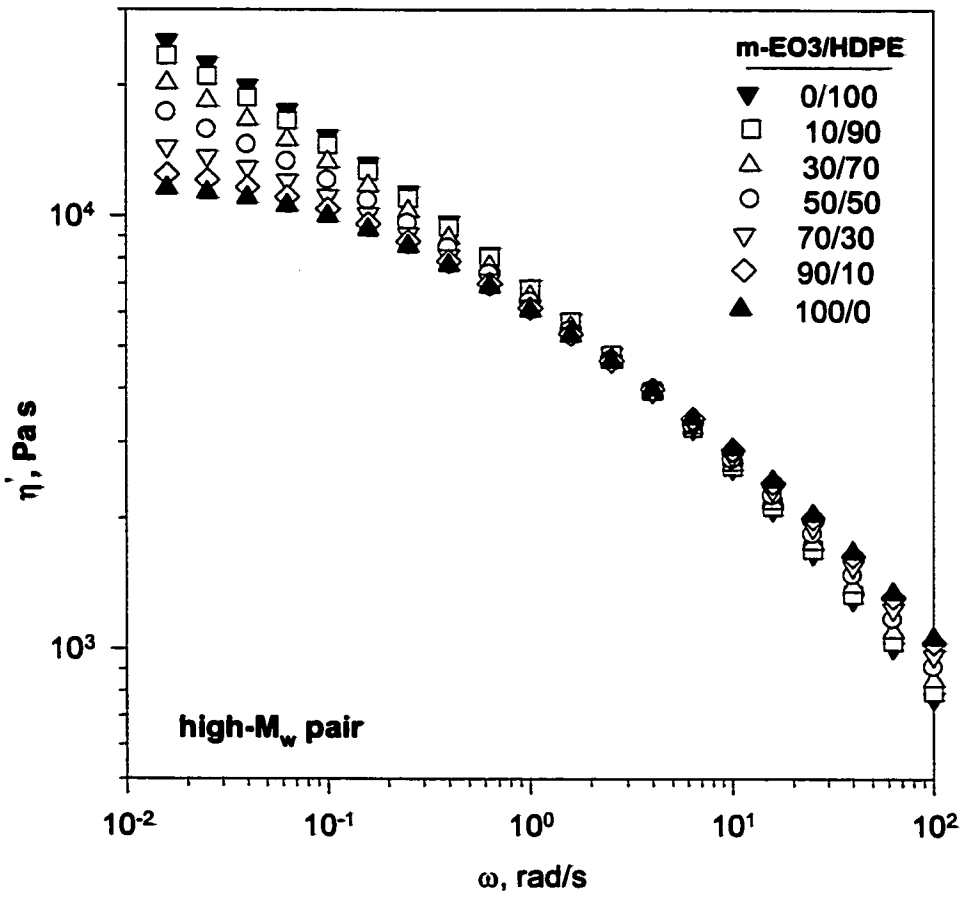

Figure 5.10 Cole-Cole plot m-EO1 blends with HDPE

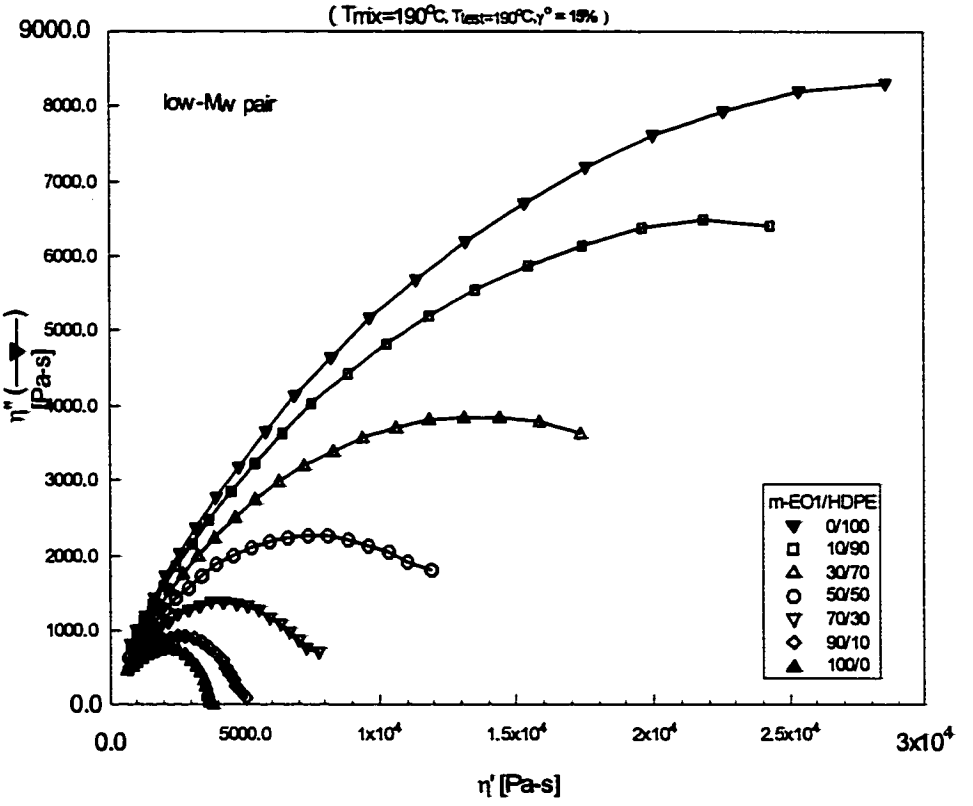

rise to a composition independent correlation, when G' is plotted against G''. This was not the case with m-LLDPE blends system investigated. Note that the two different blends systems of (m-EO1 and m-EO3) gives rise to composition dependent correlation when G' plotted against G''. For m-EO3 blends with HDPE (Appendix, Figure B.6), the same slopes were observed. However, in the case of low-M_w (Appendix, Figure C.6) the slopes of pure components were different from those of the blends. In particular, at low values of G' and G'', downward tailing was occurring and it was steeper in HDPE than m-EO1. The dependence of $\eta'(\phi)_{\omega=0.1}$ is shown in Figures 5.11a & b for the high-M_w (m-EO3) and low -M_w (m-EO1) blends respectively. Note that these plots were extracted from $\eta'(\omega)$ data shown in earlier in Figures 5.9a & b. For the high-M_w pair (Figure 5.11a), the viscosity follows the log-additivity rule, suggesting the miscibility of the high-M_w blends. Similarly, for the low-M_w pair (Figure 5.11b) $\eta'(\phi)_{\omega=0.1}$ follows the same behavior.

On the other hand, logarithmic plots of $G'(\phi)_{\omega=0.1}$ were similar to their counterparts of $\eta'(\phi)_{\omega=0.1}$ with a slight PDB in the case of low-M_w pair as shown in (Appendix, Figure C.3 & C.4). Further, it can be observed from Figure C.3 that the model does not fit the data very well. However, the slight PDB behavior and poor agreement of the experimental data and the emulsion model suggest that both blends of the low-M_w and high-M_w pairs are miscible. Or, M_w has almost no effect on the miscibility of m-LLDPE blends with

Figure 5.11a $\eta'(\phi)$ for blends of m-EO3 with HDPE
(T_{mix}=190°C, T_{test}=190°C, γ^o=15%)

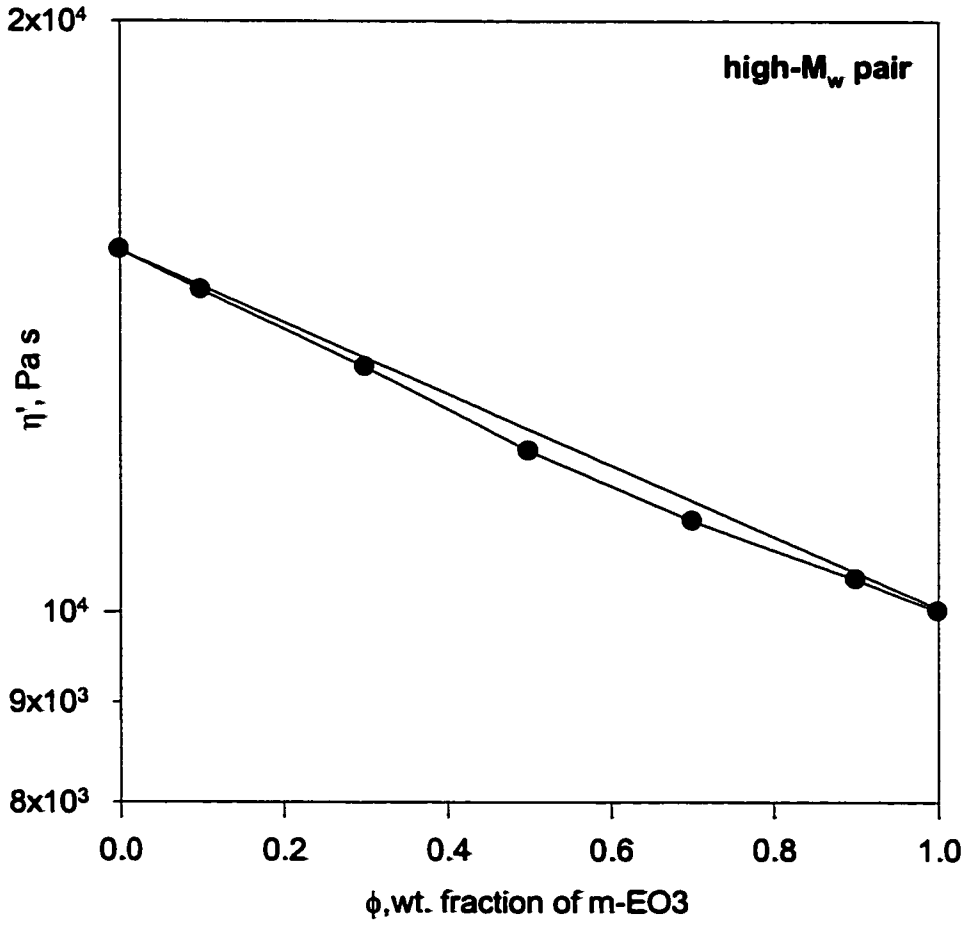

Figure 5.11b η' for blends of m-EO1 with HDPE
(T_{mix}=190°C, T_{test}=190°C, γ^{o} =15%)

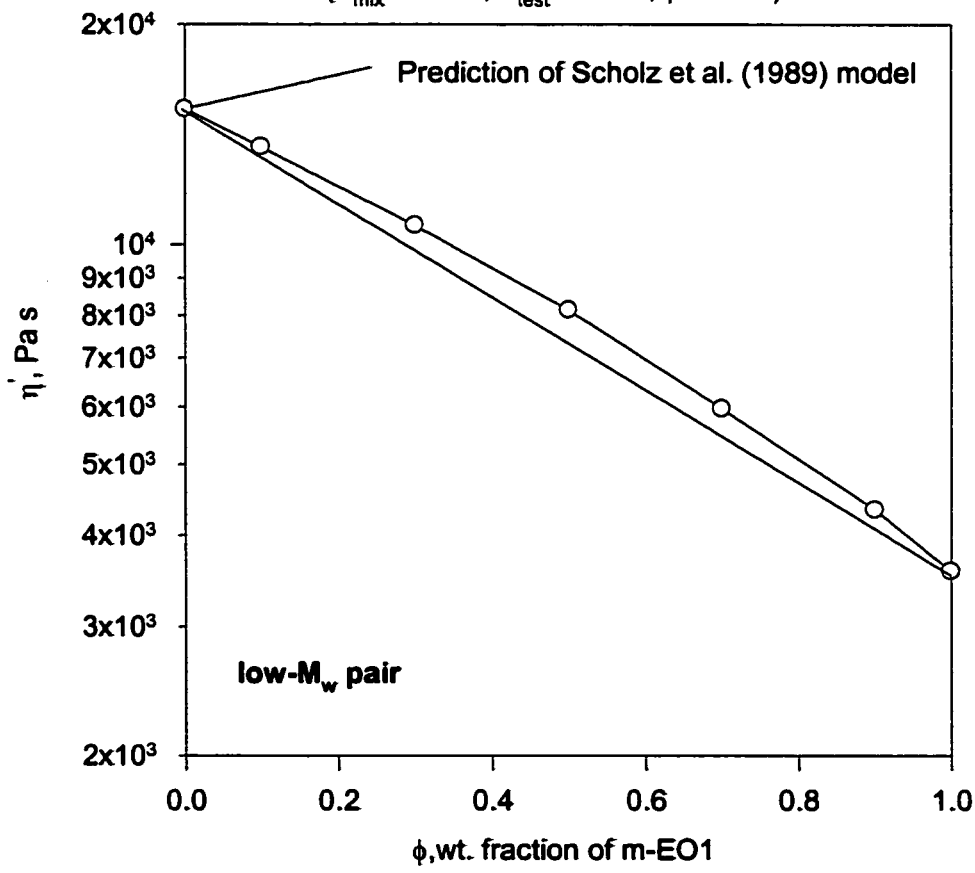

HDPE. It should be noted that the M_w of m-LLDPE studied here is 70-100 kg/mole.

Plots of $\eta_o(\phi)$ were also explored for assessing the miscibility of blends. Among the various available models, the Cross model was found to give a reasonably good fit to the $\eta'(\omega)$ data. $\eta_o(\phi)$ for both m-EO3 and m-EO1 and their blends are shown in Figures 5.12a & b respectively. For the low-M_w pair (Figure 5.12b), the blends exhibit a slight PDB from log-additivity rule, similar to that observed in the plot of $\eta'(\phi)_{\omega=0.1}$ (Figure 5.11b). On the other hand $\eta_o(\phi)$ for the high-M_w pair (Figure 5.12a) follow the log-additivity quite well. The above behavior indicates no influence for M_w on the blends miscibility. However, to clarify the miscibility of the low-M_w pair, the dilute emulsions model of Einstein (Eq. 2.2) was used to fit η_o for the 10% m-EO1 blend with HDPE. As shown in Figure 5.12b, the deviation between experimental data and prediction of emulsion model are quite large. This further supports the miscibility of m-EO1 and m-EO3 blends with HDPE. Also, these results suggest no influence for M_w in the range 70-100 kg/mol on miscibility. Nevertheless, Scholz et al. (1989) model (Eq. 2.1) was used to calculate the ratio of interfacial tension to the droplet radius (α/R) from low-ω $G'(\omega)$. The calculated value of (α/R) was found to be close to zero.

Further, steady shear measurements were performed to investigate the miscibility of the blends.

Figure 5.12b $\eta_o(\phi)$ for blends of m-EO1 with HDPE computed from Cross Model

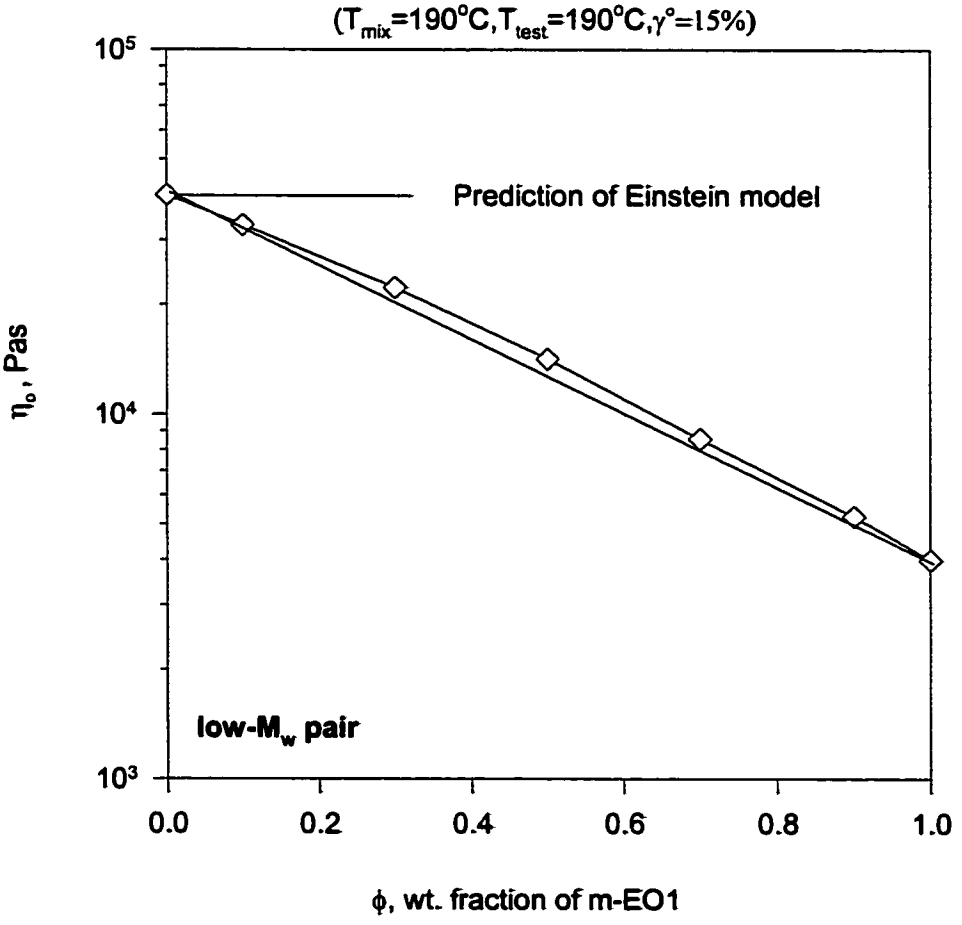

As pointed out by different researchers (Utracki and Schlund, 1987; Chuang and Han 1984), the similarity of dynamic and steady-shear properties e.g., between η and η', and between N_1 and G' must not be expected for immiscible blends. For miscible blends Utracki and Schlund (1987) have suggested that, $\eta'(\omega) \cong \eta\ (\dot{\gamma})$ for $\omega=\dot{\gamma}$. The steady shear measurements for all blends of m-EO1 and m-EO3 with HDPE were obtained at 190°C in the range 0.01 to 1.0 s^{-1} with a 3-miunite time-before-measurement (tbm) and a 30 seconds measurement-time (mt).

The steady shear data for the low-M_w blends are given in Figure 5.13a. At low $\dot{\gamma}$ $N_1(\dot{\gamma})$ values for all blends were lower than those obtained at high $\dot{\gamma}$. Also, $N_1(\dot{\gamma})$ increased in proportion to the increase in the more elastic component, the HDPE suggesting the miscibility of these blends. For the high-M_w pair, the results shown in figure 5.13b are very similar with weak PDB. However, $N_1(\dot{\gamma})$ for all blends did not exceed the values for the pure components. Hence, immiscibility is likely to develop when M_w is much higher 100 kg/mol. Again, in the studied range M_w has no significant role on miscibility. Furthermore, Cox-Merz rule (1958) was used to examine the miscibility of the blends. The comparison of $\eta(\dot{\gamma})$ and $\eta^*(\omega)$ at 190°C for m-EO1/HDPE and m-EO3/HDPE blends is displayed in Figures 5.14 and Figure 5.7a, respectively. Open symbols

Figure 5.13a $N_1(\gamma)$ for blends of m-EO1 with HDPE

(T_{mix}=190°C, T_{test}=190°C)

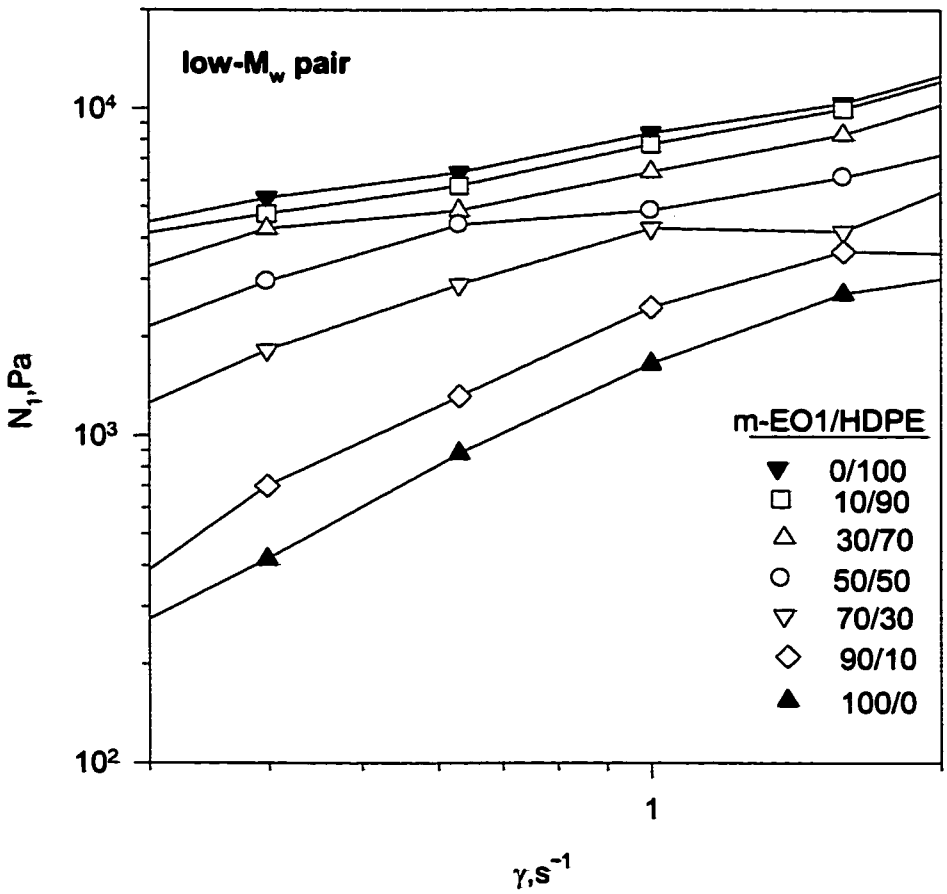

Figure 5.13b $N_1(\gamma)$ for blends of m-EO3 with HDPE
(T_{mix}=190°C, T_{test}=190°C)

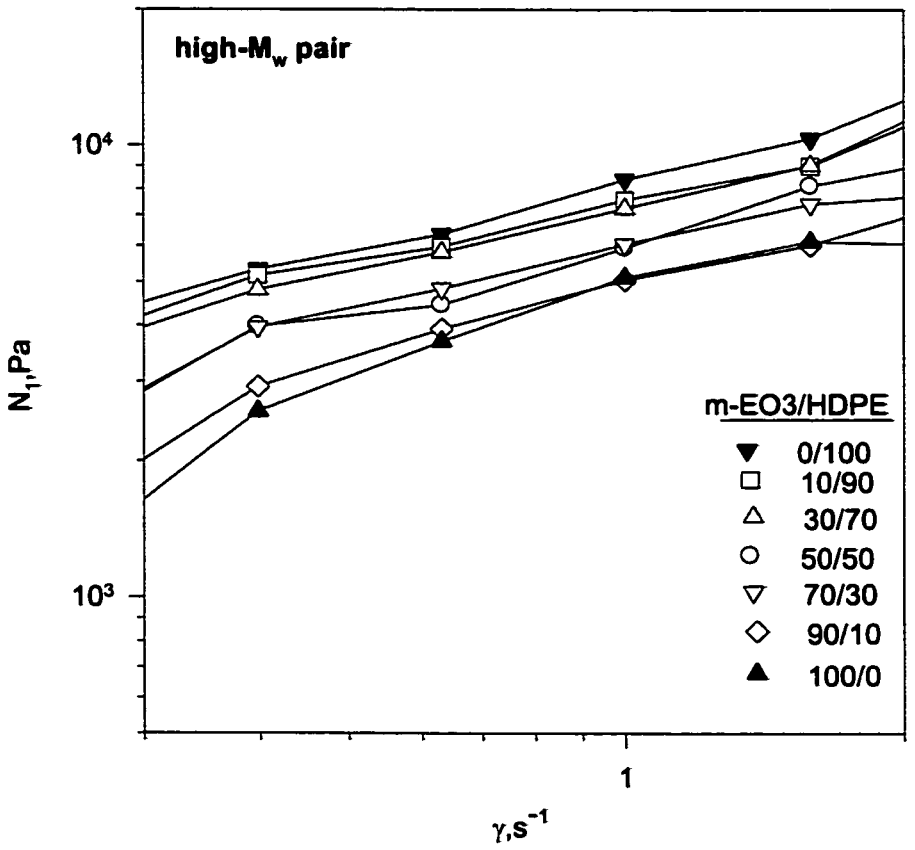

Figure 5.14 comparison of $\eta^*(\omega)$ and $\eta(\gamma)$ for blends of m-EO1 with HDPE

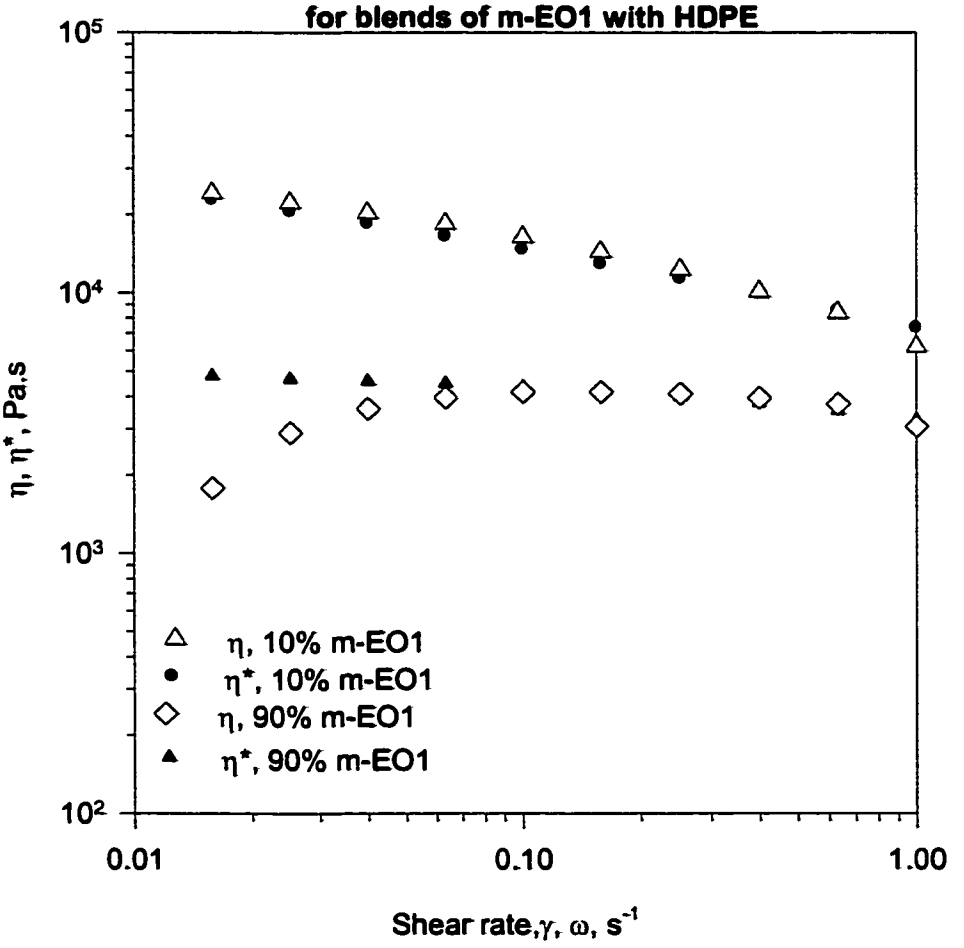

represent $\eta(\dot{\gamma})$ and filled symbols represent $\eta^*(\omega)$. For blends of m-EO1 with HDPE (Figure 5.14), good superposition was observed for both the 10% and the 90% blend of m-EO1 with HDPE in the low shear region suggesting miscibility of the blends in the whole composition range. Also, for the m-EO3 blend with HDPE, one can observe that the Cox-Merz rule (1958) is quite well verified over a broad range. Moreover, stress relaxation measurements were performed for the blends and pure resins of sample m-EO1 and m-EO3, using cone-and-plate geometry. As an example, $N_1(t)$ data for high-M_w (m-EO3) is presented in Figure 5.15, which is similar to $N_1(\dot{\gamma})$ presented earlier. As an example, N_1 (t) data for high-M_w (m-EO3) is presented in Figure 5.15, which is similar to $N_1(\dot{\gamma})$ presented earlier.

The above different rheological measurements provide means for inferring the effect of M_w on the phase behavior of m-EO blends with HDPE. All blends appear to be miscible in the whole composition range with no influence for M_w of m-EO in the range 70-100kg/mol on its miscibility with HDPE. The predictions of emulsion models (Einstein and Scholz et al. models) were found to be in disagreement with experimental data. This provides further support to the miscibility of m-EO blends with HDPE.

Figure 5.15 N1(t) for blends of m-EO3 with HDPE

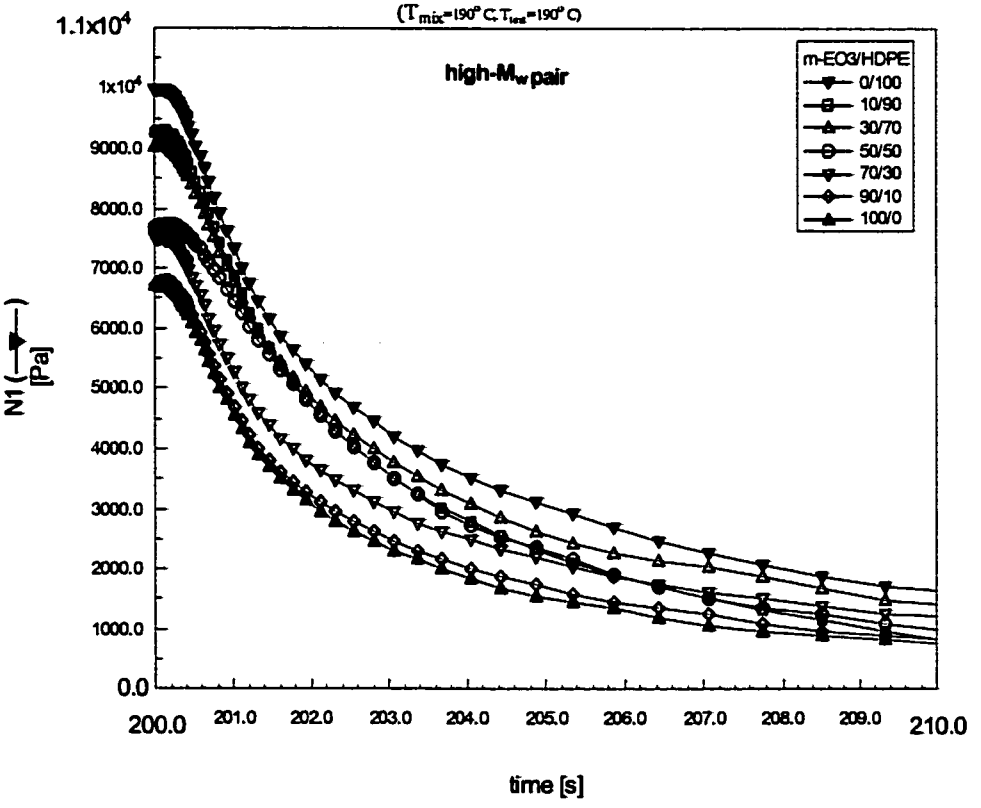

figure 5.16 $\eta'(\omega)$ for ZN-EO blends with HDPE
(T_{mix}=190°C, T_{test}=190°C, γ^{o}=15%)

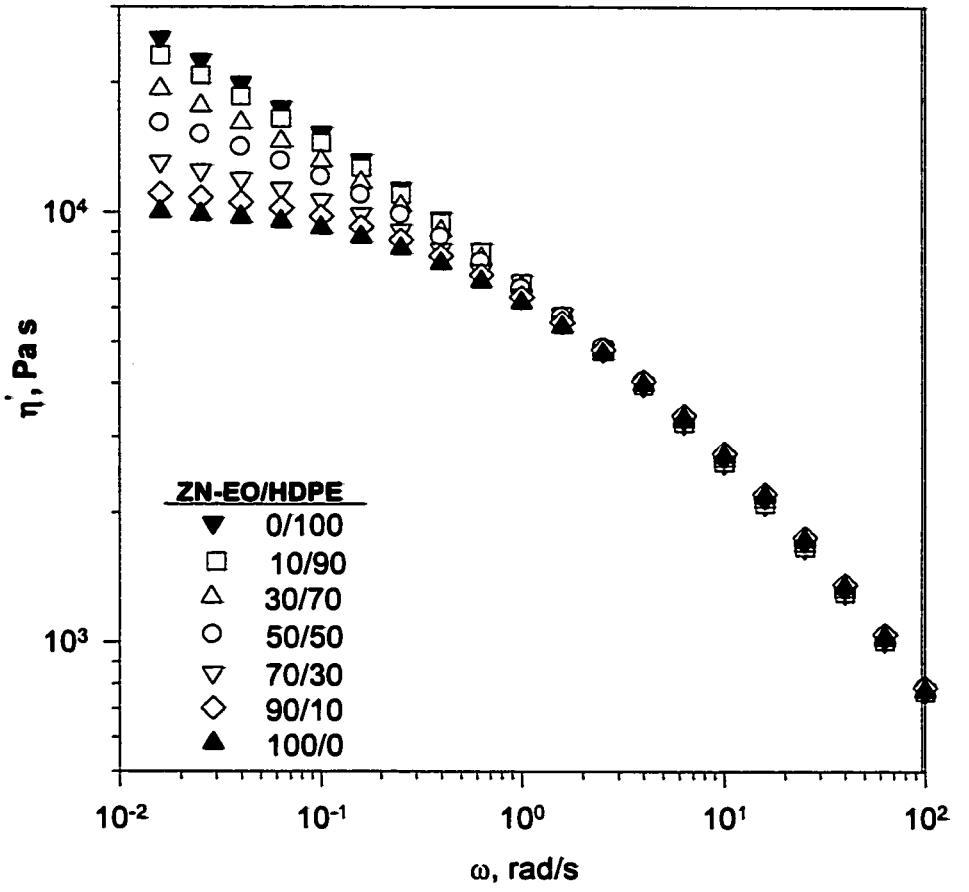

HDPE-rich blends, $\eta'(\omega)$ decreases with the increase of the portion of m-EO2 in the blend. The m-EO2 is the resin of the lowest viscosity. On the other hand, the 70% and 90% m-EO2 blends with HDPE show $\eta'(\omega)$ that are identical to that of pure m- EO2. Or, the addition of up to 30% of the more viscous blend component (HDPE) to m-EO2 did not change the viscosity of m-EO2. This observation suggests the immiscibility of m-EO2-rich blends and the miscibility of HDPE-rich blends. The trend of $G'(\omega)$ data is similar (see Figures D.1 & D.2). Here, the ZN-EO blends with HDPE show high degree of miscibility than metallocene resins.

The rheological behavior of the ZN-EO/HDPE and m-EO2/HDPE system was further investigated by using the Cole-Cole plots. As shown in Figures 5.17 and Figure 5.3a the curves for ZN-EO blends with HDPE are close to semicircular indicating the miscibility of these blends. On the other hand, the m-EO2-rich blends with HDPE are different with η' and η'' data for the 70% and 90% m-EO2 blends almost the same. Furthermore, plot of log G' versus log G'' are displayed in (Appendix, Figures D.5 &D.6). At low-ω (low G'), blends of ZN-EO with HDPE show slopes that are almost the same as those of pure resins. However, slopes of the m-EO2-rich blends are different suggesting the immiscibility of these blends. The $\eta'(\phi)$ data obtained at low-ω (ω=0.1 rad/s) are plotted in Figures 5.18 and Figure 5.4a for ZN-EO and m-EO2 blends with HDPE, respectively. In Figure 5.18, ZN-EO with HDPE blends show $\eta'(\phi)$ data that

Figure 5.17 Cole-Cole plot for blends of ZN-EO with HDPE

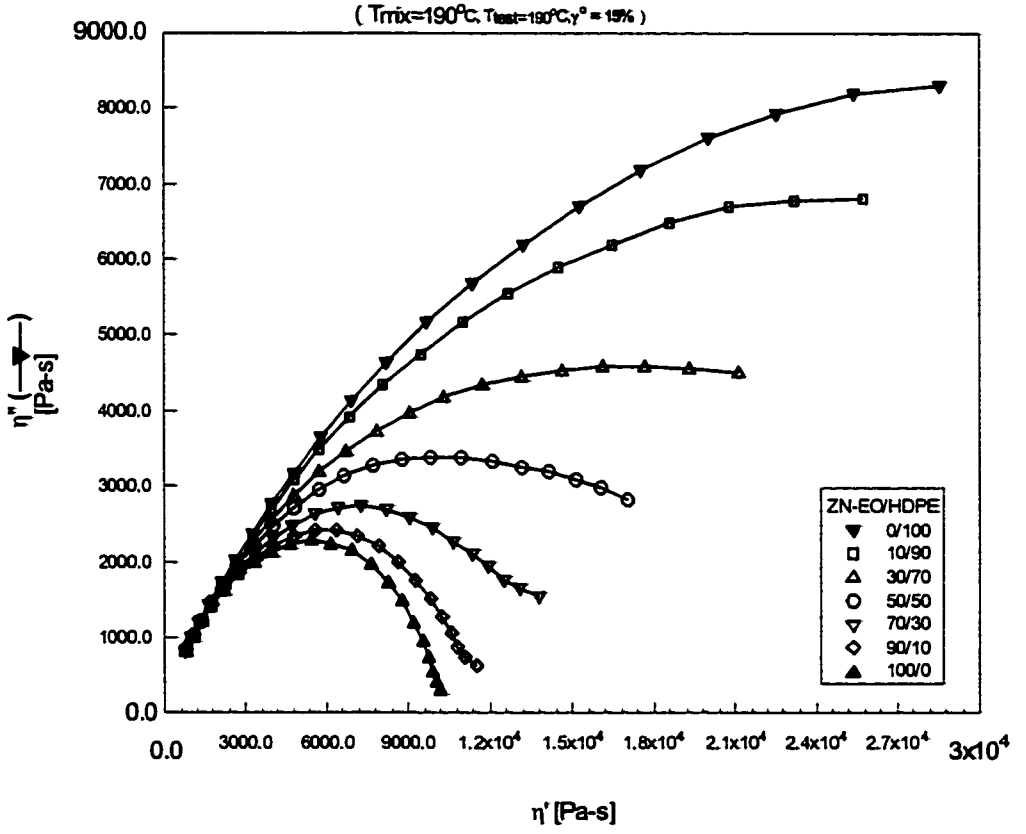

Figure 5.18 $\eta'(\phi)$ for blends of ZN-EO with HDPE

(T_{mix}=190°C, T_{test}=190°C, γ^o =15%, ω=0.1rad/s)

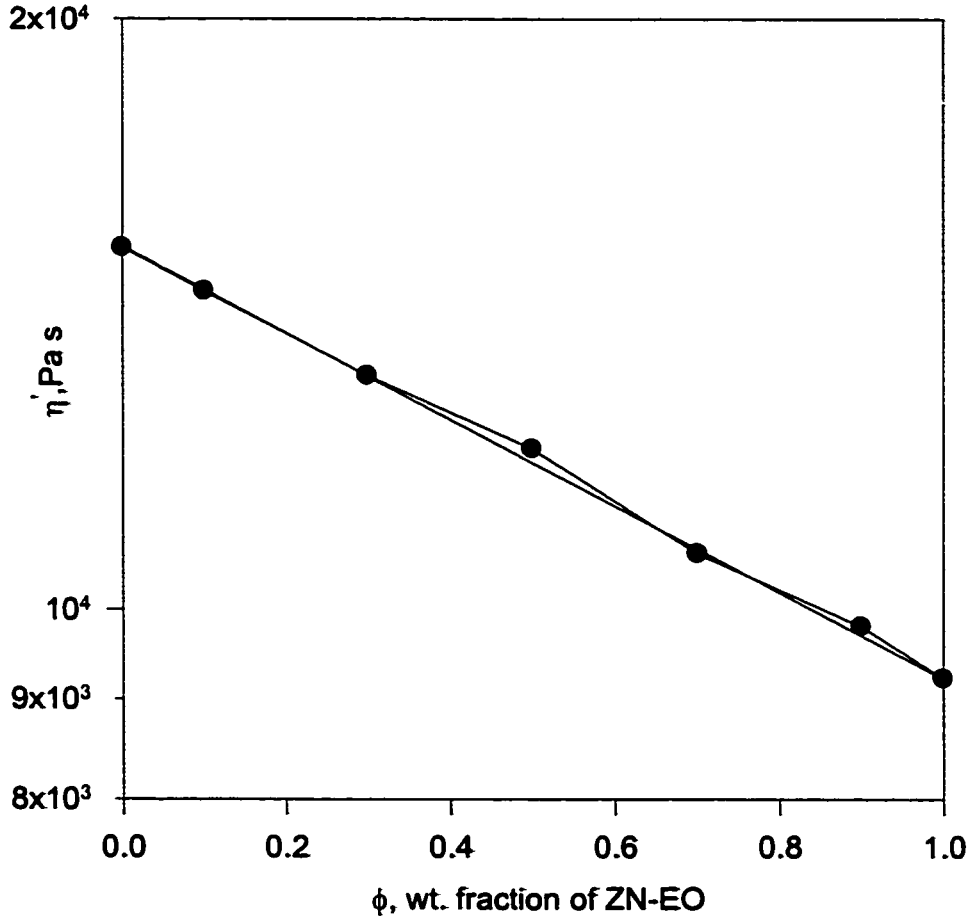

Figure 5.19 $\eta_o(\phi)$ for blends of ZN-EO with HDPE computed from Cross model
(T_{mix}=190°C, T_{test}=190°C, γ^o=15%)

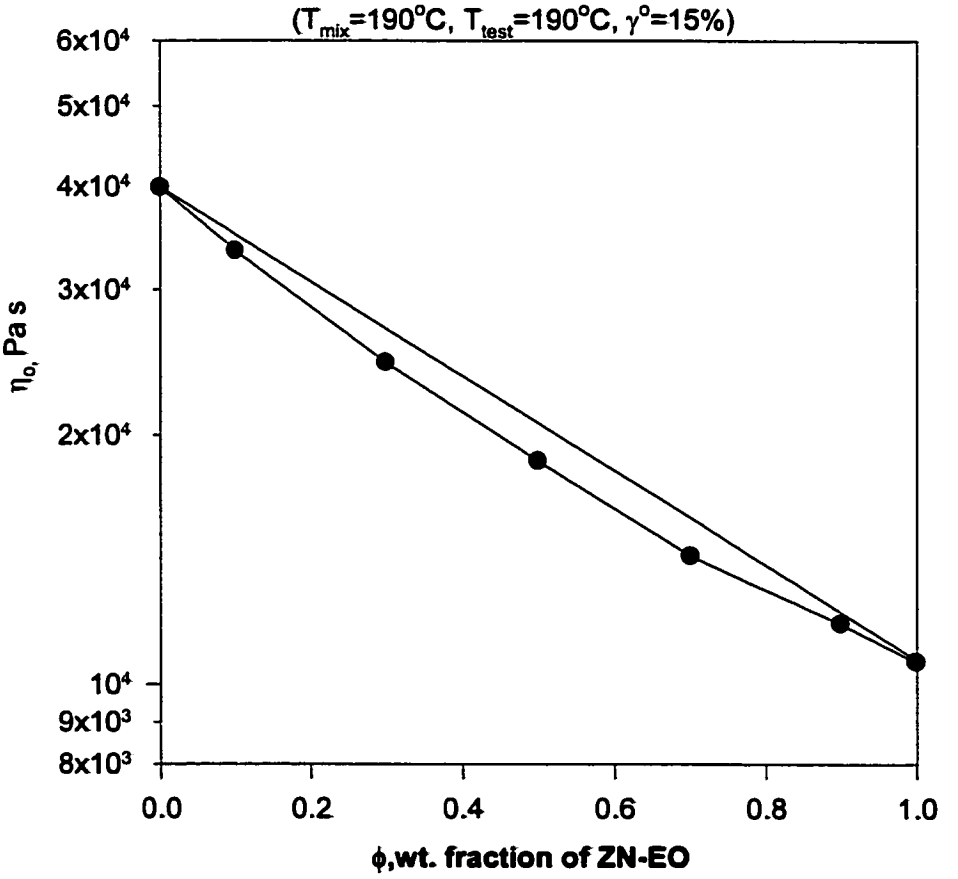

The current results suggest that ZN-EO is more miscible than m-EO2 blends with HDPE. This is in fact seems to be logical since ZN-EO contains linear molecules and hence better miscibility is expected with linear HDPE. However, these rheological results are inconsistent with TEM findings of Hill's group (Hill and Barham, 1997), which suggest no influence for catalyst type. On the other hand, Zhao et al. (1997) concluded that the cocrystallization is much lower in blends with single-site materials than in blends involving ZN materials. Also, Lee et al. (1997) observed that ZN-LLDPE to be more miscible with HDPE than the m-LLDPE. Tanem and Stori (2001) obtained similar results from TEM suggesting ZN-LLDPE to be more miscible with HDPE than m-LLDPE.

Furthermore, $\eta(\dot{\gamma})$ and $\left|\eta^*(\omega)\right|_{\gamma=\omega}$ are displayed together for ZN-EO and m-EO2 blends with HDPE; in Figures 5.20 and Figure 5.7b, to facilitate the comparison, respectively. Here, only 10% and 90% blends of ZN-EO with HDPE are selected to represent the LLDPE-rich and HDPE-rich blends. For both blends, it can be observed that the 90% and 10% m-EO2 blends with HDPE, $\eta(\dot{\gamma})$ appears to superimpose very well with $\eta^*(\omega)$ (Figures 5. 7b). Also, for the 10% and the 90% ZN-EO blend with HDPE Cox-Merz was also verified (Figure 5.20). This indicates that Cox-Merz rule failed to show the immiscibility of m-EO2-rich blends, which was predicted by the previous methods of

Figure 5.20 Compairson of $\eta^*(\omega)$ and $\eta(\gamma)$ for the blends of ZN-EO with HDPE

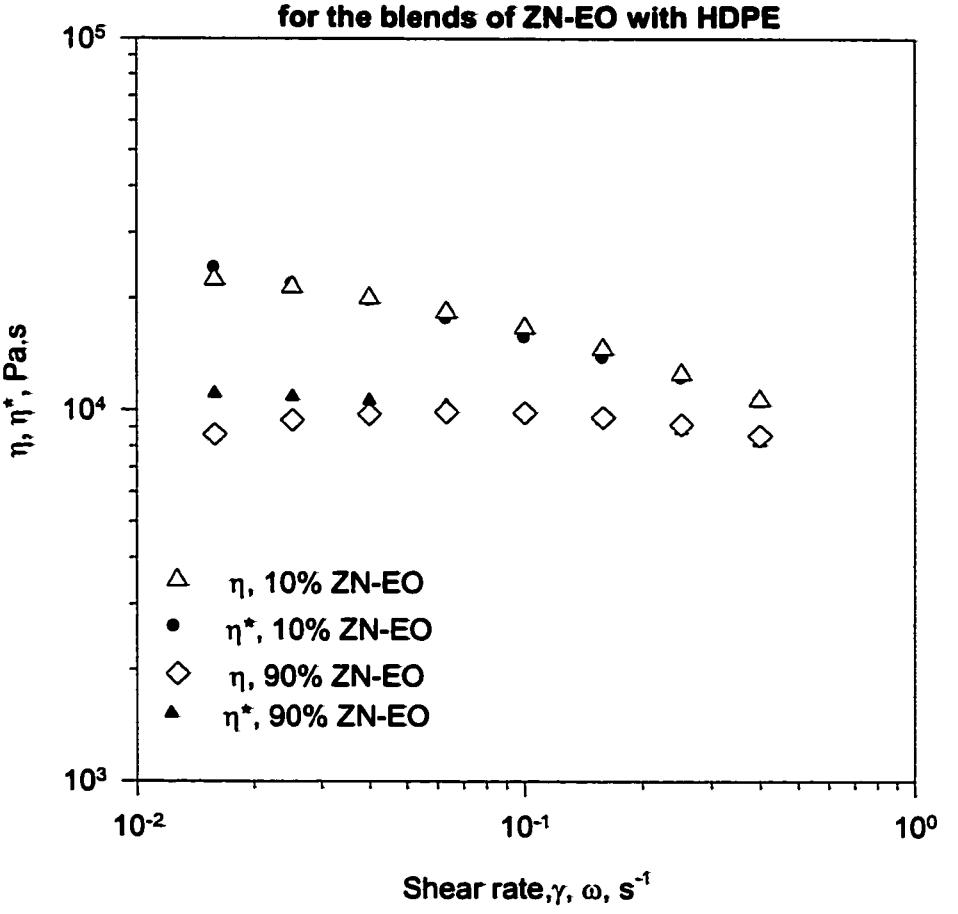

data analysis. In addition, steady-shear and transient measurements were performed using cone-and-plate geometry. The steady shear measurements of $N_1(\dot{\gamma})$ for ZN-EO blends with HDPE were displayed in Figure 5.21. Over a wide range of $\dot{\gamma}$, $N_1(\dot{\gamma})$ values for all blends were found to lie between those of the pure resins and it increased in proportion to the increase in the ratio of the more elastic component (HDPE) suggesting miscibility of ZN-EO with HDPE blends. These results provide further support to the previous finding from dynamics measurements. However, $N_1(\dot{\gamma})$ data for m-EO2 blends with HDPE were different as discussed earlier (Figure 5.6a). The $N_1(\dot{\gamma})$ measurements suggest partial miscibility of the m-EO2/HDPE blends, which is in agreement with previous conclusions of the dynamic shear measurement.

The stress relaxations data, $N_1(t)$, for blends of m-EO2 and ZN-EO with HDPE are obtained and shown in Figures 5.8a and Figure 5.22, respectively. As seen in these Figures, $N_1(t)$ for the m-EO2 and ZN-EO blends with HDPE followed the same pattern of the $N_1(\dot{\gamma})$ data (Figures 5.21 & Figure 5.6a). Also, the relaxations of the m-EO2-rich blends are almost the same as that of m-EO2 over the whole period as discussed earlier. For HDPE-rich blends, the decrease in $N_1(t)$ followed the decrease in the fraction of HDPE suggesting the miscibility of HDPE-rich blends. For ZN-EO blends with HDPE results are given in Figure 5.22. Here, $N_1(t)$ data smoothly correlated to ϕ

Figure 5.21 $N_1(\gamma)$ for blends of ZN-EO with HDPE
(T_{mix}=190°C, T_{test}=190°C)

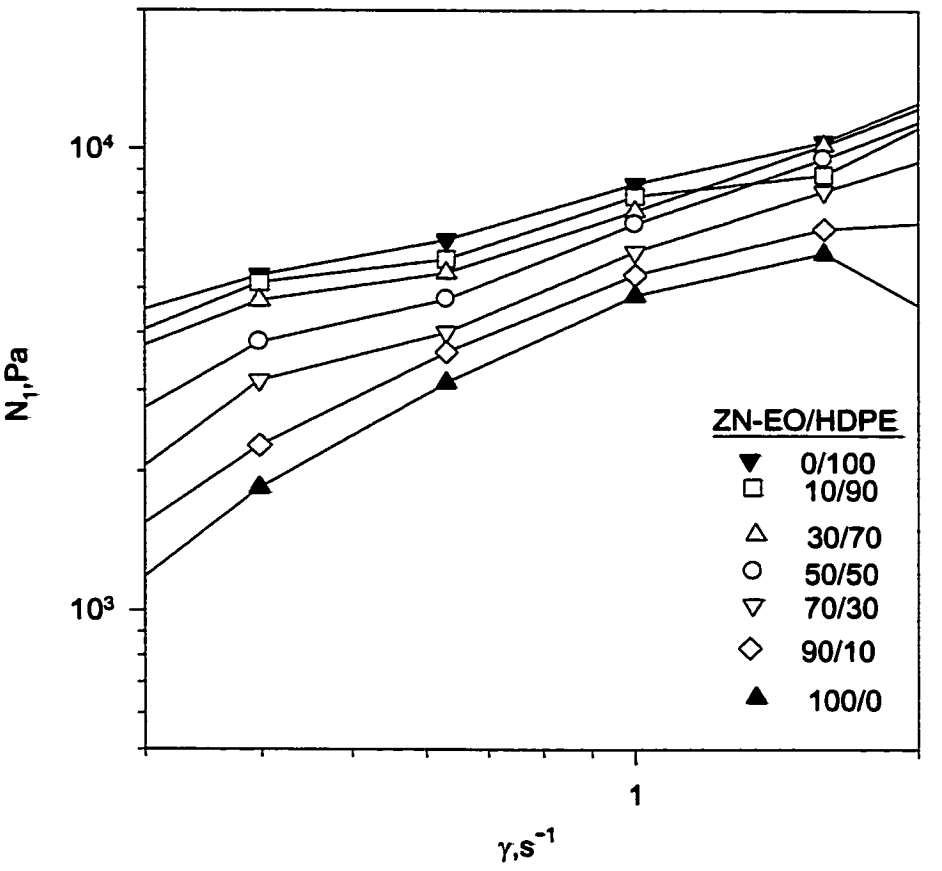

Figure 5.22 $N_1(t)$ for blends of ZN-EO with HDPE

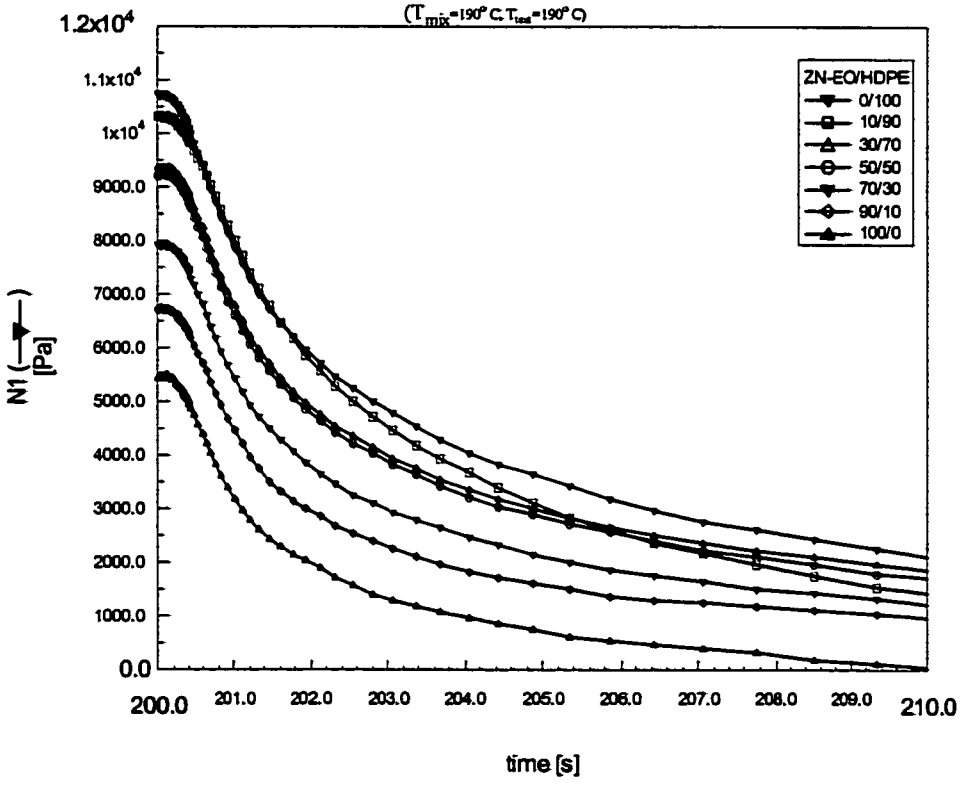

cause phase-separation rather than the addition of a small amount of m-LLDPE to HDPE. Or, the immiscibility of m-LLDPE/HDPE blends is nonsymmetric with respect to composition. This nonsymmetric behavior of PE/PE blends was predicted by Fredrikson and co-workers (Fredrickson and Liu, 1995; Fredrickson et al., 1994; Bates and Fredrickson 1994). The mismatch of the molecular conformation of m-LLDPE and HDPE is shown by the MD simulations to be the reason behind the immiscibility and also predicted from the theoretical work of Fredrickson and co-workers. The MD simulation result and rheological techniques integrate to provide insight into the effects of molecular parameters on immiscibility of HDPE/LLDPE blends and highlight the reasons behind immiscibility. Both the MD simulation and the experimental work are in agreement with theoretical predictions in the case of the influence of BC.

CHAPTER 6

Conclusions and Recommendations

6.1 Conclusions

In this work, the miscibility of PE/PE blends has been reviewed with special attention to HDPE/LLDPE blends. MD simulations and rheological techniques were employed to study the effects of molecular parameters (molecular weight, branch content and composition distribution) on the miscibility of LLDPE with HDPE in the melt state. A series of octene-based metallcene (m-LLDPE) and conventional (ZN-LLDPE) resins were blended with HDPE to investigate the melt miscibility of blends. Resins were paired to study one variable at a time and avoid interactions of molecular parameters that occurred in most of the previous studies. Based on the materials employed and the experimental techniques used, the following conclusions are reached:

6.1.1 Molecular Dynamics Simulation Technique

The study shows that miscibility of HDPE and LLDPE was found to be a strong function of branch content. Blends were miscible in melt state up to a branch content of LLDPE of 30 branches/1000C. At 40 branches/1000C, blends start to phase separate and complete phase separation was observed at 60 branches/1000C. The source of

immiscibility is suggested to be due to the preference of the two polymers to assume different conformations in the melt state. Mismatch of the conformations of blend components was observed at high branch contents.

6.1.2 Rheological Measurements

Several rheological measurements and data treatment methods were employed to study the rheological behavior of a series blend of octene-base m-LLDPE and ZN-LLDPE with HDPE in the melt state. In particular, the steady shear flow behavior both at low and high-shear rates were analyzed. The results of dynamic shear measurements in terms of dynamic viscosity η', storage modulus, G', and loss modulus, G'', were also reported. The rheological data namely, G', G'', η' and η'', were used to analyze blend miscibility. Cole-Cole plots and modified Cole-Cole plots were used. Also, the zero-shear viscosity, η_o (ϕ), determined by fitting the η' (ω) data to the Cross model was employed in the analysis. Further, plots of η' (ϕ) and $G'(\phi)$ were found to be very helpful in assessing the miscibility of blends. In addition, N_1 ($\dot{\gamma}$) and N_1 (t) data were analyzed. Einstein and Scholz et al. emulsion models were used to compare experimental results to different model predictions. Also, BPU and Lin's models were used to describe the NDB

Interlayer slip factors were obtained for immiscible systems. Based on the experimental procedures employed in this work, the most important findings are:

a. Varying the M_w of m-LLDPE in the range 70kg/mol to 95 kg/mol has no effect on the melt miscibility of m-LLDPE/HDPE blends. Miscibility was observed in the whole composition range.

b. Blends of octene-base m-LLDPE and HDPE are miscible at low branch content of m-LLDPE (BC=17 branches/1000C). However, increasing the branch content to 32 branches/1000C has resulted in partial immiscibility. Immiscibility is likely to develop in the m-LLDPE-rich range. These results are in agreement with the MD simulation results, where phase separation has started to develop above 30 branches/1000C.

c. The LLDPE with a heterogeneous composition distribution (ZN-LLDPE) was found to be more miscible with HDPE than the LLDPE with a homogeneous composition distribution (m-LLDPE). This observation is suggested to be due to the presence of linear molecules in ZN-LLDPE that act as a compatiplizer. However, immiscibility can occur if the ZN-LLDPE contains fractions of highly branched molecules.

d. In the region of LLDPE-rich blends phase separation is likely to occur. Thus in terms of improved processability addition of a small amount of HDPE is expected to lower the viscosity and elasticity of the blend.

e. The miscibility of the high-BC octene-based m-LLDPE varies with blend composition. For HDPE-rich blend, the addition of small amount of LLDPE is likely to cause miscibility, while the addition of small amount of HDPE favors the immiscibility. Or, immiscibility of m-LLDPE and HDPE blends is nonsymmetric with respect to composition. This nonsymmetric effect was predicted by theory (Fredrickson et al., 1994; bates and Fredrickson, 1994; Fredrickson and Liu, 1995) and now proved by rheological experiments.

f. MD simulations suggest that mismatch of the molecular conformations is believed to be the reason behind immiscibility of LLDPE/HDPE blends. Branch content was found to have a strong influence on molecular conformations and hence on miscibility of different blend components.

g. The immiscibility of the blends due to interlayer slip leads to decrease in the viscosity (NDB rheology) that can be explained by BPU and Lin's models. Agreement between model predictions and experimental data was obtained for LLDPE-rich blends.

6.2 Recommendations for Future Work

As shown in this thesis, the application of the rheological and MD simulation techniques to the melt miscibility studies on polyethylene blends is quite successful. Most of the results from the two techniques agree well with the experimental observation of others. However, the future work should address the following:

1) The processing and mechanical properties of ZN and m-LLDPE/HDPE blends to study the influence of these molecular parameters on the processing and final properties of blends.
2) Investigation of the influence of molecular parameters and conformations of pure polymers in solid and liquid phase.
3) Study the influence of long-chain branches of LLDPE on its miscibility with LLDPE

Appendix A

Supplement to Chapter 3

Figure A.1 NMR Spectrum of Sample m-EO1

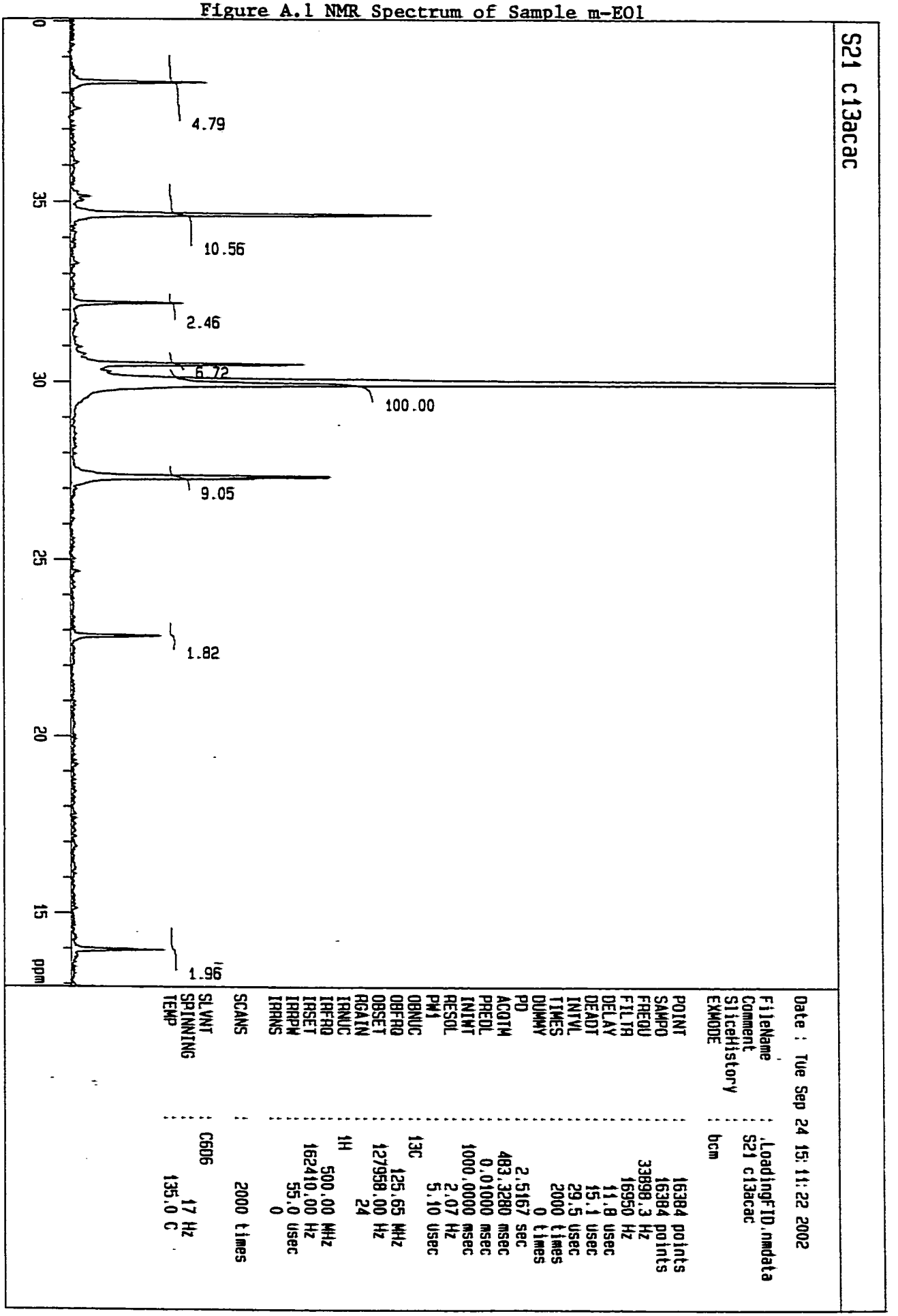

Figure A.2 NMR Spectrum of Sample m-EO2

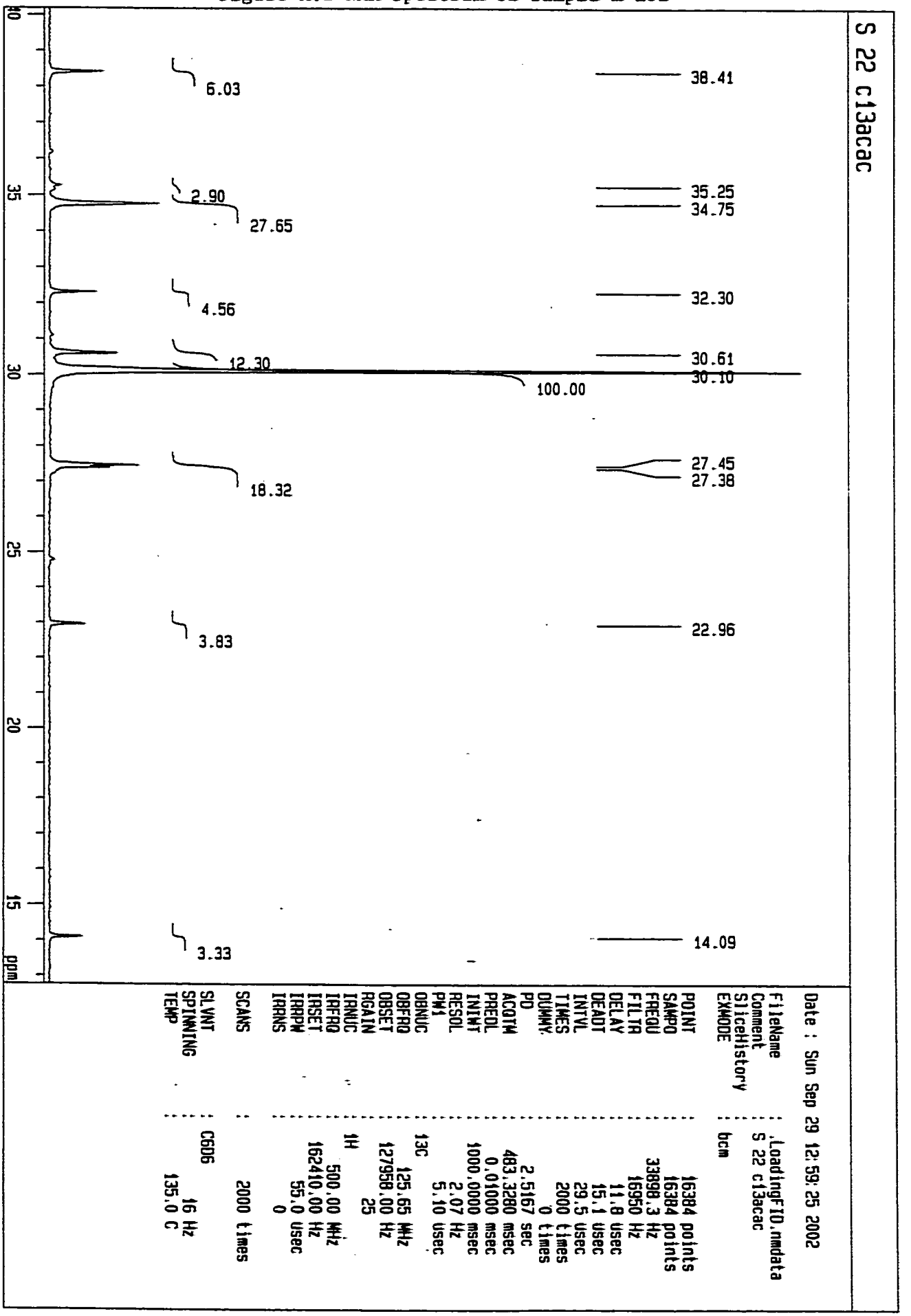

Figure A.3a NMR Spectrum of Sample m-EO3

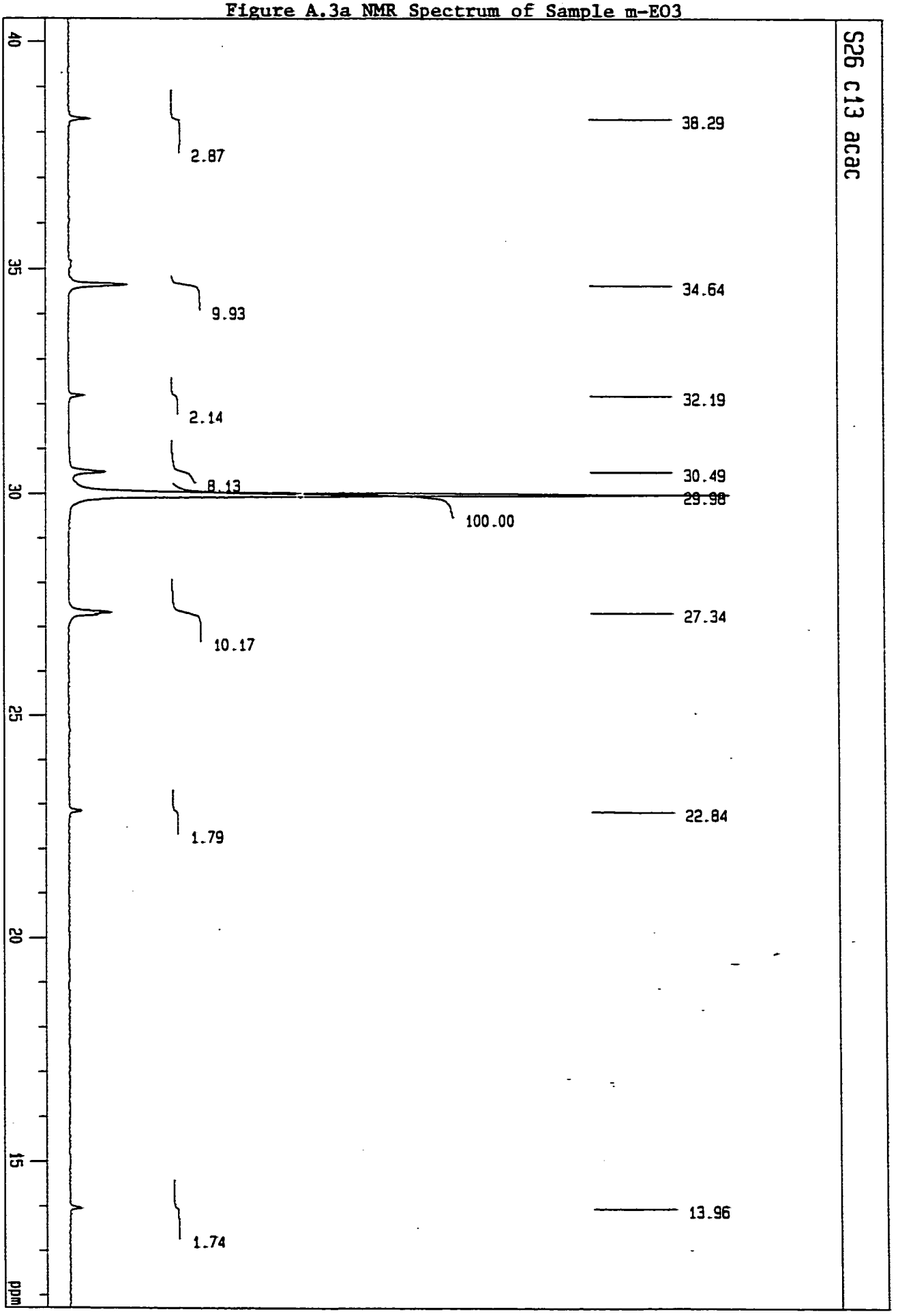

Appendix B

Supplement to Chapter 5.1

Figure B.1 G'(ω) for m-EO2 blend with HDPE

(T_{mix}=190°C, T_{test}=190°C, γ^{o}=15%)

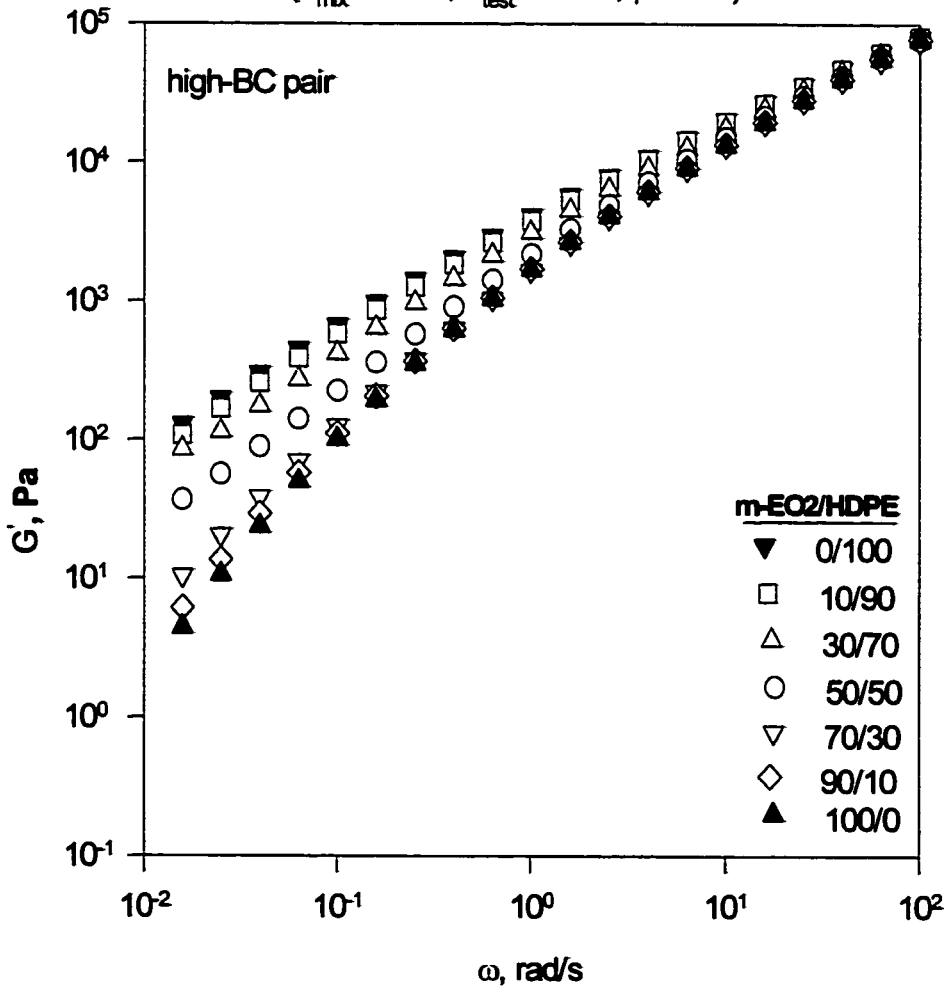

Figure B.2 $G'(\omega)$ for m-EO3 blend with HDPE
(T_{mix}=190°C, T_{test}=190°C, γ^{o}=15%)

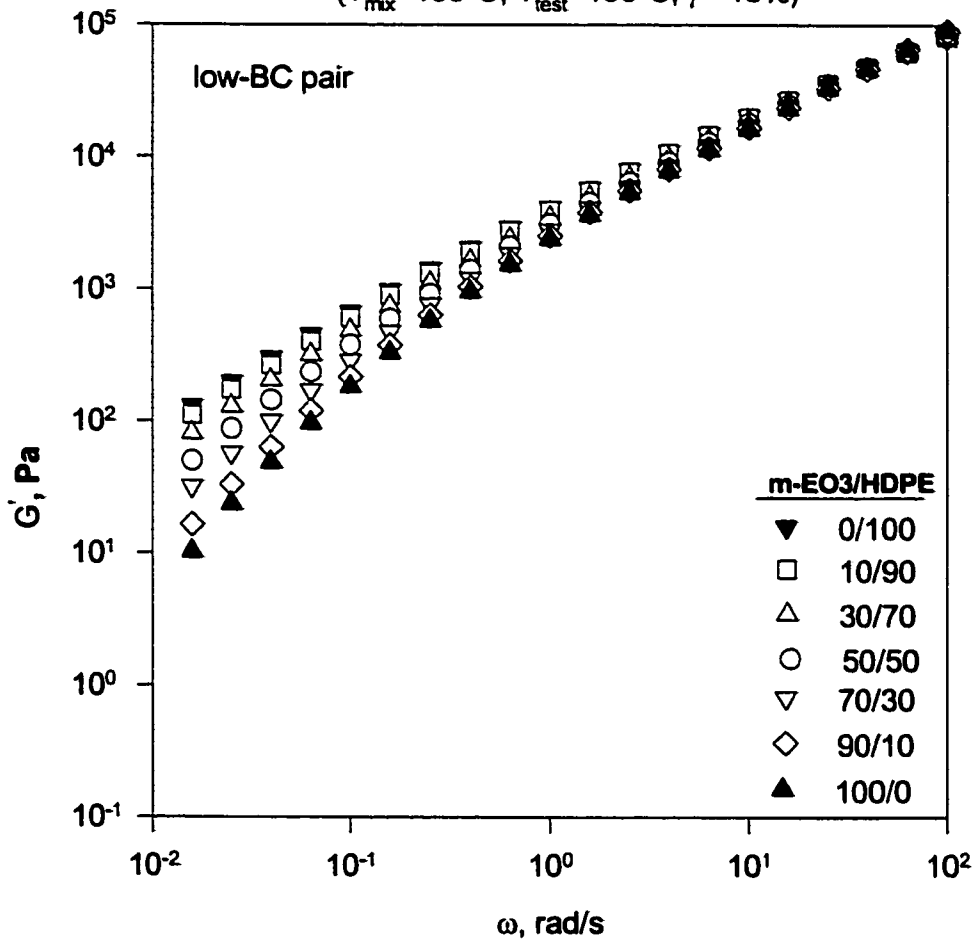

Figure B.3 G'(ϕ) for blends of m-EO2 with HDPE

(T_{mix}=190°C, T_{test}=190°C, γ^{o} =15%)

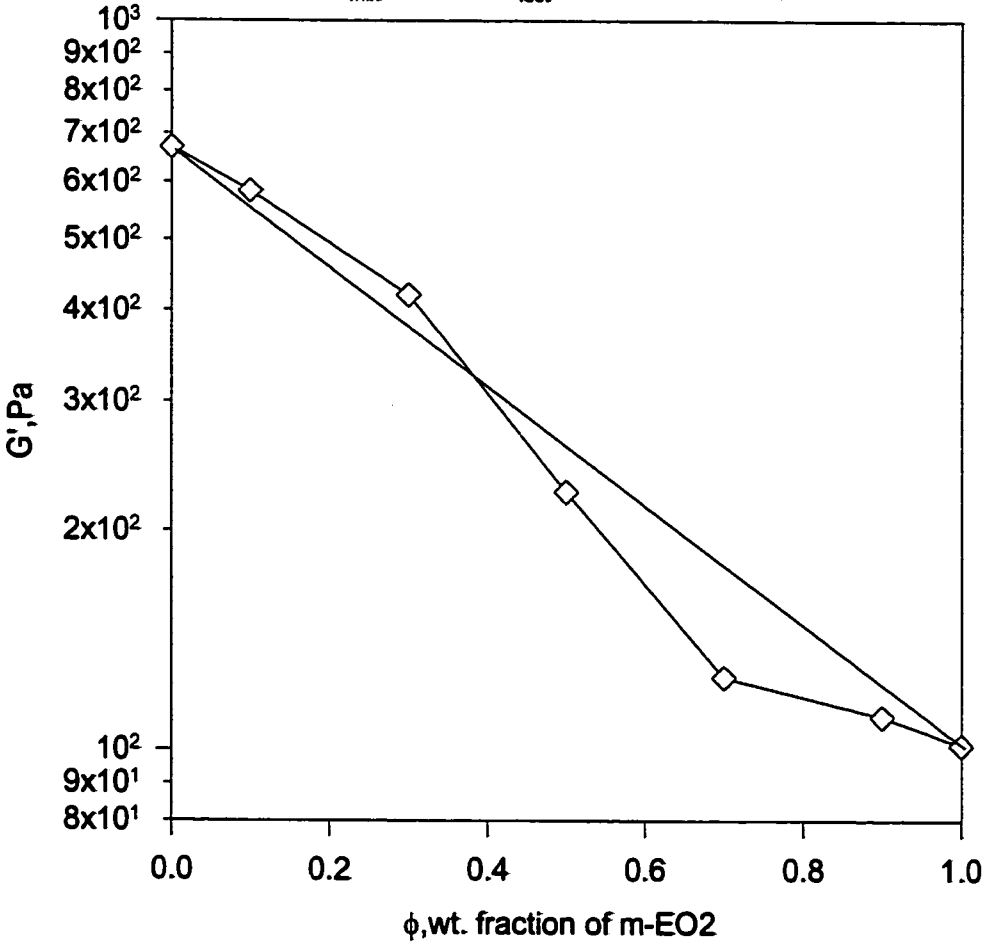

Figure B.4 G'(ϕ) blend of m-EO3 with HDPE

(T_{mix}=190°C, T_{test}=190°C, γ° =15%)

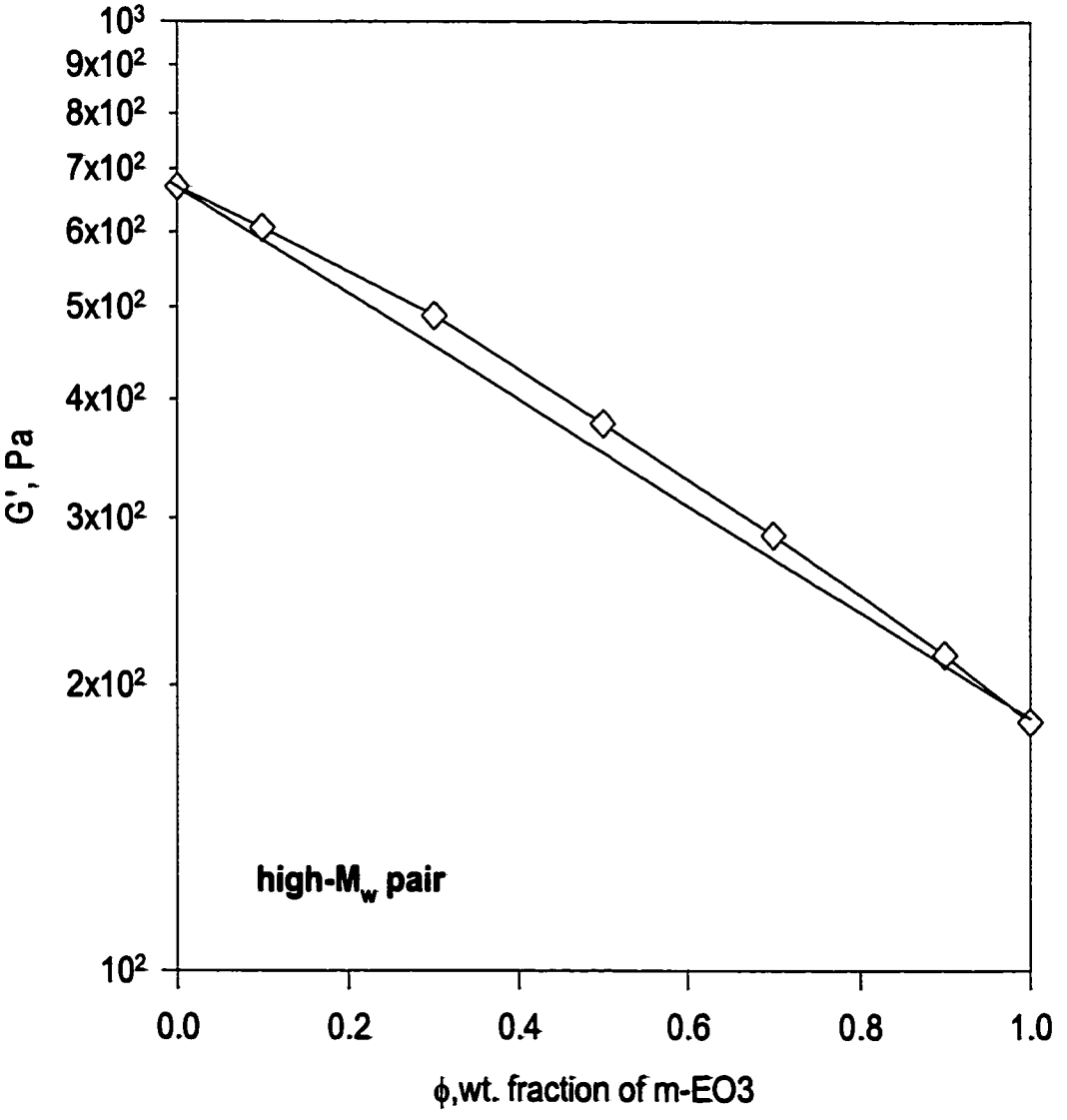

Figure B.6 Modified Cole-Cole plot for beinds of m-EO3 with HDPE
(T_{mix}=190°C, T_{test}=190°C,γ^{o}=15%)

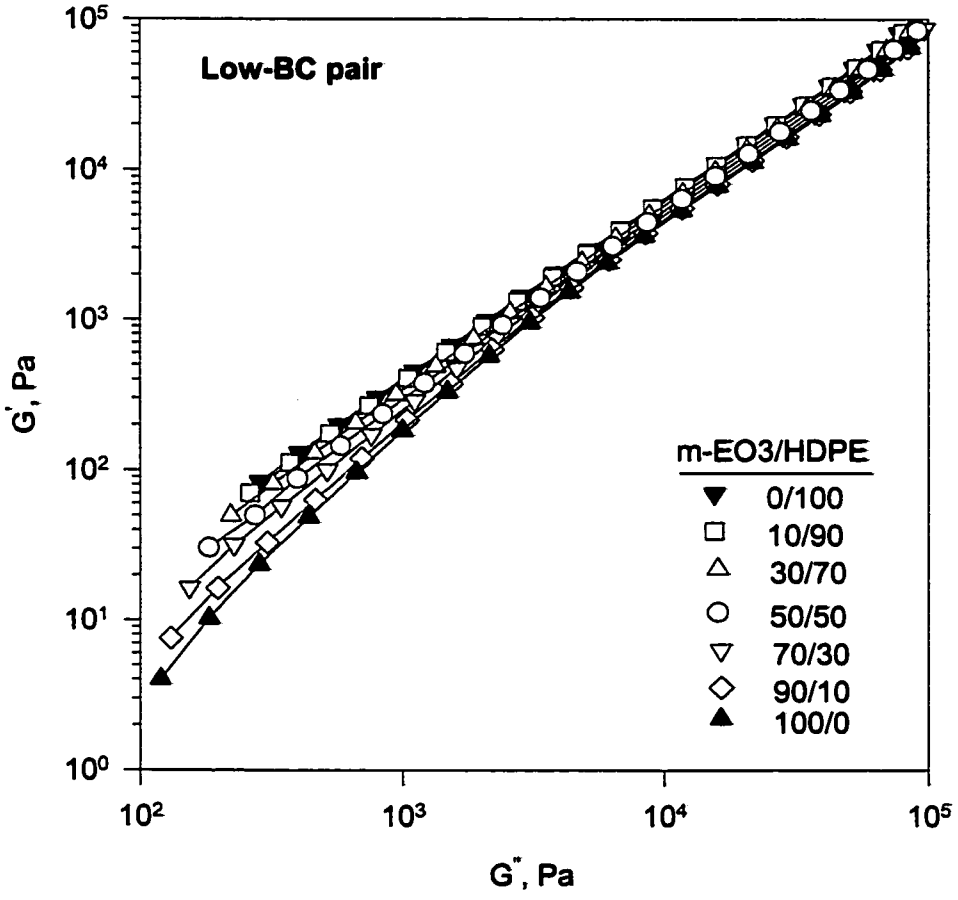

Figure B.7 $N_1(\phi)$ for blends of m-EO2 with HDPE

(T_{mix}=190°C, T_{test}=190°C,$\dot{\gamma}$ =0.4 s^{-1})

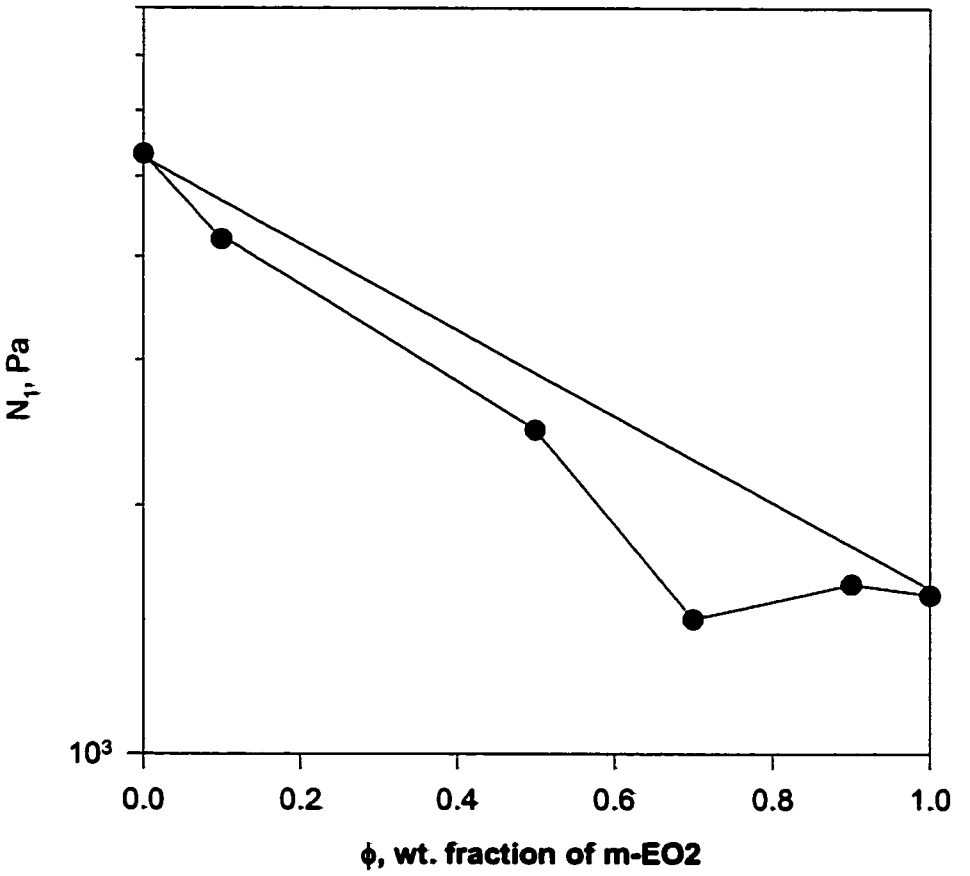

Figure B.8 $N_1(\phi)$f or blends of m-EO3 with HDPE

(T_{mix}=190°C, T_{test}=190°C,$\dot{\gamma}$ =0.4 s^{-1})

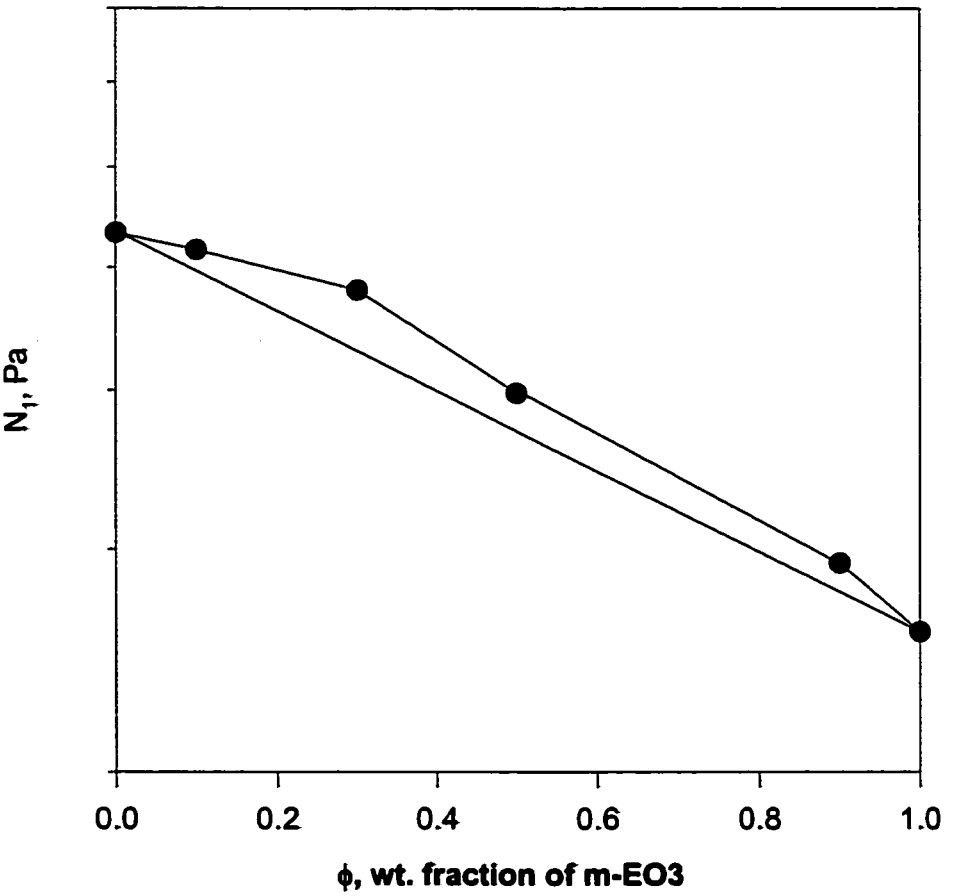

Appendix C

Supplement to Chapter 5.2

Figure C.1 G'(ω) for m-EO1 blend with HDPE

(T_{mix}=190°C, T_{test}=190°C, γ^{o}=15%)

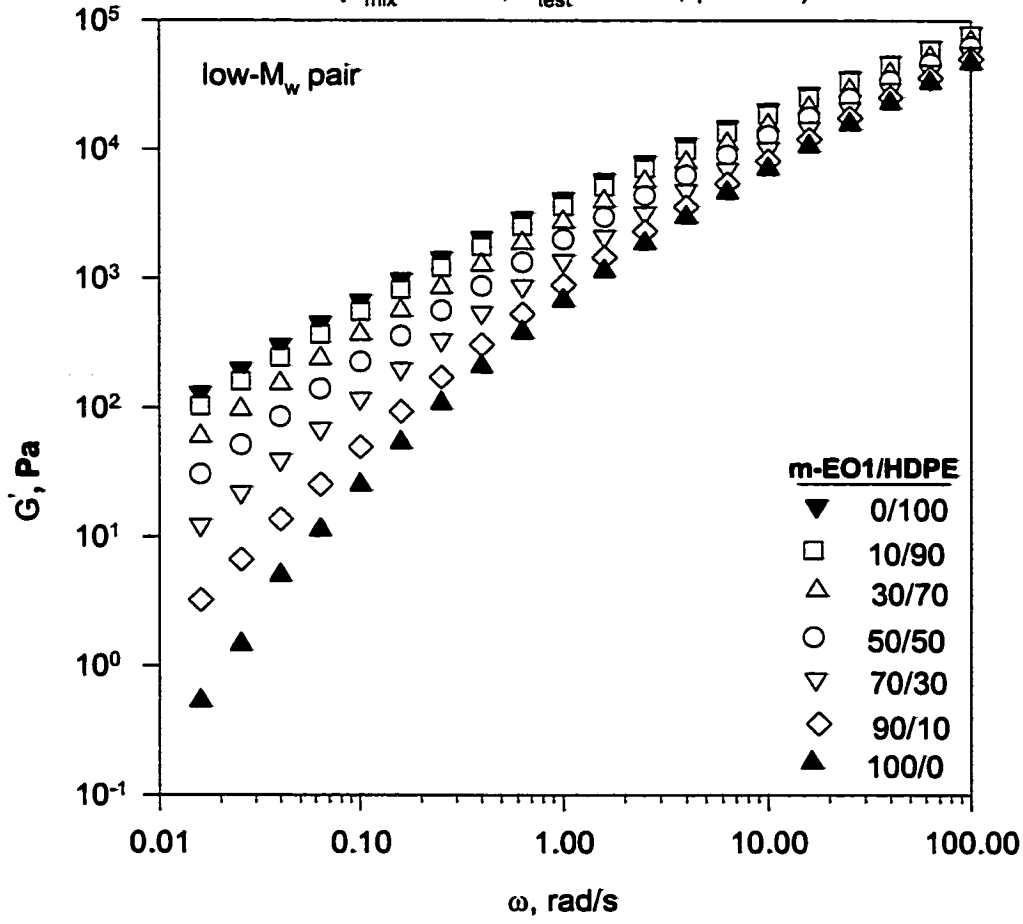

Figure C.2 G'(ω) for m-EO3 blend with HDPE
(T_{mix}=190°C, T_{test}=190°C, γ^{o}=15%)

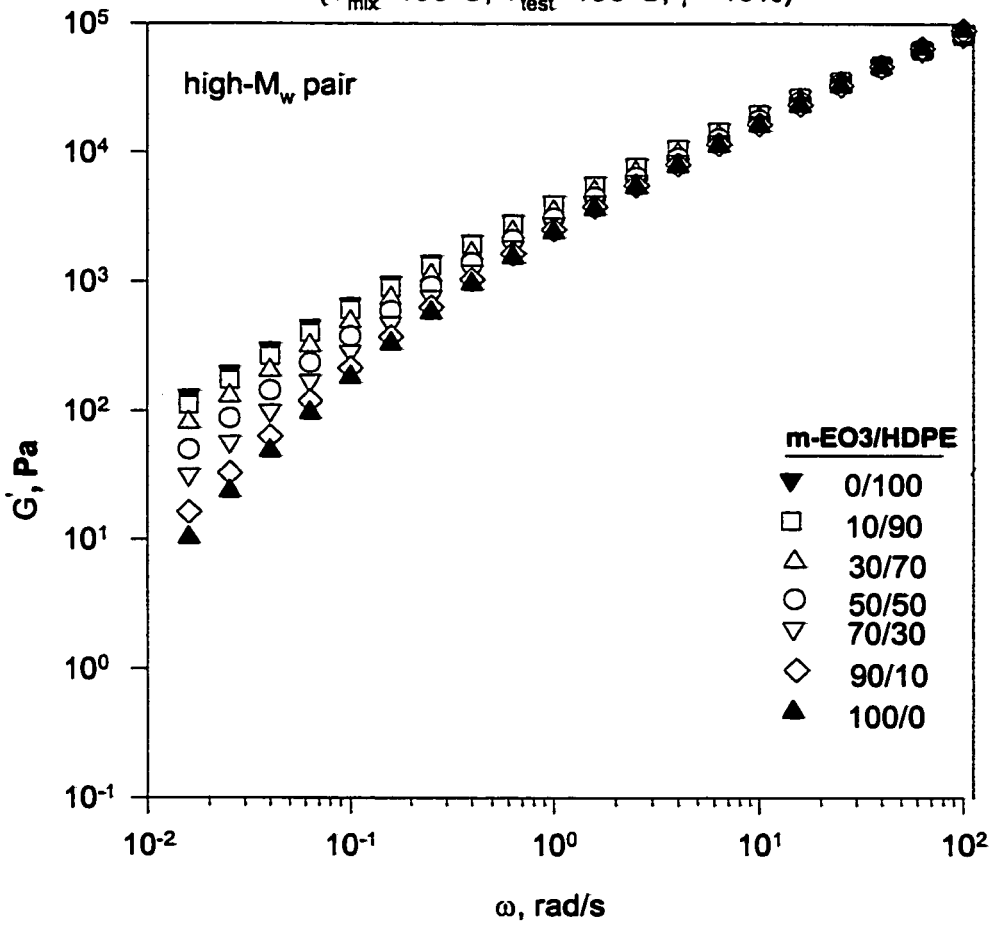

Figure C.3 G'(ϕ) for blends of m-EO1 with HDPE
(T_{mix}=190°C, T_{test}=190°C, γ°=15%)

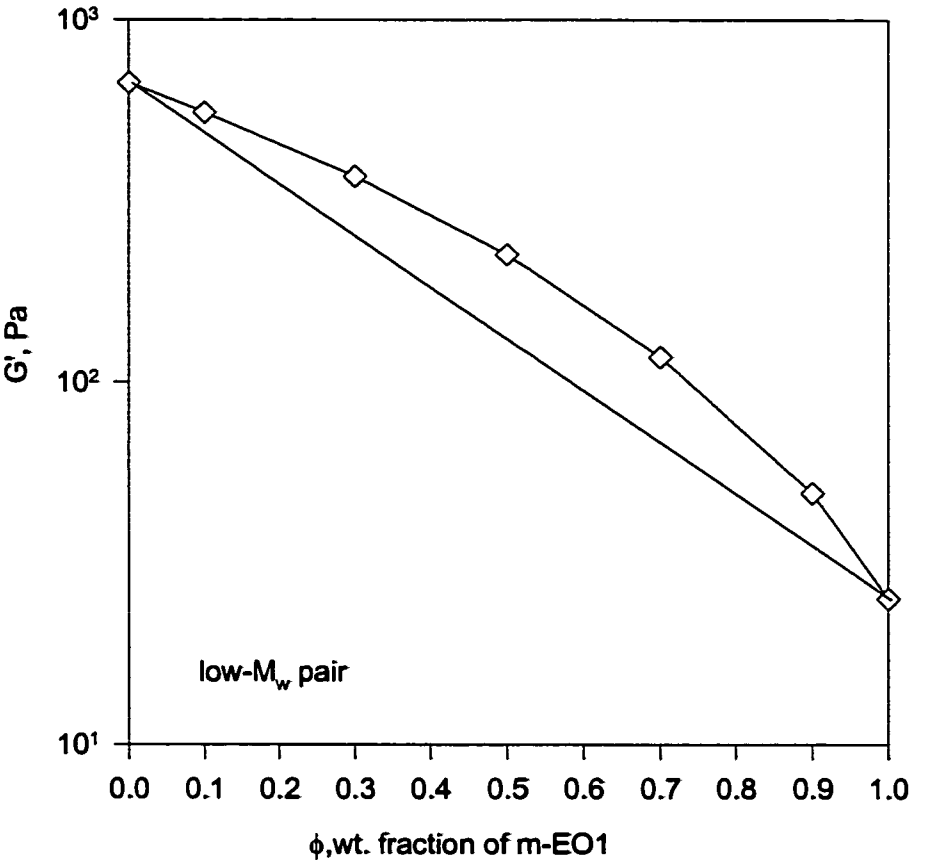

Figure C.4 $G'(\phi)$ for blends of m-EO1 with HDPE
(T_{mix}=190°C, T_{test}=190°C, $\gamma°$ =15%)

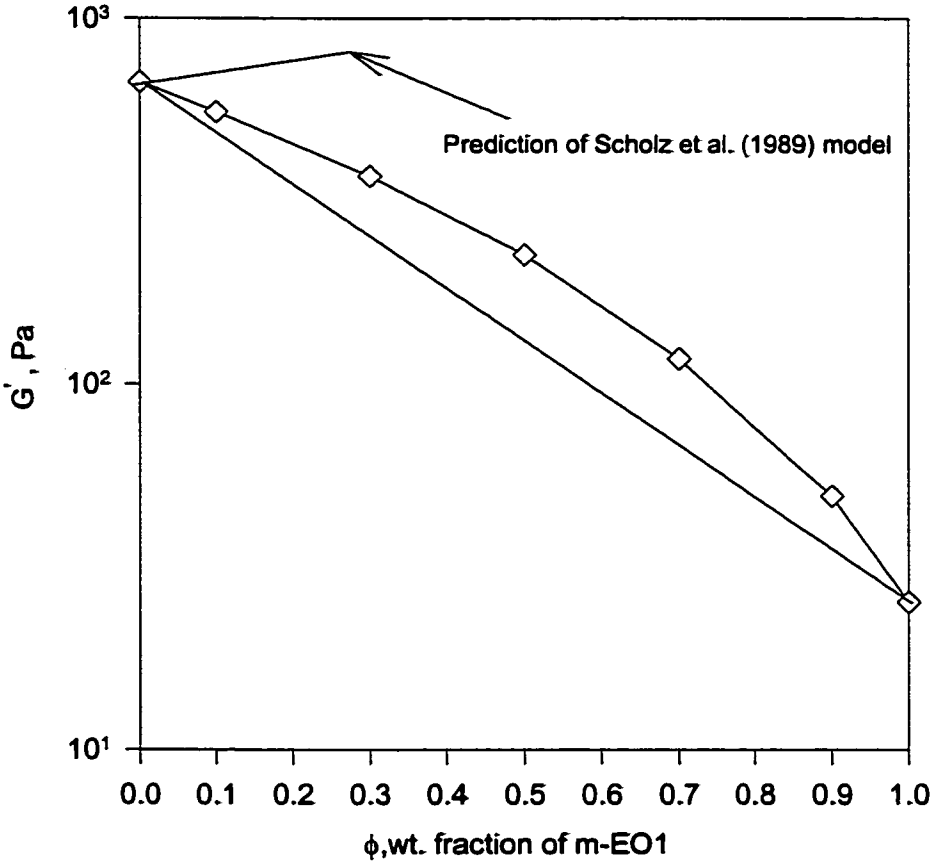

Figure C.5 G'(ϕ) blend of m-EO3 with HDPE

(T_{mix}=190°C, T_{test}=190°C, γ° =15%)

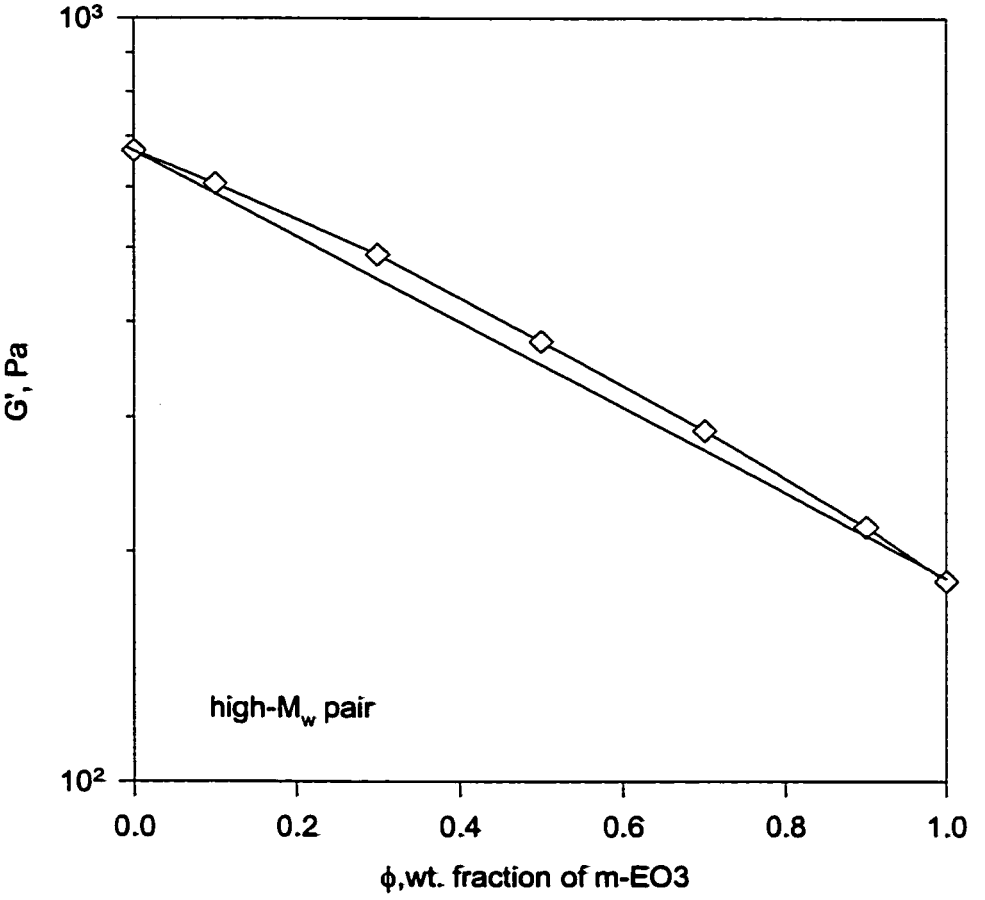

Appendix D

Supplement to Chapter 5.3

Figure D.1 $G'(\omega)$ for m-EO2 blends with HDPE
(T_{mix}=190°C, T_{test}=190°C, γ^{o}=15%)

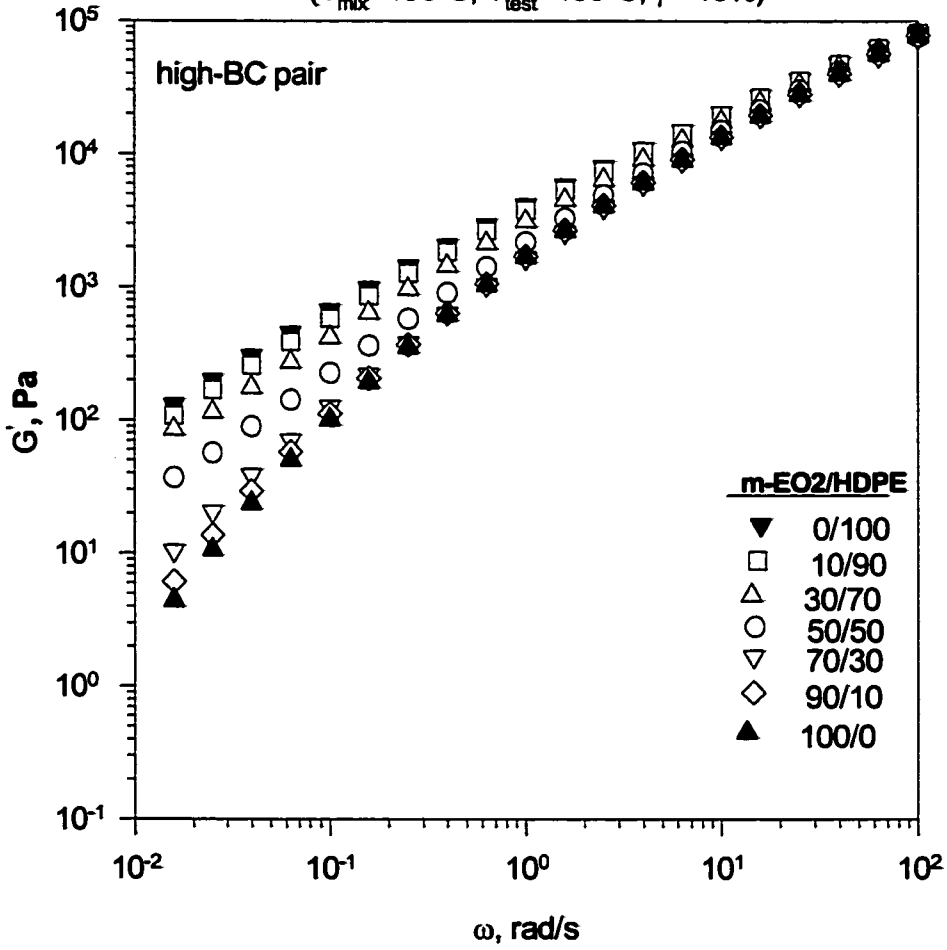

Figure D.2 G'(ω) for ZN-EO blend with HDPE
(T_{mix}=190°C, T_{test}=190°C, γ°=15%)

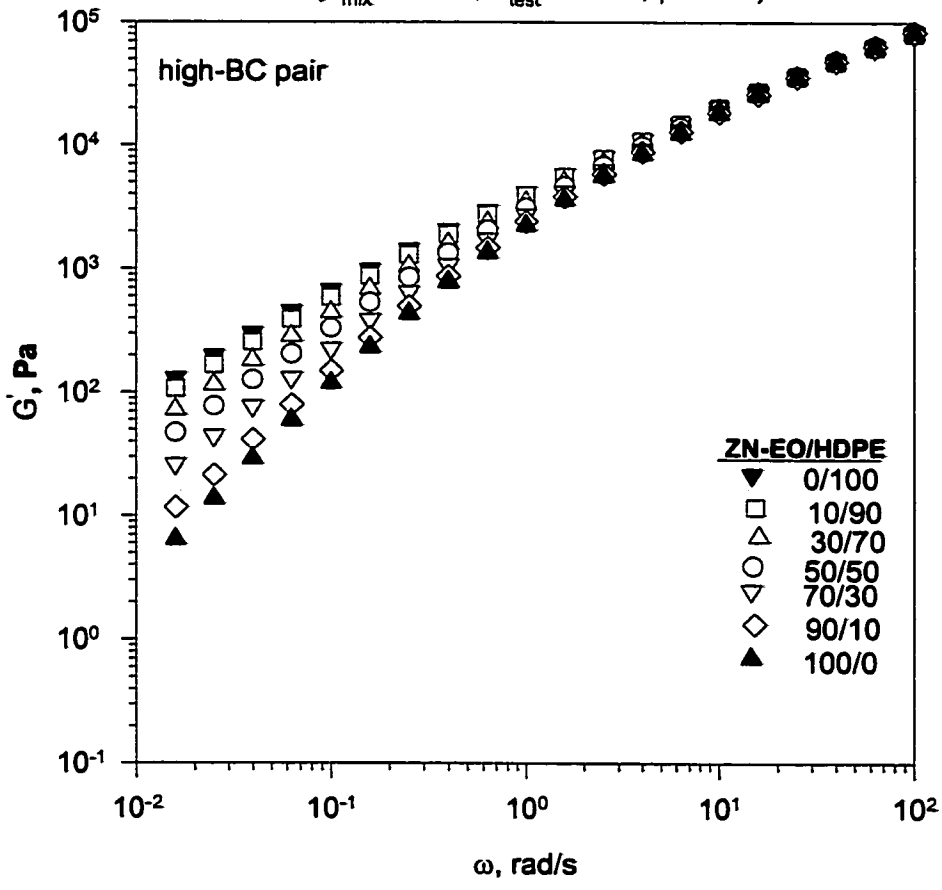

Figure D.3 G'(ϕ) for blends of m-EO2 with HDPE

(T_{mix}=190°C, T_{test}=190°C, γ° =15%)

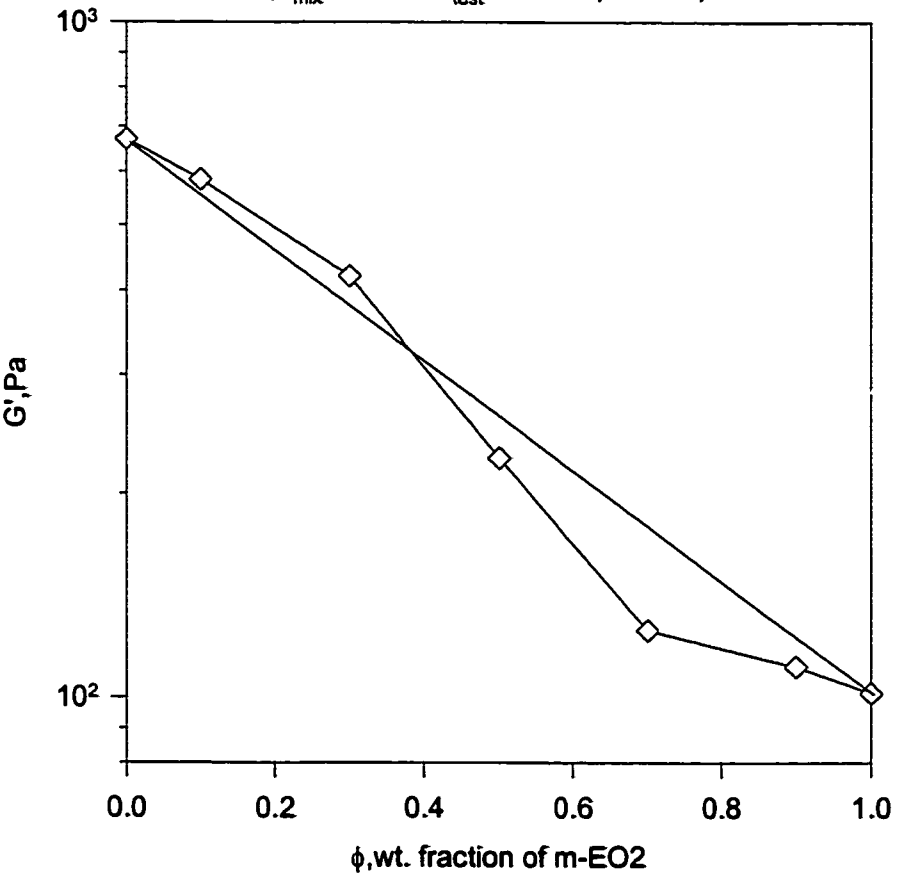

Figure D.4 $G'(\phi)$ for blends of ZN-EO with HDPE

(T_{mix}=190°C, T_{test}=190°C,γ^{o} =15%)

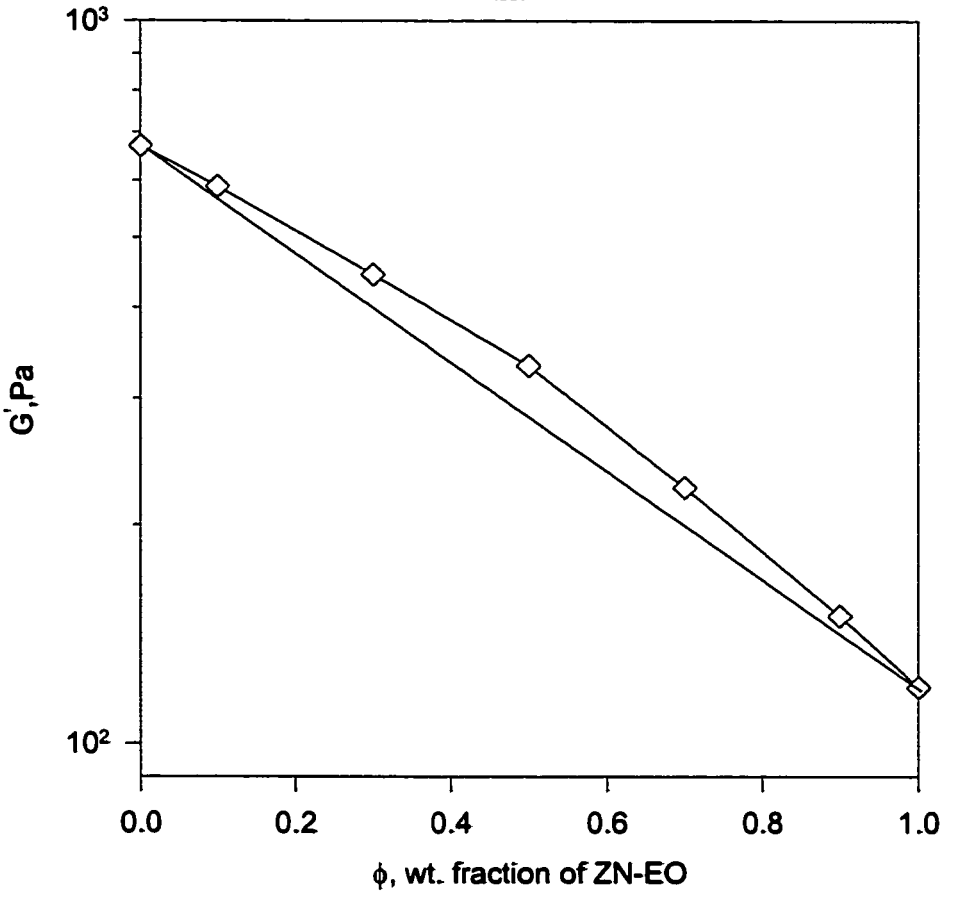

Nomenclature

A	Avogadro's constant
ARES	Advance Rheometric Expansion system
E_{vdw}	total interaction energy for van der Waals, kj/mol
ΔE_v	total vaporization energy for a material, kj/mol
G'	storage (elastic) modulus
G''	loss modulus
G^*	Complex modulus=$\sqrt{G'^2 + G''^2}$
ΔG_{mix}	Gibbs free energy change on mixing, kJ/mol
HDPE	high-density polyethylene
ΔH_{mix}	enthalpy change on mixing, kJ/mol
LLDPE	linear low-density polyethylene
M_n, M_w, M_z	number-average, weight-average, and Z-average
MD	molecular dynamics
n_1	number of moles of solvent
n_2	number of moles of polymer segment
N_1	first normal stress difference
N_2	second normal stress difference
N_i	degree of polymerization
NDB	negatively deviating blends
NPDB	negatively positively deviating blends

PDB	positively deviating blends
PNDB	positively negatively deviating blends
S	entropy of a system, kJ/mol/K
ΔS_{mix}	entropy change on mixing kJ/mol/K
T	absolute temperature, K
T_{test}	test temperature in AERS
T_{mix}	melt conditioning temperature in the blender
U	internal energy of a system, kJ/mol
V	total volume of a material, m^3
V_s	the molar volume of solvent for polymer-solvent mixture
γ	strain
γ^o	strain amplitude in dynamic shear
$\dot{\gamma}$	strain rate; steady shear rate
χ_{12}	Flory-Huggins interaction parameter
δ	Hildebrand solubility parameter, $(kJ/m^3)^{1/2}$
Δ	difference
η	Non-Newtonian viscosity
η'	Dynamic viscosity
η''	Elastic component of the complex viscosity
η^*	Complex viscosity $= \sqrt{\eta'^2 + \eta''^2}$

η_o	zero shear viscosity
ϕ	volume fraction
Π	internal pressure
θ	instantaneous bond angle
θ_o	equilibrium bond angle
ρ	density
ω	frequency

References

Abu-Sharkh B. F; **Hussein,** I.A., "MD simulation of the influence of branch content on collapse and conformation of LLDPE chains crystallizing from highly dilute solutions", Polymer, 42, 6333-6340, **2002.**

Allen, M.P.; **Tildesley,** D. J., "Computer Simulation of liquids", Oxford University Press: Oxford, **1987.**

Alamo, R.G.; **Londono**, J.D; Mandelkern, L.; Stehling, F.C.; Wignall, G.D., "Phase behavior of blends of linear and branched polyethylenes in the molten and solid states by small-angle neutron scattering", Macromolecules, 27, 411-417, **1994.**

Alamo, R.G.; **Graessley,** W.W.; Krishnamoorti, R.; Lohse, D.J.; Londono, J.D; Mandelkern, L.; Stehling, F.C., Wignall, G.D., "Small angle neutron scattering investigations of melt miscibility and phase segregation in blends of linear and branched polyethylenes as function of the branch content", Macromolecules, 30, 561-566, **1997.**

Agamalian, M.; **Alamo,** R.G.; Kim, M.H.; Londono, J.D.; Mandelkern, L.; and Wignall, G.D., "phase behavior of blends of linear and branched polyethylenes on micron length scales via ultra-small-angle neutron scattering", Macromolecules, 32, 3093-3096, **1999.**

Ajji, A.; **Choplin,** L., "Rheology and dynamic near phase separation in a polymer blend: Model and scaling analysis", Macromolecules, 24, 5221-5223, **1991.**

Bair, H.E, "Thermal analysis of additives in polymers in thermal characterization of polymeric materials 2nd ed. Edited by Edith Turi Vol 2 Academic press, **1997.**

Barham, P.J.; **Hill**, M.J; Keller, A and Rosney, C.C, "Phase separation in polyethylene melts" J. Material Sci. letters, 7, 1271-1275, **1988.**

Barham, P.J.; **Hill**, M.J; and Goldbeck-Wood, "A qualitative scheme for the liquid phase separation in blends of homopolymer with their branched copolymer", Polymer; 34, 2981-2988, **1993.**

Bates, F. S.; Fredrickson, G. H., "Conformation Asymmetry and polymer-Polymer thermodynamics", Macromolecules, 27, 1065-1067, **1994.**

Bin, S. E.; **Baird**, D. G., J Rheol, 44, 1151, **2000.**

Fredrickson, G. H.; **Liu**, A." Design of miscible polyolefin copolymer blend" J. J. Polym Sci: Part B: Polym. Phys., 33,1203-1212, **1995.**

Fredrickson, G. H.; **Liu**, A. J.; Bates, F. S., "Entropic correction to the Flory-Huggins theory of polymer blends: Architectural and conformational effects", Macromolecules, 27, 2503-2512, **1994.**

Flory, P.J., "Thermodynamics of high polymer solutions", J. Chem. Phys., 9, 660-661, **1941.**

Fujimura, M.; Kawasaki, Y., "Rheological properties of polyethylene/high-density polyethylene blend melts. II. Dynamic viscoelastic properties. J Appl Polym Sci 42, 481-488,**1991.**

Garcia-Rejon, A.; **Alvarez**, C., "Mechanical and flow properties of high-density polyethylene/low-density polyethylene blends", Polym Eng Sci 27(9), 640-646, **1987.**

Graebling, D,; **Muller, R.**; Palierne J.F., "Linear viscoelastic behavior of some incompatible polymer blends in melt. Interpretation of data with a model of emulsion of viscoelastic liquids", Macromolecules, 26, 320-329, **1993.**

Gramespacher, H.; **Meissner**, J., "Interfacial tension between polymer melts measured by shear oscillations of their blends", J. Rheol. 36(6), 1127-1141, **1992.**

Hameed, T; **Hussein**, I. A., "rheological study of the influence of M_w and comonomer type on the miscibility of m-LLDPE and LDPE blends", Polymer, 43, 6911-6929, **2002.**

Hansen, E. W.; **Blom**, R.; Bade O. M., "n.m.r. Characterization of polyethylene with emphasis on internal consistency of peak intensities and estimation of uncertainties in derived branch distribution numbers", Polymer, 38(17), 4295-4304, **1997.**

Heitmiller, R, F; **Naar**, R. Z.; Zabusky H. H., J. Appl. Polym. Sci., 8, 873, **1964.**

Hussein, I.A.; **Ho**, K.; Goyal, S.K.; Karbashewski, E.; Williams, M.C., "Polymer degradation and stability", 68(3), 381-392, **2000.**

Hussein, I.A; **Williams**, M. C., "Rheological study of the miscibility of LLDPE/LDPE blends and the influence of T_m" Polym. Eng. & Sci., 41, 696-701, **2001.**

Hill, M. J.; **Barham**, P. J.; Keller, A., "Phase segregation in blends of linear with branched polyethylene: the effect of varying the molecular weight of the polymer", Polymer, 33, 2530-2541, **1993.**

Hill, M. J.; **Barham**, P. J.; Roseny, C.C.A, "Phase segregation in melts of blends of linear and branched polyethylene", Polymer, 321384-1393, **1991.**

Hill, M. J.; **Barham**, P. J. "interpretation of behavior of blends containing linear low-density polyethylenes using a ternary phase diagram" Polymer, 34, 1802-1808, **1994.**

Hill, M.J. and **Barham**, P.J., "Absence of phase separation effects in blend of linear polyethylene fractions of differing molecular weight", Polymer, 36, 1523-1530, **1995.**

Hill, M.J.; **Puig**, C.C., "Liquid-liquid phase separation in blends of a linear low-density polyethylene with a low-density polyethylene", J. Appl. Polm. Sci. 65, 1921-1931, **1997.**

Hill, M.J. and **Barham**, P.J., "Liquid-liquid phase separation in blends containing copolymers produced using metallocene catalysts", Polymer, 38, 5595-5601, **1997.**

Huggins, M.L., "Thermodynamic properties of solutions of long chain compounds", Ann. N.Y. Acad. Sci., 43, 1-32, **1942.**

Hildebrand, J.H.; **Scott** R.L., "The solubility of non-electrolytes", Dover, New York, **1964.**

Han, C.D.; **Villamizer**, C. A., "Effects of molecular weight distribution and long-chain branching on the viscoelastic properties of high-and low-density polyethylene melts", J. Appl. Polym. Sci., 22, 1677-1681, **1978.**

Han, C.D.; **Kim**, J., "On the use of time-temperature superposition in mullticomponent/multiphase polymer systems", Polymer, 34, 2533-2539, **1993.**

Hu, S.R.; **Kyu**, T.; Stein R S., "Characterization and properties of polyethylene blends of a linear low-density polyethylene with high-density polyethylene", J Polym Sci: part B: Polym Phys 25, 71-87, **1987.**

Kazatchkov, I.B.; **Bohnet**, N., Goyal S.K.; and Hatzikiriakos S.G., "Influence of molecular structure on the rheological and processing behavior of polyethylene resins" Polym. Eng. and Sci., **1999.**

Karbashewski, E.; **Kale**, L.; Ruden, A.; Tchir, W. J.; Cook, D.G.; Pronovst, J., "Characterization of linear low density polyethylene by temperature arising elution fractionation and by differential scanning calorimetry", J. Appl. Poly. Sci., 44, 425-434, **1992.**

Mayo, S. L.; **Olafson**, B. D.; Goddard, W.A., "Deriding: generic force field for molecular simulations", J. Phys. Chem., 94, 8897-8909, **1990.**

Martuscelli, E., Macromol Chem. Rapid Commun , 5, 255, **1984.**

Mendelson, R.A.; Bowles, W.A., Finger F.L., "Effect of molecular structure on polyethylene melt rheology. II.Shear-dependent viscosity", J. Polym Sci.: Part A-2, 8, 127-141, **1970.**

Mark, J., "Handbook of Polymer Properties", American Institute of physics press, Woodbury, 257, **1996.**

Minale, M.; Moldenaers, P.; Mewis, J., " Effects of shear history on the morphology of immiscible polymer blends", Macromolecules, 30, 5470-5475, **1997.**

Martinez-Salazar, J.; **Cuesta**, M.S.; Plans, J., "on phase separation in high and low density polyethylens blends: 1. melting point depression analysis", Polymer, 32(16), 2984-2988, **1991**.

Michael, M. C.; **John,** F. G.; Paul, C. P., "Specific interactions and the miscibility of polymer blends", Technomic Publishing Co. Inc., **1991.**

Munoz-Escalation, A.; Lafuente, P.; Vega, J. F.; Munoz, M. E.; Santamaria, A., "Rheological behavior of metallocene catalyzed high density polyethylene blends" Polymer , 38, 589-594, **1997.**

Muller, A.J; Balsamo, V., "Thermal characterization of low density and linear low density polyethylene blends in advances in polymer blends and alloys technology", Ch. 1, 1-21, K. Findayson Ed., Technomic Publishing company, Lancaster, **1994.**

Nicholson, J.C.; **Fineman,** T.M.; and Crist P., "Thermodynamics of polyolefin blends: small-angle neutron scattering studies with partially deuterated chains", Polymer, 31, 2287-2293, **1990.**

Nose' S., "A unified formulation of the constant temperature molecular dynamics methods", J. Chem. Phys., 81, 511-519,**1984.**

Nose' S., " A molecular dynamics method for simulations in the canonical ensemble", Molecular Physics, 52, 255-268, **1984.**

Palierne, J.F., "linear rheology of viscoelastic emulsions with interfacial tension" Rheol Acta, 29, 204-214, **1990;** Erratum,30, 497, **1991.**

Plans, J.; **Cuesta,** S.; Marteniez-salazar, J.; "on phase separation in high and low density polyethylens blends: 2. A working model", Polymer, 32(16), 2989-2991, **1991.**

Plochocki, A.P., "polyolefin blends: rheology melt mixing, and application in polymer blends" Vol 2 edited by Paul D.R., Newman S., Academic press., **1978.**

Randall, J. C., Ed. "NMR and Macromolecules", Am. Chem. Soc. Symp. Ser. , 247, **1984.**

Rana, D.; Kim, H.L.; Kwag, H.; Rhee, J.; Cho, K.; Woo, T.; Lee, B.H.; Choe, S., "Blends of ethylene 1-octene copolymer synthesized by Ziegler-Natta and metallocene catalysts. II. Rheology and mechanical behaviors", J Appl Polym. Sci, 76 1950-1964, **2000.**

Rigby, D.; **Sun,** H.; **Eichinger,** B.E., "Computer simulations of poly (ethylene oxide): force field, PVT diagram and cyclization behavior", Poly. Int., 44, 311-330, **1997.**

Rego lopez, J. M.; **Gedde,** U.W., "Crystallization and morphology of binary blends of linear and branch polyethylene: polarized light microscopy, small-angle light scattering and thermal analysis", Polymer, 30, 22-26, **1989.**

Rhee, J.; **Crist,** B., "Thermodynamics and phase separation in the melt blends of polyethylene and model copolymer", Macromolecules, 24, 5663-5669, **1991.**

Rudin, A.; **Chee,** K.K; Shaw, J.H, "Specific volume and viscosity of polyolefin melts", J Polym Sci, part C, 30, 415-427, **1970.**

Scholz, P.; **Froelich,** D.; Muller, R., " viscoelastic properties and morphology of two-phase polypropylene/polyamide 6 blends in the melt. Interpretation of results with emulsion model", J. Rheol., 33, 481-489, **1989.**

Shroff, R. N.; **Mavridis,** H., Macromolecules, 32, 8454, **2000.**

Tashiro, K.; **Stein,** R. S.; Hsu, S.L., "1. Thermal and vibrational spectroscopic study by utilizing the deuteration technique", Macromolecules, 25, 1801-1808, **1992.**

Tanem, B.S.; **Stori,** A., "Blends of single-site linear and branched polyethylene: Morphology characterization 11", Polymer, 42, 6609-6618, **2001.**

Tanem, B.S.; **Stori**, A., "Investigation of phase behavior in the melt in blends of single-site based linear polyethylene and ethylene-1-alkene copolymer", Polymer, 42, 4309-4319, **2001.**

Tanem, B.S.; **Stori**, A., "phase separation in melt blends of single-site linear and branched polyethylene", Polymer, 42, 5689-5694, **2001.**

Tanem, B.S.; **Stori**, A., "Blends of single-site linear and branched polyethylene.1. Thermal characterization", Polymer, 42, 5389-5399, **2001.**

Usami, T.; **Gotoh**, Y; Takayama, S., "Generation mechanism of short-chain branching distribution in linear low-density polyethylenes", Macromolecules 19, 2722-2726, **1986.**

Utracki, L. A.; **Schlund**, B., " linear low density polyethylens and their blends: Part 2. Shear flow of LLDPE's" Polym Eng and Sci, 27(5) 367-379, **1987.**

Utracki, L. A.; **Schlund**, B., "Linear low-density polyethylens and their blends: Part 4 Shear flow of LLDPE blends with LLDPE and LDPE", Polym Eng Sci, 27, 1512-1522, **1987.**

Utracki, L.; **Kamal**, M. R., "melt rheology of polymer blends" Polym Eng Sci, 22(2), 96-114, 1982.

Utracki, L. A., "On the viscosity-concentration dependence of immiscible polymer blends", J Rheol. 35(8), 1615-1637, **1991.**

Utracki, L. A., "viscoelastic behavior of polymer blends", Polym Eng Sci, 28(21), 1401-1404,**1988.**

Qi, L.; **Xigao**, J., J. Chem. Phys. 107, 613, **1997.**

Verlet, L., "Computer 'experiments' on classical fluids. 1. Thermodynamical properties of Lennard-Jones molecules", Physical Review, 159, 98-103, **1967.**

Vega, J.F.; **Munoz-Escalona**, A.; Santamaria, A.; Munoz M.E.; Lafuente, P., "Comparison of the rheological properties of metallocene-catalyzed and conventional high-density polyethylenes", macromolecules, 29, 960-965, **1996.**

Vinkier, I, **Moldenaers** P, Mewis J. "stress relaxation as a microstructural probe for immiscible blends", Rheol Acta, 36, 513-523, **1997.**

Wardhaugh, L.T. **Williams**, M.C.,"Blockiness of olefin copolymers and possible microphase separation in the melt", Polym Eng Sci, 35(1), 18-27, **1995.**

Wignall, G.D.; **Alamo**, R. G.; Londono, J.D.; Mandelkern, L., and Stehling, F.C., "Small angle neutron scattering investigation of liquid-liquid phase separation in heterogeneous linear low-density polyethylene", Macromolecules, 29, 5332-5335,**1996**.

Wignall, G.D.; **Alamo**, R. G.; Londono, J.D.; Mandelkern, L.; Kim, M. H.; Lin, J. S.; Brown, G. M., "Morphology of blends of linear and short-chain branched polyethylenes in the solid state by Small-Angle Neutron and X-ray Scattering, Differential Scanning Calorimetry, and Transmission Electron microscopy", Macromolecules, 33, 551-5761, **2000.**

Wood-Adams, P.; **Dealy**, J. H., "Using Rheological data to Determine the branching level in Metallocene polyethylenes", Macromolecules, 33, 7481-7488, **2000.**

Zhang, M.; **Lynch**, D.T.; Wanks, S.E., "Effect of molecular structure distribution on melting and crystallization behavior of 1-butene/ethylene copolymers", Polymer, 42,3067-3075, **2001**.

Zhao, Y.; **Liu**, S.; Yang, D., "Crystallization behavior of blends of high-density polyethylene with novel linear low-density polyethylene", Macromol. Chem. Phys., 198, 1427-1436, **1997.**

Yang, L. Y.; **Smith**, T.G.; Bigio, D., " melt blending of linear low density polyethylene and polystyrene-Effects of processing conditions, composition, and compatiplizer upon morphology development", ANTEC, 2428-2432, **1994.**

Vita

Name: Adam Musa Giri

Education

M. Sc., Chemistry, December 1998
University of Gezira, Wad-Medani, Sudan

B. Sc., Chemical Engineering, March 1989
University of Gezira, Wad-Medani, Sudan

Past Experience

March 1989- August 1990

Teaching Assistant
Applied Chemistry and Chemical Technology Department
University of Gezira, Wad-Medani, Sudan

April 1996- December 1998

Research Assistant
Applied Chemistry and Chemical Technology Department
University of Gezira, Wad-Medani, Sudan

January 1998- August 2000

Lecturer
Faculty of Petroleum & Ground Water
University of Western Kordofan, EN-Nuhud, Sudan

September 2000- January 2003

Research Assistant
Department of Chemical Engineering
King Fahd University of Petroleum & Minerals, Dhahran 31261, Saudi Arabia